

**University of Alberta**

**Protein Elution through Packed Capillaries**

by

Jing Wen



A thesis submitted to the Faculty of Graduate Studies and Research in partial fulfillment of  
the  
requirements for the degree of Master of Science

Department of Chemistry

Edmonton, Alberta  
Spring 2006



Library and  
Archives Canada

Bibliothèque et  
Archives Canada

Published Heritage  
Branch

Direction du  
Patrimoine de l'édition

395 Wellington Street  
Ottawa ON K1A 0N4  
Canada

395, rue Wellington  
Ottawa ON K1A 0N4  
Canada

*Your file* *Votre référence*

*ISBN: 0-494-13907-2*

*Our file* *Notre référence*

*ISBN: 0-494-13907-2*

#### NOTICE:

The author has granted a non-exclusive license allowing Library and Archives Canada to reproduce, publish, archive, preserve, conserve, communicate to the public by telecommunication or on the Internet, loan, distribute and sell theses worldwide, for commercial or non-commercial purposes, in microform, paper, electronic and/or any other formats.

The author retains copyright ownership and moral rights in this thesis. Neither the thesis nor substantial extracts from it may be printed or otherwise reproduced without the author's permission.

#### AVIS:

L'auteur a accordé une licence non exclusive permettant à la Bibliothèque et Archives Canada de reproduire, publier, archiver, sauvegarder, conserver, transmettre au public par télécommunication ou par l'Internet, prêter, distribuer et vendre des thèses partout dans le monde, à des fins commerciales ou autres, sur support microforme, papier, électronique et/ou autres formats.

L'auteur conserve la propriété du droit d'auteur et des droits moraux qui protègent cette thèse. Ni la thèse ni des extraits substantiels de celle-ci ne doivent être imprimés ou autrement reproduits sans son autorisation.

---

In compliance with the Canadian Privacy Act some supporting forms may have been removed from this thesis.

Conformément à la loi canadienne sur la protection de la vie privée, quelques formulaires secondaires ont été enlevés de cette thèse.

While these forms may be included in the document page count, their removal does not represent any loss of content from the thesis.

Bien que ces formulaires aient inclus dans la pagination, il n'y aura aucun contenu manquant.

  
**Canada**

*To my parents and my family*

## Abstract

The miniaturization of separation systems has been widely applied to the area of protein analysis. This work focuses on the use of packed capillary columns for liquid chromatography (LC). Both electrokinetic pumping as used in capillary electrochromatography (CEC) and pressure based pumping will be explored. The fabrication of packed capillary with two kinds of stationary phases is addressed. A splitless-flow nano-LC system in combination with laser induced native fluorescence detection was developed, which showed separation efficiency of  $9.9 \times 10^4$  for tryptophan and mass detection limit of 5.1 fmol for  $\alpha$ -lactalbumin. Factors affecting band broadening were investigated: injector, connecting tubing and detector. To contribute to the understanding of the mechanism of protein concentration found in CEC columns packed with nano-porous particles, this thesis explores the behavior of protein in nano-porous stationary phase used for electrokinetic chromatography. Further, protein separation was demonstrated in pressure assisted size-exclusion electrochromatography (pSEEC).

## **Acknowledgments**

I am deeply indebted to my supervisor, Dr. D. Jed Harrison. Without him, none of this work would have been possible. I thank him for his patience and encouragement that carried me on through difficult times, and for his insights and suggestions that helped to shape my research skills.

I would like to acknowledge Dr. Charles A. Lucy for serving in my thesis committee and for allowing me to use his lab to finish some experiments. I would also like to acknowledge another committee member, Dr. Jonathan W. Martin. The valuable feedback from them helped me to improve the thesis in many ways.

I am grateful for the support by former and present members of the Harrison group. Thanks especially to Dr. Jianbin Bao, Dr. Guifeng Jiang, Dolores Martinez, Kowlasar Misir, Zhen Wang and Yong Zeng for all inspiring discussions and contributions to my work. Thanks also to Arlene Figley for her kind help.

Special thanks go to Dr. Hyuk Jeong for the fruitful co-operations. Many thanks to staff members in machine shop for capillary-holder fabrication and pump repair.

Finally, I would like to thank my parents for always being there when I needed them most, and for the support they provided me through my entire life. I dearly thank my husband Shengli for his love and caring and my lovely daughter Emma for the joy she brings to me.

## Table of Contents

### Chapter 1: Introduction

1.1 Objective	1
1.2 Nano Liquid Chromatography	2
1.2.1 Application of nano-LC	2
1.2.2 Fundamental Aspects of Size-Exclusion Chromatography	3
1.3 Capillary Electrochromatography	6
1.3.1 History	6
1.3.2 Fundamental Aspects	7
1.3.3 Application of CEC in Protein Analysis	11
1.3.3.1 Packed Capillary	11
1.3.3.2 Monolithic Capillary	12
1.3.3.3 Open Tubular CEC	13
1.4 Size Exclusion Electrochromatography	13
1.4.1 Historical Perspective and Fundamentals	13
1.4.2 Application of SEEC	14
1.5 Capillary Packing	15
1.5.1 Packing Material	16
1.5.2 Capillary Packing Technology	16
1.5.3 Retaining Frit	17
1.6 Scope of the Thesis	18
1.7 References	19

### Chapter 2: Nano-Liquid Chromatography

2.1 Introduction	24
2.2 Experimental	25



2.3.4 Attempt of Capillary Coating	54
2.3.5 Detection with Reversed Phase Nano-LC	56
2.3.5.1 Peptide Mixture	56
2.3.5.2 Digested Protein	57
2.4 Conclusion	58
2.5 References	59

### **Chapter 3: Size-Exclusion Electrochromatography**

3.1 Introduction	61
3.2 Experimental	62
3.2.1 Reagent and chemicals	62
3.2.2 Instrumentation and Apparatus	63
3.2.3 Fabrication of Packed Capillary	63
3.2.3.1 Silanization of Capillary Wall	64
3.2.3.2 Frit Fabrication and Polymer Bead Column Packing	64
3.2.4 Protein Labeling	66
3.2.5 Measurement of Protein Electrophoretic Mobility	66
3.2.6 Size-Exclusion Electrochromatography	67
3.3 Results and Discussion	67
3.3.1 Capillary Packing with Polymer Beads	67
3.3.1.1 Information of Polymer Beads	67
3.3.1.2 Activation of Capillary Wall	68
3.3.1.3 Frit Fabrication	68
3.3.1.4 Capillary Packing	72
3.3.2 SEEC with BioSep-S2000 Column	72
3.3.2.1 Concentration Effect	72
3.3.2.2 Pressure Assisted SEEC	75

3.3.3 SEEC with PolySep-P Column	76
3.3.3.1 Relationship between Current and Voltage	76
3.3.3.2 Effect of Injection Time	77
3.3.3.2.1 Models for Concentration Effect	78
3.3.3.2.2 Possible Mechanism in This Work	80
3.3.3.2.3 Modification of EOF Calculation in a Packed Capillary	82
3.3.3.3 Elution of Various Proteins	85
3.3.3.4 Pressure Assisted SEEC	86
3.3.3.5 Effect of Pore Size	89
3.3.3.6 Effect of Ionic Strength	90
3.3.3.7 Effect of pH	91
3.3.3.8 Study of DMSO Velocity	92
3.4 Conclusion	94
3.5 References	94

## **Chapter 4: Summary**

4.1 Conclusion and Future Work	96
4.2 Reference	97

## List of Tables

Table 1-1	Names and definitions for HPLC techniques	2
Table 2-1	Technical information of Biosep-SEC-S2000	32
Table 2-2	Reproducibility study in nano-SEC	36
Table 2-3	Contribution of each extra band broadening	40
Table 2-4	Variation of peak height and noise with concentration of $\alpha$ -lactalbumin	42
Table 2-5	Resolution comparison in various buffers	45
Table 2-6	Effect of injection volume on resolution	49
Table 2-7	Effect of flow rate on resolution	50
Table 2-8	Separation efficiency for each component in sample mixture	54
Table 3-1	Technical data for PolySep-GFC-P beads	68
Table 3-2	Calculated $\mu_{ep}$ for several proteins	81
Table 3-3	Parameters used for EOF calculation in packed capillary	84
Table 3-4	Resolution at different voltages	89

## List of Figures

Figure 1-1	Cartoon of the principle of SEC	4
Figure 1-2	Flow profile in CEC and HPLC	7
Figure 1-3	localization of the induced bulk charge layer and electrosmotic whirlwind around a spherical ion exchanger particle	9
Figure 1-4	Change of the average EOF velocity with the electric field strength for different conductivity ratio	10
Figure 1-5	Change of the average EOF velocity versus the electrical field strength for different particle sizes	10
Figure 2-1	Cartoon of packing system	26
Figure 2-2	Scheme of capillary packing	27
Figure 2-3	Confocal epiluminiscent setup	29
Figure 2-4	Pictorial representation of the instrumental setup of nano-SEC	30
Figure 2-5	Scanning electron micrographs of capillary packed with silica beads	33
Figure 2-6	Chromatogram of 50 $\mu\text{M}$ tryptophan	34
Figure 2-7	van Deemter plot for 100 $\mu\text{M}$ W	35
Figure 2-8	Plot of S/N and plate height as a function of tryptophan concentration	41
Figure 2-9	Plot of S/N as a function of $\alpha$ -lactalbumin concentration	42
Figure 2-10	Protein separation in two different buffers	44
Figure 2-11	Effect of sample solvent on protein elution	46
Figure 2-12	Elution of adsorbed protein after injection of ACN	47
Figure 2-13	Effect of injection volume on protein separation	48
Figure 2-14	Protein separation at different flow rates	49
Figure 2-15	Van Deemter plots for two proteins	50
Figure 2-16	Plate height vs. sample amount	52

Figure 2-17	Separation of mixture of proteins and peptide	52
Figure 2-18	Plot of retention time vs. log molecular weight	53
Figure 2-19	Separation of mixture of proteins and amino acid	54
Figure 2-20	Schematic representation of the coating procedure	55
Figure 2-21	Separation of mixture of three peptides at different flow rate	56
Figure 2-22	van Deemter plots for several peaks	56
Figure 2-23	Detection of trypsin digested $\alpha$ -lactalbumin	58
Figure 3-1	Cartoon of a conventional capillary electrophoresis system	64
Figure 3-2	Scheme of capillary packing with polymer beads	65
Figure 3-3	UV absorption spectrum of benzoin methyl ether	70
Figure 3-4	Scanning electron micrographs of capillary packed with polymer beads	71
Figure 3-5	BSA elution with LC and CEC mode	73
Figure 3-6	Elution profiles of 5 $\mu$ M BSA under pressure after applying voltage	74
Figure 3-7	Fluorescence images of frits	74
Figure 3-8	Effect of changing injection time for 5 $\mu$ M BSA	75
Figure 3-9	Elution profiles of pSEEC for $\beta$ -lactoglobulin	76
Figure 3-10	Current as a function of voltage for packed capillary	77
Figure 3-11	Effect of injection time on different proteins	78
Figure 3-12	Electrochromatograms of various proteins in SEEC	85
Figure 3-13	Elution profiles of various proteins in pSEEC	87
Figure 3-14	Protein separation with pSEEC and CE	88
Figure 3-15	Elution profiles of two proteins in pSEEC	90
Figure 3-16	Effect of ionic strength on protein elution in pSEEC	91
Figure 3-17	BSA elution in pSEEC at different pH	91
Figure 3-18	DMSO velocity in SEEC at various voltages	93

## Abbreviations

ACN	acetonitrile
BME	benzoin methyl ether
BSA	bovine serum albumin
CE	capillary electrophoresis
CEC	capillary electrochromatography
CZE	capillary zone electrophoresis
DMSO	dimethyl sulphoxide
DTT	<sub>DL</sub> -dithiothreitol
EOF	electroosmotic flow
GMA	glycidyl methacrylate
HETP	height equivalent to a theoretical plate
i.d.	inner diameter
IAA	iodoacetamide
IgG	immunoglobulin G
LIF	laser induced fluorescence
LINF	laser induced native fluorescence
LOD	limit of detection
MW	molecular weight
Nd:YAG	neodymium yttrium aluminum garnet
o.d.	outer diameter
pI	isoelectric point
pSEEC	pressure assisted size exclusion electrochromatography
PMT	photomultiplier tube
SDS	sodium dodecyl sulfate
SDBS	sodium dodecylbenzene sulphate

SEC	size exclusion chromatography
SEEC	size exclusion electrochromatography
SOS	sodium octyl sulphate
S/N	signal to noise
TEMED	N,N,N',N'-tetramethylethylenediamine
TFA	trifluoroacetic acid
THF	tetrahydrofuran
TRIM	trimethylolpropane trimethacrylate
UV	ultra violet
W	tryptophan

## Chapter 1: Introduction

### 1.1 Objective

Microseparation has drawn considerable attention from researchers over the past two decades, since minute sample analysis is widely needed in various fields such as environmental, clinical, forensic and pharmaceutical chemistry. Besides the small sample volume, miniaturization of separation systems offers many advantages such as high sensitivity, rapid analysis, low reagent consumption, portability and automation. These properties are very attractive for the development of versatile separation technologies.

This thesis will examine the use of packed capillary columns for liquid chromatography (LC). Both electrokinetic pumping as used in capillary electrochromatography (CEC) and pressure based pumping will be explored.

CEC is an attractive technology because it does not require pumps. Despite the obvious interest, CEC of proteins has not been very successful. In bead packed beds, the few authors that have reported results have found pressure was also required. Other authors have reported unusual protein stacking effect that may be related to double layer effects in charged nano-scale pores.

This thesis explores the behavior of proteins in nano-porous stationary phases used for electrokinetic chromatography. The main goal is to contribute to the understanding of the mechanism of protein concentration observed in these columns. As a part of this project the results with the packed columns were compared to pressure driven flow in a nano-LC format, leading to the development of a nano-LC size exclusion chromatography (SEC). The following sections review some of the important background in nano-LC, SEC, application of CEC in protein analysis, size exclusion electrochromatography (SEEC) and capillary packing technology.

## 1.2 Nano-Liquid Chromatography

### 1.2.1 Application of nano-LC

In the 1980's, packed columns using fused silica capillaries with a 20-250  $\mu\text{m}$  inner diameter and a flow rate of 0.02-10  $\mu\text{L}/\text{min}$  were developed to miniaturize high performance liquid chromatography (HPLC) in order to improve separation efficiency<sup>3-7</sup>. Theoretically, if other parameters remain constant and the injection amount is the same, the enhanced sensitivity factor ( $f$ ), after reducing the column's inner diameter from  $d_1$  to  $d_2$  is given by

$$f \sim \frac{d_1^2}{d_2^2} \quad (1-1)$$

Decreasing columns from 4.4 mm i.d. to 50  $\mu\text{m}$  i.d. could in principle result in sensitivity improvement by almost 8,500 times. In practice, smaller columns often require smaller injection volumes, to avoid overloading.

HPLC techniques were divided into five categories by Chervet<sup>8</sup> based on the size of the columns. The classification scheme is given in Table 1-1. Chervet also theoretically investigated instrumental requirements such as flow rate, connecting tubing, detection and injection volumes for nano-LC. Compared to conventional HPLC, nano-LC has several advantages: high separation efficiency, high sensitivity, fast analysis time and low consumption of sample and mobile phase. However, the limited injection volume required counterbalances the sensitivity improvement provided by Eq. (1-1). Additionally,

Column i.d.	Flow rate	Name
3.2-4.6 mm	0.5-2.0 mL/min	Conventional HPLC
1.5-3.2 mm	100-500 $\mu\text{L}/\text{min}$	Microbore HPLC
0.5-1.5 mm	10-100 $\mu\text{L}/\text{min}$	micro-LC
150-500 $\mu\text{m}$	1-10 $\mu\text{L}/\text{min}$	capillary LC
10-150 $\mu\text{m}$	10-1000 nL/min	nano-LC

**Table 1-1 Names and definitions for HPLC techniques.**

the instrument and packed columns used for nano-LC are expensive. To get the desired small injection volume and low flow rate for nano-LC, a flow splitter is often added to a conventional LC system. The excess of sample and mobile phase flows to waste through the flow splitter. The drawbacks of a flow splitter are (1) the consumption of sample and mobile phase is not minimized, (2) the split ratio will change during the elution process if there is no feedback system.

Owing to its attractive properties, nano-LC has developed dramatically since 1980. Many stationary phases were used including reverse-phase,<sup>9-12</sup> normal phase,<sup>13, 14</sup> ion exchange,<sup>15</sup> and affinity<sup>16</sup>. Nano-LC has been applied to a variety of compounds such as peptides,<sup>9, 10, 12</sup> drugs,<sup>17</sup> and chiral compounds.<sup>18, 19</sup>

For many of these applications nano-LC is usually interfaced with a mass spectrometer (MS), especially for biochemical analysis. With the small injection volumes used in nano-LC, absorbance based detectors (e.g. UV) are not suitable. In contrast, MS remains a sensitive method. Electrospray (ESI) is the most versatile continuous-flow ionization technique in coupling LC and MS<sup>10, 20, 21</sup>. Recently, matrix-assisted laser desorption/ionization (MALDI) was also used as an interface between nano-LC and MS<sup>12, 22</sup>. This new interface is based on on-line introduction of analytes or off-line fractionation of analytes.

### **1.2.2 Fundamental Aspects of Size-Exclusion Chromatography**

Size-exclusion chromatography (SEC), also known as gel permeation or gel filtration chromatography uses porous particles to separate molecules of different sizes. It is generally used to separate biological molecules and to determine molecular weights and the molecular weight distribution of polymers. Analyte and solvent molecules diffuse in and out of the pores of chromatographic particles. Retention of analyte depends on the pore size and the size of the analyte. Molecules that are smaller than the pore size can enter the particles and therefore have a longer path and a longer elution time than larger

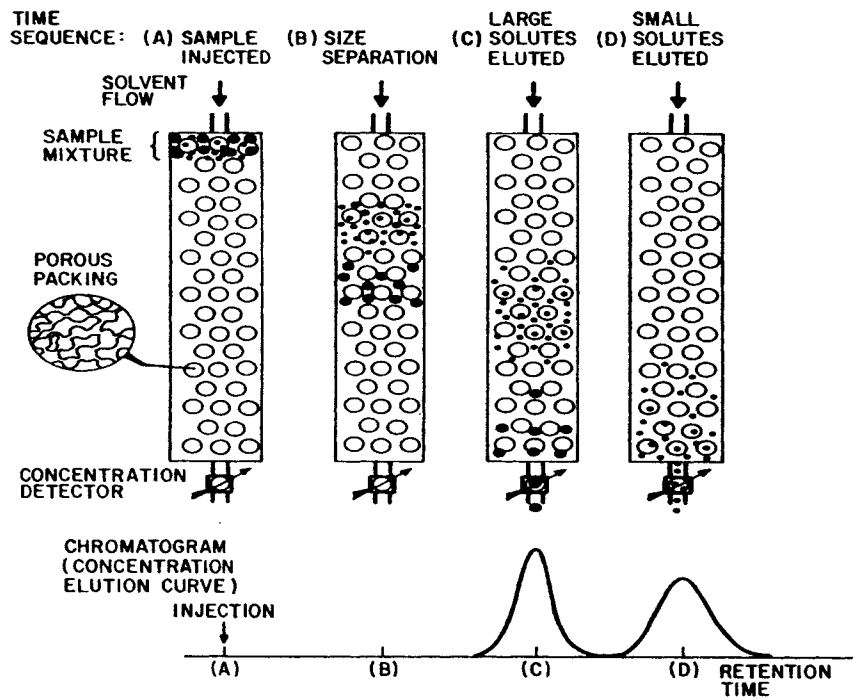


Figure 1-1 Cartoon of the principle of SEC. Adapted from Yau<sup>1</sup>.

molecules that cannot enter the particles. The principle of SEC is illustrated in Figure 1-1.

For a packed SEC column, the total volume ( $V_t$ ) is given by

$$V_t = V_g + V_i + V_o \quad (1-2)$$

where  $V_g$  is the volume occupied by stationary phase,  $V_i$  is the volume of solvent held in the pores and  $V_o$  is the free volume outside the particles. The retention volume for totally excluded molecules is  $V_o$ , while the retention volume for small molecules that can enter all the pores is  $(V_i + V_o)$ . The elution time for intermediate sized molecules is determined by the following equation.

$$V_e = V_o + KV_i \quad (1-3)$$

where  $K$  is the SEC distribution coefficient.

In SEC, an analyte is equilibrated many times between the mobile and the so-called

stationary phase during elution through the column. Each equilibration can be thought of as one theoretical plate. Assuming a Gaussian distribution for an analyte peak, the separation efficiency ( $N$ ), describing the number of theoretical plates, is related to experimental observation by

$$N = \left(\frac{t_R}{\sigma}\right)^2 = 5.54\left(\frac{t_R}{W_{1/2}}\right)^2 \quad (1-4)$$

where  $t_R$  is the elution time of the analyte,  $\sigma$  represents the variance of the Gaussian distribution function and  $W_{1/2}$  is the width at half height. The baseline peak width ( $W_b$ ) can be calculated by

$$W_b = 4\sigma \quad (1-5)$$

The height equivalent to a theoretical plate (HETP or  $H$ ) is given by

$$H = \frac{L}{N} \quad (1-6)$$

where  $L$  is the column length. HETP can also be represented by the van Deemter equation

$$H = A + B/u + Cu \quad (1-7)$$

where  $u$  is velocity and  $A$ ,  $B$  and  $C$  are related to eddy diffusion, longitudinal diffusion and mass transfer, respectively. We know that the  $B$  term decreases with increasing flow rate and the  $C$  term increases with increasing flow rate, while the  $A$  term is independent of flow rate variation. The  $C$  term is composed of three parts: a  $C_M$  term from the extraparticle effects, a  $C_{SM}$  term from stagnant mobile-phase effects and a  $C_S$  term from stationary phase mass transfer. Band broadening in SEC separation is mainly controlled by these mass transfer terms. Because the longitudinal effect ( $B$  term) is insignificant except for small molecules, a minimum HETP is not usually observed in SEC.

The resolution of two adjacent peaks, 1 and 2, is calculated from

$$R_s = \frac{2(t_{R2} - t_{R1})}{W_1 + W_2} \quad (1-8)$$

where  $t_{R1}$  and  $t_{R2}$  are the elution times of analytes 1 and 2, and  $W_1$  and  $W_2$  are the baseline peak widths.  $R_s$  is another useful measure of separation efficiency.

The observed band broadening ( $\sigma_o$ ) may originate from inside or outside of the column, which is described by

$$\sigma_o^2 = \sigma_c^2 + \sigma_e^2 \quad (1-9)$$

where  $\sigma_c$  and  $\sigma_e$  are column band broadening and extra-column band broadening, respectively. Extra-column band broadening is undesirable in SEC. It includes the contribution from the injector, detector and tubing. Through optimizing connections, minimizing injection and detection volumes, the extra-column band broadening can be reduced.

## 1.3 Capillary Electrochromatography

### 1.3.1 History

Capillary electrochromatography (CEC) was first introduced by Pretorius<sup>23</sup> in 1974. It is a hybrid separation technique which combines high performance liquid chromatography (HPLC) and capillary zone electrophoresis (CZE), and uses an electric field rather than hydraulic pressure to propel the mobile phase through a packed bed. In 1981, Jorgenson and Lukacs<sup>24</sup> showed the high efficiency of CEC with a 170  $\mu\text{m}$  i.d. packed column. Knox and Grant<sup>25,26</sup> established a theoretical study of CEC in the late 1980s. Later, CEC became a popular field for separation scientists.

CEC preserves and exploits the good aspects of both CZE and HPLC. The advantages of CEC such as high efficiency, high resolution, high selectivity, high speed and compatibility with mass spectrometry (MS) make it a powerful separation technique. The electroosmotic flow (EOF) induced plug-like profile shown in Figure 1-2 minimizes the band broadening resulting from parabolic flow in HPLC, and gives much higher separation efficiency than that afforded by HPLC. Fujimoto<sup>27</sup> summarized the efficiency of CEC and found that the efficiency can reach as high as 700,000/m. Consequently, this high efficiency enhances resolution as well as peak capacity. Since EOF is independent of the particle diameter, very small particles can be used to get better separation efficiency

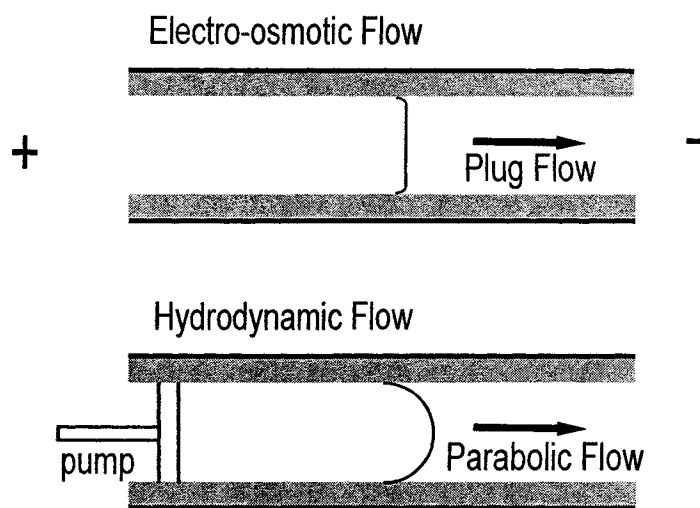


**Figure 1-2 Flow profile in CEC and HPLC.**

without the back pressure limitation existing in HPLC. Low consumption of sample and solvent makes CEC an economic and environmentally friendly method.

However, some practical difficulties hinder the wide application of CEC. Capillary packing procedures are not well standardized, leading to poor reproducibility in packing performance. CEC is not ideal for charged species because the interaction with the capillary wall and bead surfaces will change the EOF, resulting in migration time shifts. Additionally, bubbles can be generated by the applied voltage destroying the integrity of the packing bed and interrupting solvent flow. This problem can be alleviated by thorough degassing of the buffer, working at a reduced temperature (e.g. 15°C) and applying pressure at both ends of the capillary.

### 1.3.2 Fundamental Aspects

In CEC, the flow of eluent is driven by an electric field applied across the packed capillary, instead of using hydrodynamic flow provided by a pressure pump. Normally, the column includes two parts: a packed bed and an open section. The driving force, EOF, is the most important parameter in CEC. However, EOF in CEC has not been fully

studied. So far, people have developed two models for the theoretical study of EOF.

The first model is based on Overbeek's work<sup>28</sup> which is also related to von Smoluchowski's theory. EOF increases linearly with electric field. Eq. (1-10) is the well-known von Smoluchowski equation used to describe linear EOF velocity ( $u$ ).

$$u = -\frac{\varepsilon\varepsilon_0\zeta E}{\eta} \quad (1-10)$$

where  $\varepsilon$  is the dielectric constant of the medium,  $\varepsilon_0$  is the permittivity of the vacuum,  $E$  is the applied electric field,  $\eta$  is the viscosity of the bulk solution and  $\zeta$  is the zeta potential. The EOF increases with dielectric constant, surface charge on the capillary inner wall and applied voltage, while it decreases with viscosity. If the stationary phase used in CEC is porous, the definition of EOF needs to be modified. The expression for the average EOF velocity is then given by

$$u_r = u_p \left[ 1 + \left( \frac{d_p}{R} \right) \left( \frac{2}{\beta} \right) \left( \frac{\zeta_w}{\zeta_p} \right) \right] \quad (1-11)$$

where  $u_r$  is the average velocity,  $u_p$  is the electroosmotic velocity generated at the particle surface,  $d_p$  is the packing particle diameter,  $R$  is the radius of the packed capillary,  $\zeta_w$  is the zeta potential at the capillary wall,  $\zeta_p$  is the zeta potential at particle surface, and  $\beta$  is a dimensionless parameter described by following equation

$$\beta = 3\sqrt{\frac{\alpha(1-\varepsilon_c)}{2}} \quad (1-12)$$

where  $\varepsilon_c$  is the total column porosity and  $\alpha$  is another dimensionless factor related to the structure of the packing and shape of the particles. In Eq. (1-11), the contribution of wall effects were taken into consideration. Such wall effects increase with particle diameter and the zeta potential ratio between the capillary wall and the particle surface. EOF velocity that is generated locally at the particle surface can be described by

$$u_p = -\frac{\varepsilon\varepsilon_0\zeta_p E}{\eta} \left( \frac{\sigma_p}{\sigma_b} \right) \quad (1-13)$$

where  $\sigma_p$  and  $\sigma_b$  are the conductivities of the packed column and the open capillary with the same buffer solution.

Dukhin<sup>29, 30</sup> proposed the second model: electroosmosis of the second kind, which departs from the classical Smoluchowskian model. When the particles' conductivity is higher than the electrophoretic medium, an unexpectedly high EOF is produced in a very high field. The tangential and normal components of the electric field at the charged surface of the curved particle induce bulk charges, further enhancing EOF. A partial reason for such EOF enhancement is an "electroosmotic whirlwind"<sup>2</sup> around a conductive spherical particle with a polarized double layer. This "electroosmotic whirlwind" is depicted in Figure 1-3.

Eq. (1-13) still can be applied to predict the EOF velocity. However, the apparent zeta potential ( $\zeta_p^+$ ) represents a much higher zeta potential than that of the capillary wall. In this model, the wall effect is negligible. The EOF can be enhanced by an increase in both the surface conductivity of particle and the particle size. The effect is shown in Figure 1-4 and Figure 1-5.

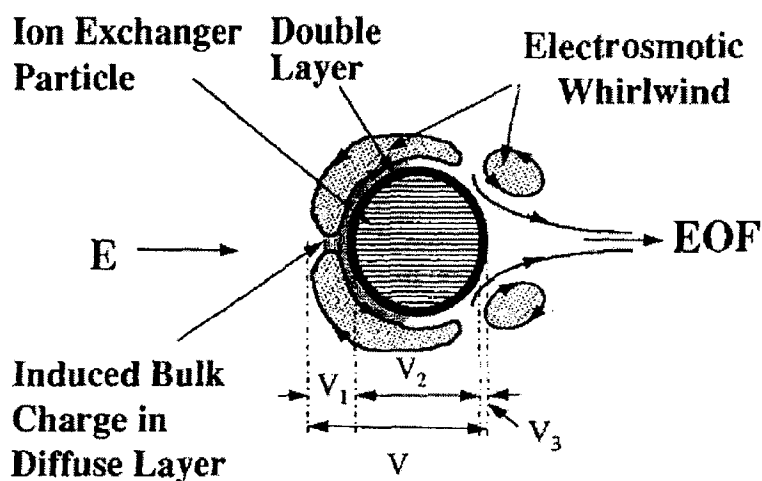


**Figure 1-3 Schematic illustration of the localization of the induced bulk charge layer and electroosmotic whirlwind around a highly conductive spherical ion exchanger particle immersed in an electrolyte solution of relatively low conductivity under the influence of high electric field. Adapted from Horváth<sup>2</sup>.**

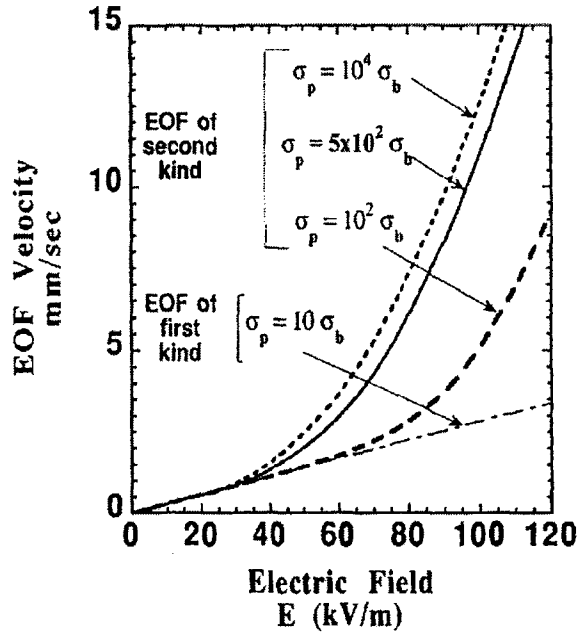


Figure 1-4 Plots of the average EOF velocity versus the electric field strength for different conductivity ratios. Conditions;  $d_p = 5 \mu\text{m}$ , pore size  $\delta = 500 \text{ \AA}$ , zeta potential  $\zeta_w = \zeta_p = 100 \text{ mV}$ ,  $\epsilon = 80$ ,  $\epsilon_0 = 8.85 \times 10^{-12} \text{ C V}^{-1} \text{ m}^{-1}$ ,  $\eta = 10^{-3} \text{ kg s}^{-1} \text{ m}^{-1}$ . Adapted from Horváth<sup>2</sup>.

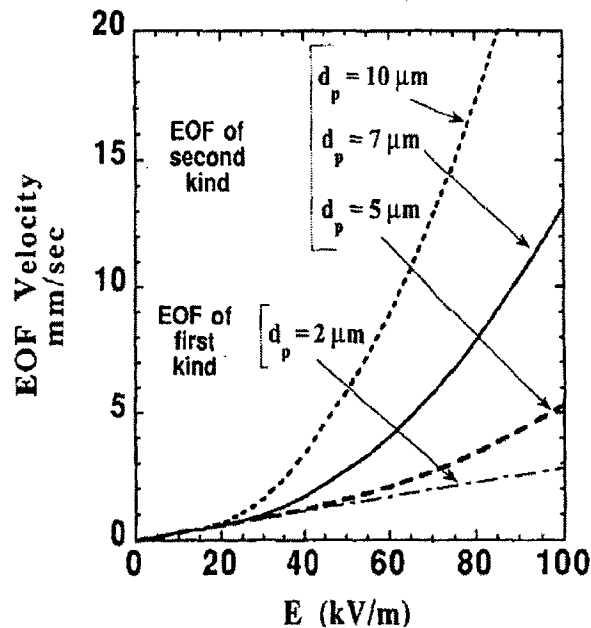


Figure 1-5 Plots of the average EOF velocity versus the electrical field strength for different particle sizes. Conditions:  $\sigma_p/\sigma_b = 5 \times 10^2$ , pore size  $\delta = 500 \text{ \AA}$ , zeta potential  $\zeta_w = \zeta_p = 100 \text{ mV}$ ,  $\epsilon = 80$ ,  $\epsilon_0 = 8.85 \times 10^{-12} \text{ CV}^{-1} \text{ m}^{-1}$ ,  $\eta = 10^{-3} \text{ kgs}^{-1} \text{ m}^{-1}$ . Adapted from Horváth<sup>2</sup>.

### 1.3.3 Application of CEC in Protein Analysis

The many applications of CEC include impurity analysis, chiral separation, assays of major components of samples and trace determinations. Researchers have demonstrated the power of CEC in separation of neutral pharmaceuticals<sup>31,32</sup>, peptides<sup>33,34</sup>, chiral compounds<sup>35,36</sup>, etc. Yet, only a scant number of papers deal with proteins in CEC. The sharp, symmetrical peaks and the possibility of further enhancing resolution by the use of counteracting EOF and electrophoretic force (EPF) makes CEC a promising technique for biopolymer separations. However, this application is limited by several factors, which include: (1) irreversible protein adsorption to the surface of capillary wall and/or packing material, (2) electrostatic interaction between charged moieties within the protein structure and charged packing. These problems can cause peak tailing which leads to poor column efficiency, and an EOF change that results in poor reproducibility.

To date, the majority of biopolymer applications of CEC are for peptides. Novotny<sup>37</sup> achieved good separation for model peptides with a capillary filled with a macroporous polyacrylamide/poly(ethylene glycol) matrix, derivatized with C<sub>12</sub> ligand (29%) and containing acrylic acid. However, proteins did not elute out of the same monolithic capillary. The authors thought the high hydrophobicity was responsible for the complete protein retention.

#### 1.3.3.1 Packed Capillary

Packed beds are most commonly used for CEC. However, only a few papers report the application of CEC to protein analysis with packed capillaries, despite a decade of research. Preliminary studies on protein separation under an electric field by Basak<sup>38</sup> was accomplished in a column (15 mm i.d.) filled with gels. To avoid Joule heating, a very low electric field was applied across the column together with a pressure flow. Later, the same group separated a binary protein mixture with a Sephadex gel column<sup>39</sup>. With the combination of pressure and voltage, Cole<sup>40</sup> purified four major whey proteins with

various size-exclusion gels. Yet, the peaks shown in these papers were broad and the separation time was long. In 2005, Sun<sup>41</sup> performed separations of three proteins within 40 min with a low-voltage electric field perpendicular to the liquid phase streamline. Horváth<sup>42</sup> investigated proteins with anion-exchanger capillary in isocratic CEC mode in which EOF was the only driving force. In this ion-exchange model, salt concentration had a strong effect on protein retention. From the above work we see that CEC of proteins required both electrical and pressure driven flow. Only for the ion-exchange based resins was pressure not required.

### 1.3.3.2 Monolithic Capillary

CEC separation on monoliths has attracted great interest because the stationary phase is easy to prepare and retaining frits are not necessary. Hjertén<sup>43</sup> successfully separated four proteins with a continuous bed derivatized with both C<sub>18</sub> and ammonium groups by using both normal-flow and counter-flow gradients. At pH = 2.0, both the proteins and the EOF-generating ligands have positive charges, therefore the electrostatic interaction is eliminated. With a similar pH (= 2.5), Horváth's group<sup>44</sup> studied peptide and protein separation with a cationic acrylic monolith and believed that the separation was determined by a dual mechanism involving selective chromatographic retention and differential electrophoretic migration. Later, the same group fabricated a positively charged stationary phase with fixed n-butyl chains and achieved faster protein separation at an elevated temperature (e.g. 55°C)<sup>45</sup>. Also, the separation efficiency reached up to 50,000 plates per column (effective length 30 cm). A polymer-based strong-cation-exchanger stationary phase was used to get baseline separation of basic proteins<sup>46</sup>. High separation efficiency (up to 65,000 plates per column (effective length 20 cm)) was obtained. With the presence of ion-exchange resin in polymerization mixture, a monolith functionalized with C<sub>4</sub> groups was cast in UV-transparent capillaries for protein separation<sup>47</sup>. Although the separation efficiency with this stationary phase was

lower than CZE, higher resolution was obtained due to the additional chromatographic separation mechanism. CEC with affinity chromatography was also applied to the separation of mannose-binding proteins<sup>48</sup>. Ion-exchange stationary phase still plays a major role in CEC with monolithic capillary.

### **1.3.3.3 Open Tubular CEC**

With open tubular CEC (OT-CEC), a stationary phase was applied on the inner surface of a capillary. A review by Lubman's group<sup>49</sup> listed some serious advantages of OT-CEC over a packed-bed CEC such as smaller plate height, high concentration sensitivity and higher speed. However, there are still some difficulties associated with sample injection and detection. With OT-CEC, six polyethylene glycol-modified proteins were separated in an etched C<sub>18</sub> modified capillary within 30 minutes<sup>50</sup>. McGown succeeded in the separation of very similar protein structures such as bovine milk proteins<sup>51</sup> as well as bovine albumin (BSA) from different species<sup>52</sup> using a G-quartet DNA stationary phase.

## **1.4 Size Exclusion Electrochromatography**

### **1.4.1 Historical Perspective and Fundamentals**

The study of size exclusion electrochromatography (SEEC) was initiated by two research groups in 1998<sup>53,54</sup>. Since then, only a few other groups have investigated this field, and published a very limited number of papers on SEEC. SEEC is an alternative separation technique of conventional pressure-driven SEC. Compared to SEC, SEEC has a faster elution time, higher separation efficiency and low consumption of mobile phase, similar to the advantages of CEC over LC.

In conventional SEC, no mobile phase flows through the pores of stationary particles. Molecules with different sizes enter a different fraction of the total pore volume, resulting in different elution times. The retention window ( $\tau$ ) in SEC describes the

retention time difference between the totally excluded molecules and the solvent molecules which are too small to be retained in the pores.  $\tau$  is affected by interstitial porosity ( $\varepsilon_o$ ) and intraparticle porosity ( $\varepsilon_i$ ):

$$\tau = \frac{\varepsilon_o}{\varepsilon_i + \varepsilon_o} \quad (1-14)$$

The retention window in SEEC is smaller than with pressure driven flow. This is due to a significant flow existing inside pores in SEEC, which decreases the flow velocity difference. The changed retention window is given by

$$\tau = \frac{\omega\varepsilon_i + \varepsilon_o}{\varepsilon_i + \varepsilon_o} \quad (1-15)$$

where  $\omega$  the ratio between the solvent velocity inside the pores and the velocity outside the pores. In SEEC, a retention window ranging from 0.6 to 1 could be achieved based on experiment results. It has also been proven experimentally that the retention window decreases as the ionic strength increases,<sup>54-56</sup> consistent with increased flow in small pores due to reduced double layer thickness.

Kok<sup>57, 58</sup> and Tijssen<sup>55</sup> studied the pore flow effects in electrically driven size exclusion chromatography and found  $\omega$  changed with pore size and ionic strength. SEEC has a more complicated separation mechanism than SEC. Schoenmakers<sup>59</sup> tried to evaluate SEC and SEEC calibration curves through modeling and found a higher prediction error in molecular weight calibration for SEEC.

#### 1.4.2 Application of SEEC

Most SEEC experiments were performed with non-aqueous mobile phase<sup>54, 56, 58, 60-64</sup>. This is because the main application of SEEC is for synthetic polymers, which are not water soluble. Krull<sup>61</sup> realized separation of polysaccharides in aqueous mobile phase using polymeric stationary phase, with an indirect detection method.

So far, silica beads,<sup>54-56, 58, 62</sup> polymer particles<sup>60, 61</sup> and monoliths<sup>53</sup> have been used

as stationary phases. High EOF decreases the retention window while low EOF increases the analysis time. Krull<sup>60</sup> mixed gel particles and polymer stationary phase with ion-exchange capacity to control the performance of SEEC and achieved good separation for synthetic neutral polymers.

Kok's group determined molecular mass distribution of several synthetic polymers<sup>63</sup> including polymethylmethacrylate, polycarbonate, polycaprolactam and poly(ethylene terephthalate) as well as cellulose<sup>62</sup> with the SEEC method. The results agreed well with those from SEC. Besides synthetic polymers, Krull<sup>61</sup> used SEEC for separation of a natural polysaccharide, pullulan, up to 112,000 g/mol with borate buffer. Although SEEC is not as precise as conventional SEC, it is a promising method because of its attractive properties.

## 1.5 Capillary Packing

In the last few years, capillary electrochromatography (CEC) and nano-liquid chromatography (nano-LC) have received increasing attention from researchers. For both methods, a capillary packed with the appropriate stationary phase is used. Colón<sup>65</sup> classified the packed structures into three categories: (1) capillaries packed with particles<sup>24, 66-70</sup>, (2) monolithic structures created through in situ polymerization<sup>71-76</sup>, (3) capillaries with entrapped particles<sup>77-80</sup>. This stationary phase immobilization method is the combination of the first two methods. Today, capillaries packed with chromatographic particulates are widely used in CEC and nano-LC.

Packing capillaries is considered an art, requiring a trial-and-error approach to get adequate experience. Yost's<sup>81</sup> statement of the difficulties of column packing for HPLC in 1980 can also be applied to capillary packing. Good column fabrication can give a reliable and reproducible column performance. Typically, fused-silica capillaries with inner diameters of 100  $\mu\text{m}$  or less are used for CEC, since the heat generated by applied electric field in CEC can be dissipated effectively in a tube with a small inner diameter.

### 1.5.1 Packing Material

For HPLC, the high back pressure caused by small particles in small columns limits the particle size of the stationary phase, while very small particles can be used to achieve high separation efficiency in CEC. However, the particle size ( $d_p$ ) used in CEC is still limited by the overlap of the electrical double layer in the flow channel. Rice and Whitehead<sup>82</sup> recommended that the ratio of the channel diameter to the double layer thickness ( $d_c/\delta$ ) should be larger than 20 to get a plug-like EOF flow profile. Assuming the flow channels are cylindrical, the minimum channel bore is 0.02-0.2  $\mu\text{m}$  to maintain plug-like flow for a typical 1-10 nm double layer. Based on the estimation of Knox and Grant<sup>25</sup> ( $d_c/d_p \sim 0.25$ ), the minimum particle size is 0.08-0.8  $\mu\text{m}$ . In addition, the packing material in CEC must have charged or ionizable groups to support EOF not only for neutral molecules but also for charged molecules. These criteria limit the types of particles that can be used. Bartle<sup>83</sup> and Sandra<sup>84</sup> reported a comprehensive list of packing materials and their applications in CEC. Currently, silica-based reverse-phase stationary phases such as Hypersil C<sub>18</sub> and Spherisorb ODS I are widely used for CEC.

### 1.5.2 Capillary Packing Technology

Research groups have already developed several different packing methods for capillary columns, such as supercritical carbon dioxide packing<sup>85-87</sup>, liquid slurry packing<sup>66,67,88</sup>, electrokinetic packing<sup>89-91</sup>, centripetal force packing<sup>92,93</sup>, gravity packing<sup>94</sup>, etc. Each is briefly discussed below. The most popular capillary packing method is liquid slurry packing.

For pressure packing using a slurry, a high pressure pump is used to deliver the bead slurry (10-100 mg/mL) into the capillary. The typical packing pressure is between 2,900 and 14,500 psi. Ultrasonication is often employed to aid the packing. Once the capillary is packed, a slow depressurization is needed so that the packing bed will not be disturbed by the backpressure generated by disconnection of the capillary from the slurry reservoir.

Bartle<sup>86</sup> applied a supercritical CO<sub>2</sub> packing method for CEC. The capillary is immersed into an ultrasonic bath with a temperature above the critical temperature of CO<sub>2</sub> (50-60°C). Beads are packed into the capillary at a constant pressure which is also above critical pressure of CO<sub>2</sub> (3000-4500 psi). As in pressure packing, slow depressurization is needed. Lee<sup>95</sup> packed particles ranging from 1 to 7 μm with this method.

With the electrokinetic packing method<sup>89-91</sup>, EOF is used to drive particles into a capillary having an end-frit. The electric field is applied until a desired length of capillary is packed. The tightness of the bed is determined by the applied voltage.

Colón<sup>92, 93</sup> introduced a packing method using centripetal force. A low viscosity slurry solvent is preferred to get higher particle velocity. Rotation of the packing system forces the particles to move outward to the fritted end. Both electrokinetic packing and centripetal force packing can be used to pack multiple capillaries simultaneously.

Colón's group<sup>65</sup> compared the performance of the above four methods. They fabricated columns with the same packing material and used all the same conditions except for the actual packing procedure. They found that the slurry pressure packing gave a column efficiency similar to that obtained by electrokinetic packing, but lower efficiency than that with centripetal force or supercritical CO<sub>2</sub> packing, despite the fact that slurry packing is a well established method, widely used by researchers.

### 1.5.3 Retaining Frit

Frit fabrication is a key part of a packed capillary. An ideal frit should have good mechanical strength and high permeability. In addition, it should not interact with the analytes. There are several procedures to make frits. First, frits can be made by sintering the chromatographic material at a temperature over 550°C. The smaller the capillary is, the more stable the frit. This is the most widely used approach, as it is simple and fast. However, several problems are associated with sintered frits. (1) To make frits, the

protective capillary coating is burnt away, resulting in a fragile column. (2) Sintered frits have poor reproducibility because the permeability of the frit is affected by its length, heating time and the heating elements. (3) The high temperature used for frit-formation can change the characteristics of the packing material, leading to non-homogeneous packing or stationary phase at the frit. This kind of non-homogeneous packing causes non-uniform EOF, which is partly responsible for bubble formation<sup>96-98</sup>. Also, the polysilicate frit generates peak tailing<sup>99</sup> due to variability in the particle surface caused by sintering.

Frits can be made by sol-gel technology<sup>100, 101</sup>. Mild temperatures ranging from 30 to 50 °C are used, so that the stationary phase remains intact and there is no damage to the capillary coating. A lengthy drying process is needed to obtain a gel network with enough mechanical strength.

In situ polymerization is another approach to fabricating a frit<sup>61, 69, 102</sup>. This method has proven to be reproducible. Pore size can be controlled by varying the composition of the polymerization mixture. Additionally, there is no heat damage to the stationary phase. If a normal fused-silica capillary is used for UV photopolymerization, the polymer coating needs to be removed at the frit position before the packing process. The brittle column is more difficult to handle and the overall process is time consuming compared to sintering. However, it is the most viable process for polymer bead-based stationary phases.

## **1.6 Scope of the Thesis**

This thesis work focuses on protein elution through a packed capillary, using either pressure or electrokinetically driven flow with nano-SEC column. A nano-LC system with laser induced native fluorescence detection (LINF) was tested and protein separation with nano-SEC was studied. Also the mechanism of protein concentration in SEEC was investigated. With pressure assisted SEEC (pSEEC), protein separation was tested. Three

SEC stationary phases with different separation range were used to pack capillary, and the packing technology was addressed in detail in the following two chapters.

Chapter 2 addresses some practical problems in the preparation of nano-SEC columns with silica beads and demonstrates the packing quality with tryptophan (W). A 266 nm laser was exploited as the excitation source to get an intrinsic fluorescence signal of W. A flow splitless mobile phase delivery nano pump and a laser induced native fluorescence (LINF) detector were used in the nano-SEC system. Limit of detection (LOD) was investigated for tryptophan (W) and  $\alpha$ -lactalbumin. In addition, the factors which affect band broadening and resolution such as flow rate, sample concentration, mobile phase and injection volume were studied.

In Chapter 3, the method used to fabricate packed capillary with polymer stationary phase was presented. Two different stationary phases were used to test protein elution in the SEEC mode. Pore size, pH and ionic strength of mobile phase and nature of protein were changed to improve protein retention. To estimate EOF in SEEC, the migration time of a neutral marker DMSO and IgG was tested. This chapter also describes the separation of three proteins with pressure assisted SEEC.

Finally, Chapter 4 briefly summarizes the achievement in preceding chapters and gives some suggestions for further study.

## 1.7 References

- (1) Yau, W. W.; Kirkland, J. J.; Bly, D. D. *Modern size-exclusion liquid chromatography : practice of gel permeation and gel filtration chromatography*, 1979.
- (2) Rathore, A. S.; Horváth, C. *J. Chromatogr. A* 1997, 781, 185-195.
- (3) Takeuchi, T.; Ishii, D. *J. Chromatogr.* 1980, 190, 150-155.
- (4) Takeuchi, T.; Ishii, D. *J. Chromatogr.* 1981, 213, 25-32.
- (5) Yang, F. J. *J. Chromatogr.* 1982, 236, 265-277.
- (6) Shelly, D. C.; Gluckman, J. C.; Novotny, M. *Anal. Chem.* 1984, 56, 2990-2992.
- (7) Kennedy, R. T.; Jorgenson, J. W. *Anal. Chem.* 1989, 61, 1128-1135.
- (8) Chervet, J. P.; Ursem, M. *Anal. Chem.* 1996, 68, 1507-1512.
- (9) Baggerman, G.; Clynen, E.; Huybrechts, J.; Verleyen, P.; Clerens, S.; De Loof, A.;

- Schoofs, L. *Peptides* 2003, 24, 1475-1485.
- (10) Sinnaeve, B. A.; Van Bocxlaer, J. F. *J. Chromatogr. A* 2004, 1058, 113-119.
  - (11) Fanali, S.; Aturki, Z.; D'Orazio, G.; Raggi, M. A.; Quaglia, M. G.; Sabbioni, C.; Rocco, A. *J. Sep. Sci.* 2005, 28, 982-986.
  - (12) Mirgorodskaya, E.; Braeuer, C.; Fucini, P.; Lehrach, H.; Gobom, J. *Proteomics* 2005, 5, 399-408.
  - (13) Wuhrer, M.; Koeleman, C. A. M.; Deelder, A. M.; Hokke, C. H. *Anal. Chem.* 2004, 76, 833-838.
  - (14) Wuhrer, M.; Koeleman, C. A. M.; Hokke, C. H.; Deelder, A. M. *Anal. Chem.* 2005, 77, 886-894.
  - (15) Winnik, W. M. *Anal. Chem.* 2005, 77, 4991-4998.
  - (16) Bedair, M.; Rassi, Z. E. *J. Chromatogr. A* 2005, 1079, 236-245.
  - (17) Fanali, S.; Camera, E.; Chankvetadze, B.; D'Orazio, G.; Quaglia, M. G. *J. Pharm. Biomed. Anal.* 2004, 35, 331-337.
  - (18) Mayer, S.; Briand, X.; Francotte, E. *J. Chromatogr. A* 2000, 875, 331-339.
  - (19) Fanali, S.; Aturki, Z.; Kašicka, V.; Raggi, M. A.; D'Orazio, G. *J. Sep. Sci.* 2005, 28, 1719-1728.
  - (20) Varesio, E.; Rudaz, S.; Krause, K.; Veuthey, J. *J. Chromatogr. A* 2002, 974, 135-142.
  - (21) Alpert, C.; Engst, W.; Guehler, A.; Oelschlaeger, T.; Blaut, M. *J. Chromatogr. A* 2005, 1082, 25-32.
  - (22) Preisler, J.; Foret, F.; Karger, B. L. *Anal. Chem.* 1998, 70, 5278-5287.
  - (23) Pretorius, V.; Hopkins, B. J.; Schieke, J. D. *J. Chromatogr.* 1974, 99, 23-30.
  - (24) Jorgenson, J. W.; Luckas, K. D. *J. Chromatogr.* 1981, 218, 209-216.
  - (25) Knox, J. H.; Grant, I. H. *Chromatographia* 1987, 24, 135-143.
  - (26) Knox, J. H.; Grant, I. H. *Chromatographia* 1988, 26, 329-337.
  - (27) Fujimoto, C. *Trends anal. chem.* 1999, 18, 291-301.
  - (28) Overbeek, J. T. G.; Wijga, P. W. O. *Rec. Trav. Chim.* 1946, 65, 556-563.
  - (29) Dukhin, S. S. *Adv. Colloid Interface Sci.* 1991, 35, 173-196.
  - (30) Dukhin, S. S.; Mishchuk, N. A. *J. Membr. Sci.* 1993, 79, 199-210.
  - (31) Fu, H.; Jin, W.; Xiao, H.; C.; X.; Guo, B.; Zou, H. *Electrophoresis* 2004, 25, 600-606.
  - (32) Orlandini, S.; Furlanetto, S.; Pinzauti, S.; D'Orazio, G.; Fanali, S. *J. Chromatogr. A* 2004, 1044, 295-303.
  - (33) Liang, Z.; Duan, J.; Zhang, L.; Zhang, W.; Zhang, Y.; Yan, C. *Anal. Chem.* 2004, 76, 6935-6940.
  - (34) Szucs, V.; Freitag, R. *J. Chromatogr. A* 2004, 1044, 201-210.
  - (35) Hebenstreit, D.; Bicker, W.; Lämmerhofer, M.; Lindner, W. *Electrophoresis* 2004, 25, 277-289.
  - (36) Mangelings, D.; Tanret, I.; Matthijs, N.; Maftouh, M.; Massart, L. D.; Heyden, Y. V. *Electrophoresis* 2005, 26, 818-832.

- (37) Palm, A.; Novotny, M. V. *Anal. Chem.* 1997, *69*, 4499-4507.
- (38) Rudge, S. R.; Basak, S. K.; Ladisch, M. R. *AIChE Journal* 1993, *39*, 797-808.
- (39) Basak, S. K.; Velayudhan, A.; Kohlmann, K.; Ladisch, M. R. *J. Chromatogr. A* 1995, *707*, 69-76.
- (40) Tellez, C. M.; Cole, K. D. *Electrophoresis* 2000, *21*, 1001-1009.
- (41) Tan, G.; Shi, Q.; Sun, Y. *Electrophoresis* 2005, *26*, 3084-3093.
- (42) Zhang, J.; Huang, X.; Zhang, S.; Horváth, C. *Anal. Chem.* 2000, *72*, 3022-3029.
- (43) Ericson, C.; Hjertén, S. *Anal. Chem.* 1999, *71*, 1621-1627.
- (44) Zhang, S.; Huang, X.; Zhang, J.; Horváth, C. *J. Chromatogr. A* 2000, *887*, 465-477.
- (45) Zhang, S.; Zhang, J.; Horváth, C. *J. Chromatogr. A* 2001, *914*, 189-200.
- (46) Zhang, S.; Zhang, J.; Horváth, C. *J. Chromatogr. A* 2002, *965*, 83-92.
- (47) Bandilla, D.; Skinner, C. D. *J. Chromatogr. A* 2003, *1004*, 167-179.
- (48) Bedair, M.; Rassi, Z. E. *J. Chromatogr. A* 2004, *1044*, 177-186.
- (49) Wu, J.; Qian, M. G.; Li, M. X.; Zheng, K.; Huang, P.; Lubman, D. M. *J. Chromatogr. A* 1998, *794*, 377-389.
- (50) Pesek, J. J.; Matyska, M. T.; Krishnamoorthi, V. *J. Chromatogr. A* 2004, *1044*, 317-322.
- (51) Rehder-Silinski, M. A.; McGown, L. B. *J. Chromatogr. A* 2003, *1008*, 233-245.
- (52) Dick Jr., L. W.; Swintek, B. J.; McGown, L. B. *Anal. chim. acta* 2004, *519*, 197-205.
- (53) Peters, E. C.; Petro, M.; Svec, F.; Fréchet, J. M. J. *Anal. Chem.* 1998, *70*, 2296-2302.
- (54) Venema, E.; Kraak, J. C.; Tijssen, R.; Poppe, H. *Chromatographia* 1998, *48*, 347-354.
- (55) Venema, E.; Kraak, J. C.; Poppe, H.; Tijssen, R. *J. Chromatogr. A* 1999, *837*, 3-15.
- (56) Stol, R.; Poppe, H.; Kok, W. T. *Anal. Chem.* 2003, *75*, 5246-5253.
- (57) Stol, R.; Poppe, H.; Kok, W. T. *J. Chromatogr. A* 2000, *887*, 199-208.
- (58) Stol, R.; Kok, W. T.; Poppe, H. *J. Chromatogr. A* 2001, *914*, 201-209.
- (59) Heyden, Y. V.; Popovici, S. T.; Schoenmakers, P. J. *J. Chromatogr. A* 2002, *957*, 127-137.
- (60) Mistry, K.; Cortes, H.; Meunier, D.; Schmidt, C.; Feibush, B.; Grinberg, N.; Krull, I. *Anal. Chem.* 2002, *74*, 617-625.
- (61) Mistry, K.; Krull, I.; Grinberg, N. *Electrophoresis* 2003, *24*, 1753-1763.
- (62) Stol, R.; Pedersoli Jr, J. L.; Poppe, H.; Kok, W. T. *Anal. Chem.* 2002, *74*, 2314-2320.
- (63) Ding, F.; Stol, R.; Kok, W. T.; Poppe, H. *J. Chromatogr. A* 2001, *924*, 239-249.
- (64) Oudhoff, K. A.; Macka, M.; Haddad, P. R.; Schoenmakers, P. J.; Kok, W. T. *J. Chromatogr. A* 2005, *1068*, 183-187.
- (65) Colón, L. A.; Maloney, T. D.; Fermier, A. M. *J. Chromatogr. A* 2000, *887*, 43-53.

- (66) Smith, N. W.; Evans, M. B. *Chromatographia* 1994, 38, 649-657.
- (67) Boughtflower, R. J.; Underwood, T.; Paterson, C. J. *Chromatographia* 1995, 40, 329-335.
- (68) Boughtflower, R. J.; Underwood, T.; Maddin, J. *Chromatographia* 1995, 41, 398-401.
- (69) Chen, Y.; Gerhardt, G.; Cassidy, R. *Anal. Chem.* 2000, 72, 610-615.
- (70) Kawamura, K.; Otsuka, K.; Terabe, S. *J. Chromatogr. A* 2001, 924, 251-257.
- (71) Fujimoto, C. *Anal. Chem.* 1995, 67, 2050-2053.
- (72) Liao, J. L.; Chen, N.; Ericson, C.; Hjertén, S. *Anal. Chem.* 1996, 68, 3468-3472.
- (73) Fields, S. *Anal. Chem.* 1996, 68, 2709-2712.
- (74) Peters, E. C.; Petro, M.; Svec, F.; Fréchet, J. M. J. *Anal. Chem.* 1997, 69, 3646-3649.
- (75) Ericson, C.; Liao, J.; Nakazato, K.; Hjertén, S. *J. Chromatogr. A* 1997, 767, 33-41.
- (76) Preinerstorfer, B.; Lindner, W.; Lämmerhofer, M. *Electrophoresis* 2005, 26, 2005-2018.
- (77) Asiaie, R.; Huang, X.; Farnan, D.; Horváth, C. *J. Chromatogr. A* 1998, 806, 251-263.
- (78) Dulay, M. T.; Kulkarni, R. P.; Zare, R. N. *Anal. Chem.* 1998, 70, 5103-5107.
- (79) Chirica, G. S.; Remcho, V. T. *Electrophoresis* 1999, 20, 50-56.
- (80) Chirica, G. S.; Remcho, V. T. *Anal. Chem.* 2000, 72, 3605-3610.
- (81) Yost, R. W.; Ettre, L. S.; Conlon, R. D. *Practical Liquid Chromatography: An Introduction*; Perkin-Elmer Corporation, 1980.
- (82) Rice, C. L.; Whitehead, R. *J. Phys. Chem.* 1965, 69, 4017-4023.
- (83) Robson, M. M.; Cikalo, M. G.; Myers, P.; Euerby, M. R. *J. Microcol. Sep.* 1997, 9, 357-372.
- (84) Dermaux, A.; Sandra, P. *Electrophoresis* 1999, 20, 3027-3065.
- (85) Malik, W.; Li, D.; Lee, M. L. *J. Microcol. Sep.* 1993, 5, 361-369.
- (86) Robson, M. M.; Roulin, S.; Shariff, S. M.; Raynor, M. W.; Bartle, K. D.; Clifford, A. A.; Myers, P.; Euerby, M. R.; Johnson, C. M. *Chromatographia* 1996, 43, 313-321.
- (87) Healy, L. O.; Owens, V. P.; O'Mahony, T.; Srijaranai, S.; Holmes, J. D.; Glennon, J. D.; Fischer, G.; Albert, K. *Anal. Chem.* 2003, 75, 5860-5869.
- (88) Lynen, F.; Buica, A.; de Villiers, A.; Crouch, A.; Sandra, P. *J. Sep. Sci.* 2005, 28, 1539-1549.
- (89) Inagaki, M.; Kitagawa, S.; Tsuda, T. *Chromatography* 1993, 14, 55R-60R.
- (90) Yan, C.: US, 1995.
- (91) Stol, R.; Mazereeuw, M.; Tjaden, U. R.; van der Greef, J. *J. Chromatogr. A* 2000, 873, 293-298.
- (92) Fermier, A. M.; Colón, L. A. *J. Microcol. Sep.* 1998, 10, 439-447.
- (93) Maloney, T. D.; Colón, L. A. *Electrophoresis* 1999, 20, 2360-2365.
- (94) Reynolds, K. J.; Maloney, T. D.; Fermier, A. M.; Colón, L. A. *Analyst* 1998, 123,

1493-1495.

- (95) Tang, Q.; Lee, M. L. *Trends anal. chem.* 2000, 19, 648-663.
- (96) Rebscher, H.; Pyell, U. *J. Chromatogr. A* 1996, 737, 171-180.
- (97) Poppe, H. *J. Chromatogr. A* 1997, 778, 3-21.
- (98) Rathore, A. S.; Horváth, C. *Anal. Chem.* 1998, 70, 3069-3077.
- (99) Behnke, B.; Jonansson, J.; Zhang, S.; Bayer, E.; Nilsson, S. *J. Chromatogr. A* 1998, 818, 257-259.
- (100) Schmid, M.; Bauml, F.; Kohne, A. P.; Welsch, T. *J. High Resol. Chromatogr.* 1999, 22, 438-442.
- (101) Zhang, X.; Huang, S. *J. Chromatogr. A* 2001, 910, 13-18.
- (102) Chen, J.; Dulay, M. T.; Zare, R. N. *Anal. Chem.* 2000, 72, 1224-1227.

## Chapter 2: Nano-Liquid Chromatography

### 2.1 Introduction

The growing interest in analyzing minute samples in various fields stimulates rapid development of microseparation techniques. Compared to conventional HPLC, nano-LC has several advantages: high separation efficiency, high sensitivity, fast analysis time and low consumption of sample and mobile phase. People have already applied nano-LC to many analytes, including peptide, pharmaceuticals, chiral compounds and others. To get the very slow flow rate required for nano-LC, either a flow splitter or some commercially available pump with a built in flow splitting system is used. Using a flow splitter without a feedback system, the splitting ratio changes with increasing column resistance or viscosity change during gradient mode operation, which is a drawback to the use of flow splitters.

In this work, a split-less flow nano-LC system was developed. A nano pump provides a very slow and stable flow rate. Unlike some other commercial nano pumps with a built in flow splitting system, this split-less flow liquid delivery system minimizes consumption of sample and mobile phase. A capillary (50  $\mu\text{m}$  i.d., 365  $\mu\text{m}$  o.d.) packed with BioSep-S2000, 5  $\mu\text{m}$  particles, was used as the SEC column. The method used for fabrication of a packed capillary was addressed. Since proteins fluoresce in the UV under ambient conditions, laser induced native fluorescence was employed to detect proteins, thus avoiding the time-consuming and problematic labeling step. Here, a preliminary study of split-less flow nano-SEC is presented. The performance of the nano-LC system was evaluated with tryptophan (W), and the limit of detection (LOD) was estimated for both W and  $\alpha$ -lactalbumin. A binary protein mixture ( $\alpha$ -lactalbumin and BSA) was baseline resolved. The effect of flow rate, injection volume and mobile phase on resolution was investigated. Additionally, the band broadening in this nano-SEC system was studied. To demonstrate the performance of the nano-LC system, a commercial reverse phase capillary was employed to analyze digested protein.

## 2.2 Experimental

### 2.2.1 Reagent and Chemicals

Doubly distilled water (Millipore Canada) was degassed with He and used to prepare all solutions.  $\alpha$ -lactalbumin from bovine milk, albumin from bovine (BSA), albumin from chicken egg (ovalbumin), immunoglobulin G from rabbit serum (IgG),  $\alpha_1$ -mating factor fragment, luteinizing hormone releasing hormone,  $\alpha_1$ -mating factor, HPLC grade acetonitrile (ACN), tetrahydrofuran (THF), trifluoroacetic acid (TFA), DL-dithiothreitol (DTT), iodoacetamide (IAA), silicon tetrachloride, ammonium bicarbonate, acrylamide, potassium persulfate, 3-(trimethoxysilyl)propyl acrylate, N,N,N',N'-tetramethylethylenediamine (TEMED), Tween 20, polyethylene glycol 8000 (PEG 8000) and 2 $\times$ SDS buffer were purchased from Sigma (USA). Tryptophan and polyethylene glycol 300 (PEG 300) were obtained from Fluka, sodium dihydrogen orthophosphate, NaOH and acetic acid from BDH Inc., sodium chloride from Merck (Germany), sodium dodecyl sulfate (SDS) from Bio-Rad and immobilized TPCK trypsin from Pierce. 5  $\mu$ m BioSep-S2000 beads were bought from Phenomenex (USA). A 75  $\mu$ m i.d. capillary with 5  $\mu$ m C<sub>18</sub> beads (20 cm packed, 30 cm total) was obtained from Unimicro (USA).

Protein stock solutions (20 mg/ml) were prepared in water filtered through a Nylon syringe filter (0.2  $\mu$ m pore size, Chromatographic Specialities Inc.). A 50 mM phosphate buffer (pH = 6.7) with or without additives was used as mobile phase. The pH of the buffer was adjusted by titration with 1 M NaOH to the required value. Buffer solutions were filtered and degassed prior to use. Bead stock solution was made by suspending 50 mg of beads in 20 mM NaH<sub>2</sub>PO<sub>4</sub> containing 10% methanol, then diluting to the desired concentration with water.

### 2.2.2 Preparation of Packed Capillary

A schematic of the packing equipment, which consisted of an HPLC pump, an

ultrasonic bath, a slurry reservoir, a capillary and temporary frit is shown in Figure 2-1. The 10 mg/ml stationary phase (5  $\mu\text{m}$  BioSep-S2000) was slurried in  $\text{H}_2\text{O}$ . Silica beads are usually heated to make frits that hold the beads. To achieve good packing, the packing solvent was degassed before use. The packed capillary (365  $\mu\text{m}$  o.d., 50  $\mu\text{m}$  i.d.) preparation procedure is as follows:

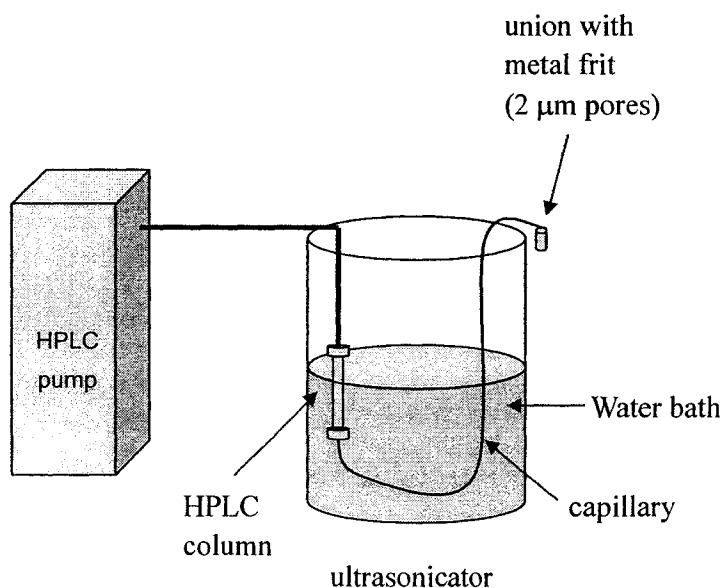


**Figure 2-1 Cartoon of packing system.**

1. Bead slurry (10 mg/ml) is vortexed for 5 min.
2. 200  $\mu\text{L}$  of the slurry is transferred to a stainless steel reservoir (7.5 cm in length, 4.6 mm i.d.).
3. The inlet of the reservoir is connected to a Waters 590 programmable HPLC pump while the outlet is connected to the inlet of a capillary. A union containing a metal screen with 2  $\mu\text{m}$  pores is used as a temporary frit at the outlet of the capillary.
4. Both the reservoir and the capillary are put into an ultrasonicator (Branson 1200, Branson Cleaning Equipment Company, USA) to prevent bead sedimentation.

H<sub>2</sub>O is used to flush the beads into the capillary at ~3,000 psi. The pump is stopped and the system depressurizes by itself for several hours, and column pressure is released when pressure is ~1,500 psi.

5. After packing, a retaining (inlet) frit is formed by threading the capillary through a hole in a Nichrome wire. Heat is applied to form the frit with H<sub>2</sub>O flushing through the column.
6. The temporary frit is removed and then the extra beads are washed out with pressure.
7. The second (outlet) frit is made as described in step 5.
8. The capillary is flushed with H<sub>2</sub>O in the reverse direction. Extra beads outside of the outlet frit are washed away.

A detection window is made near the outlet frit with a capillary burner (home built).

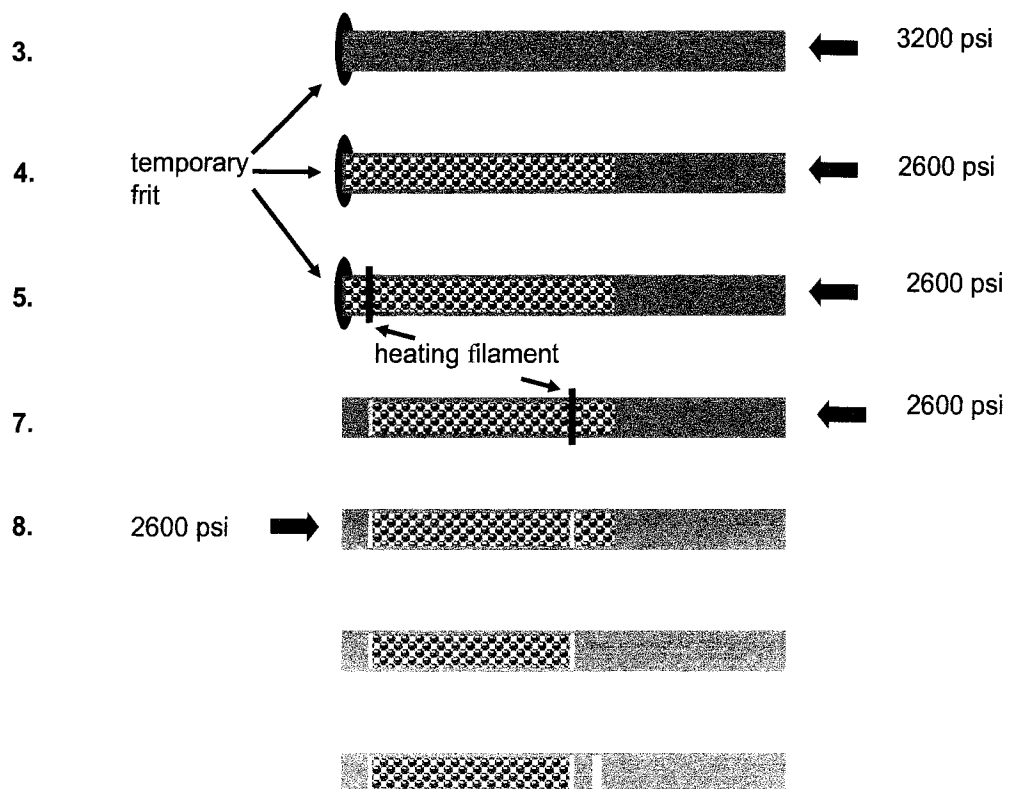


**Figure 2-2 Scheme of capillary packing.**

### 2.2.3 Instrumentation and Apparatus

A Waters 590 programmable HPLC pump (USA) was used to pack capillaries (365  $\mu\text{m}$  o.d., 50  $\mu\text{m}$  i.d.) purchased from Polymicro Technologies (USA). The capillaries were usually cut to 35 cm. Unions, fittings and a Scivex<sup>TM</sup> confluent<sup>TM</sup> nano fluidic module were obtained from Upchurch Scientific (USA). The nano pump, which can provide flow rates of 20 nL/min to 300  $\mu\text{L}/\text{min}$ , was used to pump the nano-LC system without the need for a flow splitter. A 266 nm pulsed UV laser (pulse width < 600 psec., repetition rate = 6-10 kHz, power = 2 mW) obtained from JDS Uniphase was used as an excitation light source. The syringe (5  $\mu\text{L}$ , 22 gauge) used for sample injection was from Valco Instruments Co. Inc. (Houston, TX, USA).

The diagram in Figure 2-3 illustrates the optical setup for fluorescence detection. This setup is developed from Ocvirk's design<sup>2</sup>, as modified by Misir<sup>1</sup>. Several steering mirrors (5108-A-UV, New Focus) on an optical table (Newport) directed the 266 nm UV laser beam into the microscope. A dichroic mirror (XF 2000, diameter = 25.4 mm, Omega Optical, Brattleboro, VT) reflected UV laser light toward a 13 $\times$  UV microscope objective (U-13X, NA = 0.13, clear aperture = 3.00 mm, focal length = 11.53 mm, working distance = 6.82 mm, Newport, USA). After passing through the objective, the excitation light was focused into the capillary. The fluorescence emission was collected by the same objective. The emitted light passed the dichroic mirror and was focused with a tube lens (Newport, SPX028AR.10, diameter = 25.4 mm, focal length = 200 mm) onto a pinhole (600  $\mu\text{m}$ , Melles Griot, CA, USA) located at the focal point. A photomultiplier tube (PMT) (RF 1477, bias 600 V, Hamamatsu, Tokyo, Japan) with an XF 3000 band pass filter (band pass = 100 nm, ~76% T, 290-380 nm, Omega Optical, Brattleboro, VT) was connected to the microscope tube to collect photons after spectral filtering. The analog signal was amplified by a trans-impedance amplifier (home built) and filtered with a 25 Hz low pass Bessel noise filter, corresponding to a time constant of 0.04 s. Most peaks were at least 2-3 s wide. Labview software installed in a Compaq PC was used for data

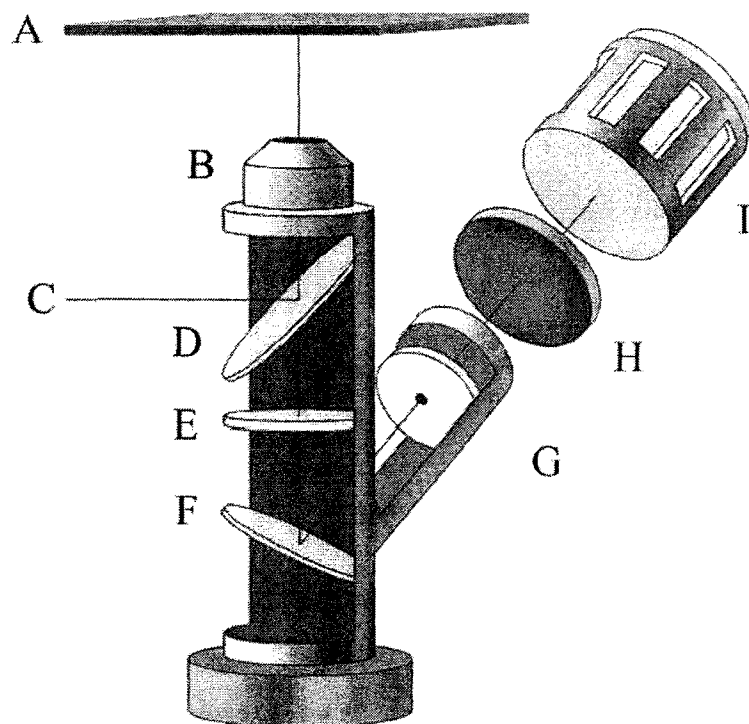


**Figure 2-3 Confocal epifluorescent setup. A, chip; B, UV objective; C, 266 Nd:YAG laser beam; D, dichroic mirror; E, tube lens; F, quartz mirror; G, pinhole, 600  $\mu\text{m}$ ; H, bandpass filter; I, PMT. Cartoon adapted from Misir<sup>1</sup>**

acquisition. All data were collected at a rate of 500 Hz which gave a data write rate of 5 Hz after averaging 100 points to one data point recorded.

Figure 2-4 shows the setup for the nano-LC. Two grooves were etched on the surface of the plexiglass holder, whose position was adjusted by xyz translation stages (Newport, #423). After mounting in the V-shaped grooves, the capillary was fixed with screws. With a nanovolume<sup>TM</sup> internal sample injector (Cheminert, Valco Instruments Co. Inc., Houston, TX, USA), 4 nL of analyte was injected into the column. Because the confluent nanofluidic module can provide very slow and stable flow, no flow splitter is needed in this system. At the end of each working day, the packed capillary was flushed

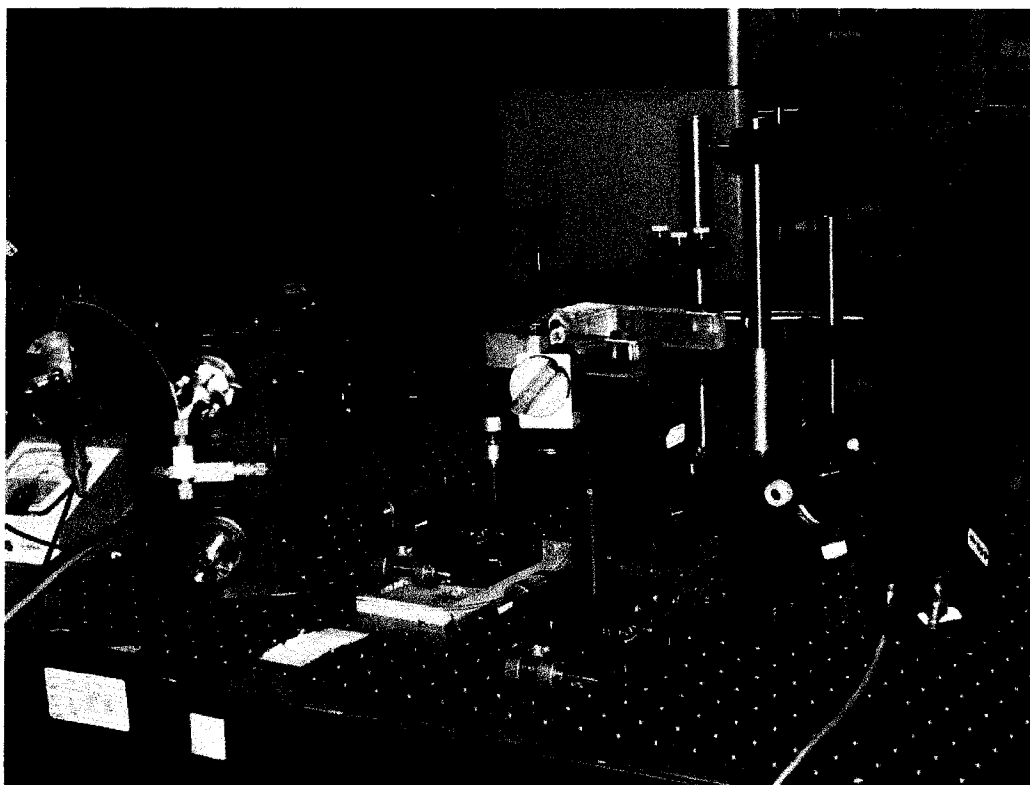


**Figure 2-4 Pictorial representation of the instrumental setup of nano-SEC. (a) solvent reservoir, (b) Upchurch nano pump, (c) Cheminert nanovolume injector, (d) packed capillary, (e) confocal epiluminescent microscope, (f) PMT.**

with H<sub>2</sub>O extensively and sealed by parafilm to prevent column drying.

#### **2.2.4 Protein Digestion**

A mix of 100  $\mu$ L 5 mg/ml  $\alpha$ -lactalbumin, 110  $\mu$ L 200 mM NH<sub>4</sub>HCO<sub>3</sub> and 20  $\mu$ L 90 mM DL-dithiothreitol (DTT) in an amber vial was incubated at 37°C for 1 hour. The solution then stood for 1 hour at room temperature in darkness, after mixing with 20  $\mu$ L of 200 mM iodoacetamide (IAA), followed by addition of 100  $\mu$ L 0.1 M NH<sub>4</sub>HCO<sub>3</sub> buffer with immobilized TPCK trypsin to the protein solution and 16-hour incubation in a shaker at 37°C. The gel with immobilized trypsin is separated from the digestion mixture by centrifugation. The digestion mixture is stored at 4°C for use.

## 2.2.5 Capillary Coating

### 2.2.5.1 PEG Coating

This method is modified from a procedure used to improve polyvinylchloride (PVC) membrane adhesion to an electrode surface<sup>3,4</sup>. The capillary was washed by 0.1M NaOH, H<sub>2</sub>O and THF for 30 minutes, respectively. Then the polymer solution (3 ml THF, 0.075 g PEG 300, 0.25% SiCl<sub>4</sub>) was transferred into the capillary. The amount of SiCl<sub>4</sub> is reported as wt.% (in the form of SiCl<sub>4</sub>) of the total amount of polymer solution. Both ends of the capillary were sealed by parafilm and left overnight. Finally, the excess polymer solution was washed out with THF. After flushing with H<sub>2</sub>O, the capillary was ready for use.

### 2.2.5.2 Polyacrylamide Coating

In the method introduced by Hjertén<sup>5</sup> to eliminate electroosmotic flow (EOF) and solute adsorption in capillary electrophoresis (CE), a bifunctional compound is used not only to react with the capillary wall but also to take part in a polymerization process. The bifunctional compound used here is 3-(trimethoxysilyl)propyl acrylate. The methoxy group reacts with the silanol groups in the capillary wall, while the acryl group reacts with acryl monomers to form a polymer.

The capillary was first treated with 0.1 M NaOH for 30 minutes, then rinsed with H<sub>2</sub>O and filled with a silane solution, which was a mixture of 80  $\mu$ L 3-(trimethoxysilyl)propyl acrylate and 20 mL of H<sub>2</sub>O (pH adjusted to 3.5 by acetic acid). After 1 hr reaction at room temperature, the capillary was flushed extensively with H<sub>2</sub>O, then 3% acrylamide solution containing the appropriate amount of catalyst (1  $\mu$ L TEMED and 1 mg potassium persulfate per ml solution) was pulled through the capillary and allowed to stand for 30 minutes. Excess (non-covalently attached) polyacrylamide was washed away with H<sub>2</sub>O. The capillary was dried with N<sub>2</sub> and the residual water was eliminated by placing the capillary in an oven at 35°C.

## 2.3 Results and Discussion

### 2.3.1 Preparation of Packed Capillary

#### 2.3.1.1 Capillary Packing

Biosep-SEC-S columns are good size-exclusion chromatographic columns for peptides and proteins. The spherical, silica-based, packing particles (5  $\mu\text{m}$ ) are bonded with a hydrophilic coating, which has limited non-specific interaction with proteins. These stationary phases showed good performance for native proteins and superior stability to protein denaturants and organic modifiers<sup>6</sup>. In this study, only Biosep-SEC-S2000 was tested. The detailed technical data are given in Table 2-1.

Material	Hydrophilic bonded silica
Particle size ( $\mu\text{m}$ )	5
Pore size ( $\text{\AA}$ )	145
Exclusion range in Daltons for proteins:	
native	1,000 – 300,000
0.5% SDS	200 – 75,000
6M Guanidine HCl (GnHCl)	500 – 100,000
pH range	2.5 – 7.5

**Table 2-1 Technical information of Biosep-SEC-S2000.**

Under high pressure, SEC beads were packed into a capillary at very high speed. Usually, it took only a couple of minutes to get the desired packing length. However, the overall column fabrication is a time consuming process, because depressurizing after packing takes several hours. All parts used for the process must be kept clean to avoid leaking or blocking in the packing system.

#### 2.3.1.2 Frit Fabrication

Frit fabrication is a key part of a packed column. A frit should be mechanically

stable enough to hold stationary phase. It also needs to be porous enough for good mobile phase flow through the bed. If the frits are made by sintering the chromatographic beads, the performance of the frits depends on the heating element and heating time. For the chosen heating element, the heating time should be optimized through a trial-and-error process.

Images of cross sections of packed capillaries are shown in Figure 2-5. Figure 2-5 (A) shows beads tightly packed in a 50  $\mu\text{m}$  i.d. capillary. The device used to make the frit is a home-built capillary burner with a Nichrome ribbon, in which a 500- $\mu\text{m}$  hole is drilled. The thickness of the Nichrome ribbon is about 300  $\mu\text{m}$ , so that the resulting frit is 1-2 mm long. The temperature for frit formation can be adjusted by the voltage across the ribbon:  $\sim 600^\circ\text{C}$  (determined by thermocouple) was used to make frits in this study. A frit prepared by sintering of coated spherical silica beads is depicted in Figure 2-5 (B). Silica beads are bonded together at their contact points. The heat needed for frit-forming burns off the polyimide protective layer of the capillary, making these parts of the column easy to break. Care must be taken during packed capillary handling. It is necessary to have  $\text{H}_2\text{O}$  flushing inside the capillary while forming frit. The heat from the Nichrome ribbon

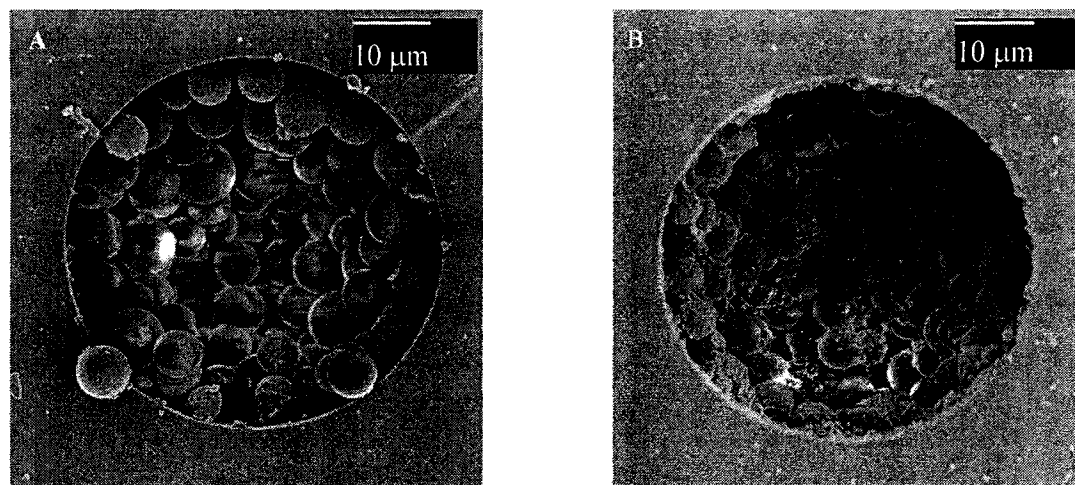


**Figure 2-5 Scanning electron micrographs of (A) embedded BioSep-SEC-S2000 beads, (B) sintered frit with embedded beads.**

can burn away beads if there is no H<sub>2</sub>O flow flush. If this happens voids will be formed. If 10 mM NaH<sub>2</sub>PO<sub>4</sub> is flushed during the frit-forming process the heating time needed decreased from 18 s to 3 or 4 s. It is found that in the presence of sodium, polysilicate can be formed by heating the silica to 550°C<sup>7</sup>. Sodium in the packing solvent speeds up fabrication of the frit to some degree. However, it is difficult to accurately control the heating time with a timer. Usually, a 1s time difference can cause a big change in frit performance. The resulting frit can collapse easily or can have poor permeability. With manual operation, there is difficulty getting reproducible frits with NaH<sub>2</sub>PO<sub>4</sub>. Therefore, H<sub>2</sub>O is preferred for frit-forming.

## 2.3.2 Detection of Tryptophan

### 2.3.2.1 Column Packing Performance

Figure 2-6 shows a typical chromatogram of 50 μM tryptophan (W). The 12.2 cm column showed good separation efficiency ( $N = 9.9 \times 10^4$  plates/m). The number of theoretical plates,  $N$ , is given by Eq. (1-4).

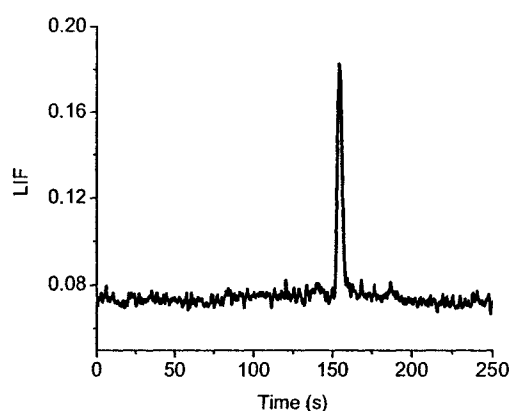


**Figure 2-6 Chromatogram of 50 μM tryptophan. mobile phase: 50 mM NaH<sub>2</sub>PO<sub>4</sub> (pH = 6.7), packing length: 12.2 cm, flow rate: 100 nL/min.**

Reduced plate height ( $h$ ) is calculated by

$$h = H / d_p \quad (2-1)$$

where  $H$  is height equivalent to a theoretical plate, and  $d_p$  is particle diameter. Usually,  $h$  is used to judge if a conventional SEC column is good or not. A “good” column has an  $h$  of  $\sim 2.0$ - $3.5$  for a totally permeating monomer such as toluene<sup>8</sup>. For Figure 2-6, the reduced plate height of 1.96 for tryptophan, which is totally retained by the SEC beads, is smaller than 3, which indicates the column is well packed.

Figure 2-7 presents a van Deemter plot for the nano-SEC column tested with W. From the van Deemter equation, the height equivalent to a theoretical plate (HETP) is given by

$$H = A + B/u + Cu \quad (2-2)$$

where  $u$  is velocity and  $A$ ,  $B$  and  $C$  are related to eddy diffusion, longitudinal diffusion and mass transfer, respectively. Because the longitudinal effect ( $B$  term) is insignificant except for small molecules, a minimum HETP is not usually observed in SEC. Table 2-2 illustrates quite good reproducibility in elution time, peak area and peak height for five consecutive runs of  $10 \mu\text{M}$  W.

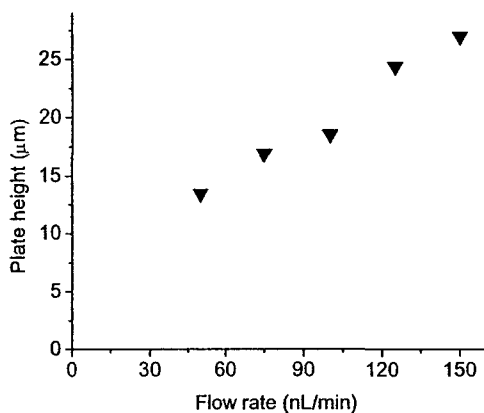


**Figure 2-7** A van Deemter plot for  $100 \mu\text{M}$  W. mobile phase:  $50 \text{ mM NaH}_2\text{PO}_4$  ( $\text{pH} = 6.7$ ), packing length:  $12.2 \text{ cm}$ , flow rate:  $100 \text{ nL/min}$ .

Run #	Elution time (s)	Peak area	Peak height
1	156.9	0.28	0.047
2	156.4	0.23	0.045
3	156.7	0.24	0.046
4	156.7	0.27	0.050
5	155.9	0.27	0.050
mean	156.5	0.26	0.048
RSD(%)	0.25	7.9	4.2

**Table 2-2 Elution time, peak area and peak height for 5 consecutive runs. Sample: 10  $\mu$ M W, mobile phase: 50 mM  $\text{NaH}_2\text{PO}_4$  (pH = 6.7), packing length: 12.2 cm, flow rate: 100 nL/min.**

Although the separation efficiency of tryptophan ( $N = 9.9 \times 10^4$  plates/m) in this work is lower than that of CE, it is comparable to other nano-LC systems. In CE, theoretical plate counts ( $N$ ) of several million can be obtained for biomolecules such as proteins and nucleotides because of slow diffusion.  $N$  is smaller for small molecules. With a “ball lens” UV-pulsed laser-induced fluorescence detector, Couderc analyzed tryptophan and tyrosine in cerebrospinal fluid in CE<sup>9</sup>, where the plate number for W was  $6.1 \times 10^5$  plates/m in a 60 cm (53 cm effective length)  $\times$  75  $\mu$ m i.d. capillary. People using a packed capillary in CEC or LC also achieved good results. With native fluorescence detection Jorgenson<sup>10</sup> achieved good separation efficiency of  $6.7 \times 10^4$  plates/m for BSA using a 50  $\mu$ m i.d. SEC column. Other than the SEC column used in this work, many researchers tested capillaries packed with a reverse phase. Welsh reported  $7.4 \times 10^4$  plates/m for small molecules by CEC with a 5  $\mu$ m  $\text{C}_{18}$  bead packed capillary (75  $\mu$ m i.d.) having a 15-cm long packing bed<sup>11</sup>. Cassidy found a better  $N$  of  $1.36 \times 10^5$  plates/m for benzyl alcohol with 5  $\mu$ m ODS2 packed capillary (75  $\mu$ m i.d., 32-cm packing length) in CEC<sup>12</sup>. For LC, the plate number is smaller than that in CE. Ursem evaluated separation

efficiency for fluorene and fluoranthene with isocratic reverse phase (5  $\mu\text{m}$  C<sub>18</sub>) liquid chromatography (75  $\mu\text{m}$  i.d.  $\times$  30 cm).<sup>13</sup> Within a flow rate range of 25-600 nL/min, the plate number changes from  $4.2 \times 10^4$  to  $1.0 \times 10^5$  plates/m. The separation efficiency of tryptophan in a nano-SEC column in this work is comparable to the values shown above, implying good performance of the nano-SEC system.

### 2.3.2.2 Band Broadening

Band broadening includes two sources: chromatographic dispersion due to the column itself and extra-column dispersion. The latter results from connections, injection volume, detection volume, etc. The total volume variance  $\sigma_{V,total}^2$  is given by Eq. (2-3)

$$\sigma_{V,total}^2 = \sigma_{V,column}^2 + \sigma_{V,injector}^2 + \sigma_{V,detector}^2 + \sigma_{V,tubing}^2 + \sigma_{V,endfitting}^2 + \sigma_{V,responsetime}^2 \quad (2-3)$$

where  $\sigma_{V,column}^2$  represents the band broadening effect from the column itself,  $\sigma_{V,injector}^2$ ,  $\sigma_{V,detector}^2$ ,  $\sigma_{V,tubing}^2$ ,  $\sigma_{V,endfitting}^2$  and  $\sigma_{V,responsetime}^2$  describe the band broadening resulting from injector, detector cell, connecting tubing, column endfittings and detector response time, respectively. Since the packed column is directly connected to an injection valve in this work, no band broadening should occur from the endfitting. Assuming that the packed capillary produces a Gaussian peak, then the observed total variance can be deduced from

$$\sigma_{V,total}^2 = \frac{V_{R,i}^2}{N} \quad (2-4)$$

where  $V_{R,i}$  is the retention volume of analyte  $i$ . The observed variance for tryptophan was 5.2 nL<sup>2</sup>.

#### 2.3.2.2.1 Injector Band Broadening

The injector used has a 4-nL volume. If it gives a “plug” injection, the band broadening from the injector is

$$\sigma_{V,injector}^2 = \frac{V_{injector}^2}{12} = \frac{(4nL)^2}{12} = 1.3(nL)^2 \quad (2-5)$$

where  $V_{injector}$  is the volume of injector. Therefore the apparent efficiency loss due to a 4-nL injector is about 25% for W. Clearly, the injector used here is not perfect for the nano-LC system. The split-less flow nano-LC system here requires an injector with very small volume. However, 4 nL is the smallest injection volume which commercially available injectors can provide. To decrease injection volume, a timed injection method was used in this work. The detailed information is given in section 2.3.3.4.

### 2.3.2.2.2 Detector Cell Band Broadening

The detector we used for nano-SEC was used previously for detection on a microchip. The 266 nm laser beam is 0.5 mm in diameter. Light waves spread as they propagate because of diffraction. Laser beam spreading can be described by

$$w(z) = w_0 \left[ 1 + \left( \frac{\lambda z}{\pi w_0^2} \right)^2 \right]^{1/2} \quad (2-6)$$

where  $z$  is the distance propagated from the plane where the wavefront is flat,  $\lambda$  is the wavelength of light,  $w_0$  is the radius of the  $1/e^2$  irradiance contour at the plane where the wavefront is flat,  $w(z)$  is the radius of the  $1/e^2$  contour after the wave has propagated a distance  $z$ . The calculated size of the laser beam reaching the objective lens is 0.56 mm. The focused laser spot size passing through a diffraction limited lens can be calculated from

$$d_{1/e^2} = \frac{1.27\lambda f}{D_{1/e^2}} \quad (2-7)$$

for a laser beam with a Gaussian intensity profile. Here,  $d_{1/e^2}$  represents laser spot diameter in the focal plane,  $\lambda$  is the wavelength of light,  $f$  is the focal length of the lens,  $D_{1/e^2}$  is the radius of the  $1/e^2$  contour before the wave propagates through the lens. By

combining the above two equations, the minimum focused spot should be 12.3  $\mu\text{m}$  in diameter. This number might be smaller than the actual focused spot size; if the spreading is not diffraction limited or the beam is not Gaussian, which it is not for this laser. The corresponding minimum detection volume for the 50  $\mu\text{m}$  i.d. capillary is 24  $\mu\text{L}$ .

A detection window is located after, but close to the packing bed. For an on-column detector cell, the band broadening is of the same form as “plug” injection and can be described by

$$\sigma_{V,\text{cell}}^2 = \frac{V_{\text{cell}}^2}{12} \quad (2-8)$$

where  $V_{\text{cell}}$  is the volume of detector cell. The detector cell produces an apparent efficiency loss of 0.01% for  $W$ , which is insignificant. Even for a larger spot size or non-gaussian beam this is clearly a negligible contribution. The detector used here is excellent for the nano-LC system.

### 2.3.2.2.3 Connecting Tube Band Broadening

There is a short distance of about 3 mm between the detection window and outlet frit. This open section will contribute to the total band broadening. The variance from the connecting tube is computed by

$$\sigma_{V,\text{tubing}}^2 \approx \frac{\pi r^4 L F}{24 D_M} \quad (2-9)$$

where  $r$  and  $L$  are the radius and length of the tube,  $F$  is the flow rate, and  $D_M$  is the diffusion coefficient. The diffusion constant for small molecules in water is  $10^{-5} \text{ cm}^2 \text{ s}^{-1}$  or less. The flow rate used for the chromatogram in Figure 2-6 is 100 nL/min. Therefore the calculated variance is  $0.26 \text{ (nL)}^2$ , which contributes 5% to the total band broadening. This value is acceptable.

### 2.3.2.2.4 Contribution of Each source to the Total Band Broadening

The extra column band broadening has been discussed in previous sections. Table 2-3 summarizes the variance from injector, detector cell and connecting tubing as well as the contribution of each source to the total band broadening in the nano-SEC system. From these data, the injection valve is not good for detection of W. Also, the contribution of connecting tubing to the total band broadening for protein is much larger than for W because of the slow diffusion of protein, which is an important factor in Eq. 2-9.

Sample			Contribution
50 $\mu$ M tryptophan	$\sigma_{V,total}^2$ (nL) <sup>2</sup>	5.2	
	$\sigma_{V,injector}^2$ (nL) <sup>2</sup>	1.3	25%
	$\sigma_{V,cell}^2$ (nL) <sup>2</sup>	0.00058	0.01%
	$\sigma_{V,tubing}^2$ (nL) <sup>2</sup>	0.26	5%
0.1 mg/ml $\alpha$ -lactalbumin	$\sigma_{V,total}^2$ (nL) <sup>2</sup>	72	
	$\sigma_{V,injector}^2$ (nL) <sup>2</sup>	1.3	1.8%
	$\sigma_{V,cell}^2$ (nL) <sup>2</sup>	0.00058	0.0008%
	$\sigma_{V,tubing}^2$ (nL) <sup>2</sup>	2.5	3.5%
0.05 mg/ml BSA	$\sigma_{V,total}^2$ (nL) <sup>2</sup>	73	
	$\sigma_{V,injector}^2$ (nL) <sup>2</sup>	1.3	1.8%
	$\sigma_{V,cell}^2$ (nL) <sup>2</sup>	0.00058	0.0008%
	$\sigma_{V,tubing}^2$ (nL) <sup>2</sup>	4.6	6.3%

**Table 2-3 Contribution of each extra band broadening. Diffusion coefficient ( $\times 10^{-7} \text{ cm}^2 \text{ s}^{-1}$ ) for BSA<sup>10</sup> and  $\alpha$ -lactalbumin<sup>14</sup> are 5.65 and 10.6, respectively.**

### 2.3.2.3 Limit of Detection

The limit of detection (LOD) ( $S/N = 3$ ) was evaluated for the nano-SEC system using UV laser induced native fluorescence detection. The noise  $N$  here is baseline noise, which is measured from the standard deviation of the baseline before the appearance of the sample peak. The  $S/N$  vs. concentration plot and calibration curve is shown in Figure 2-8. There is a linear relationship between  $S/N$  and tryptophan concentration within 10-100  $\mu\text{M}$ . The LOD ( $S/N = 3$ ) of the native fluorescence detection system was calculated to be 3.5  $\mu\text{M}$  for tryptophan. If another buffer (50 mM  $\text{NaH}_2\text{PO}_4$  ( $\text{pH} = 6.7$ ), 20% ACN) was used to obtain these plots, the extrapolated LOD ( $S/N = 3$ ) was similar, 1.9  $\mu\text{M}$ , even though the flow rate decreased from 100 nL/min to 75 nL/min. With the same detector, Misir<sup>1</sup> obtained an LOD of 230 nM for W in CE with a quartz chip.

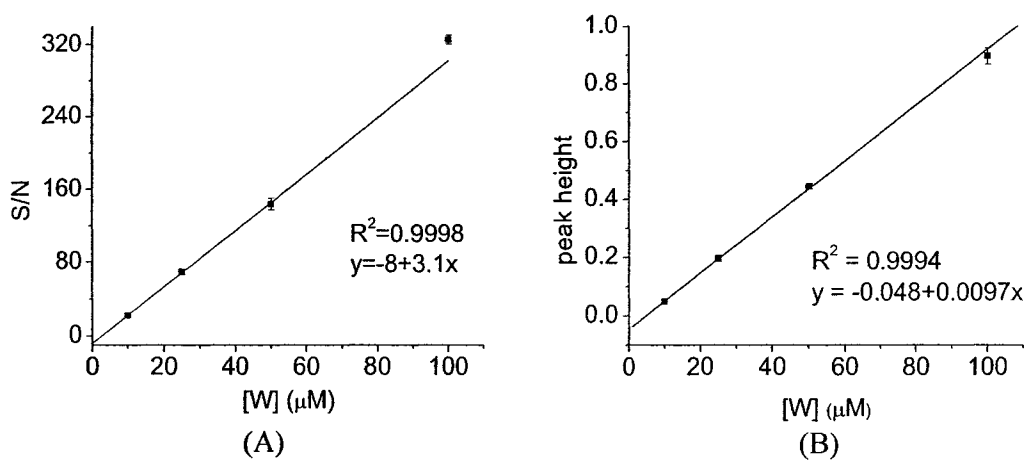


**Figure 2-8 (A) Plot of  $S/N$  as a function of tryptophan (W) concentration. (B) Peak height calibration plot for tryptophan. Mobile phase: 50 mM  $\text{NaH}_2\text{PO}_4$  ( $\text{pH} = 6.7$ ), packing length: 12.2 cm, flow rate = 100 nL/min. Error bars show standard deviation of three replicate measurements.**

### 2.3.3 Protein Detection

#### 2.3.3.1 Limit of Detection

In Figure 2-9, S/N increased linearly with the concentration of  $\alpha$ -lactalbumin within the range of 0.05-0.4 mg/ml. If the plot of S/N vs. concentration is extrapolated to S/N = 3, the deduced LOD is 18  $\mu$ g/ml (or 1.3  $\mu$ M), which is worse than the LOD of 500 nM determined from on-chip CE experiments by Misir<sup>1</sup>. Here, the variation of S/N becomes more evident at higher concentration of  $\alpha$ -lactalbumin. Peak height and noise used to calculate S/N are listed in Table 2-4. Noise increases with concentration, while peak

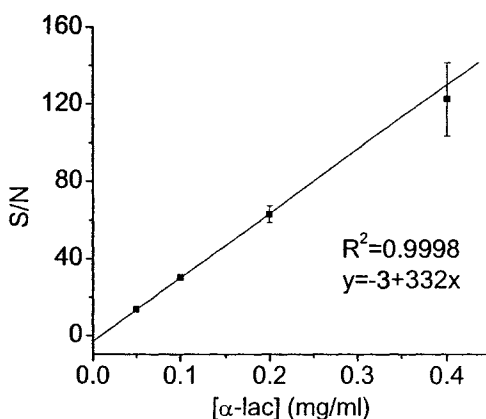


**Figure 2-9** Plot of S/N as a function of  $\alpha$ -lactalbumin concentration. Mobile phase: 50 mM  $\text{NaH}_2\text{PO}_4$  (pH = 6.7), packing length: 12.2 cm, flow rate = 100 nL/min. Error bars show standard deviation of three replicate measurements.

Concentration (mg/ml)	Peak height	Noise (N)
0.05	0.039 $\pm$ 0.002	0.0029 $\pm$ 0.0001
0.1	0.088 $\pm$ 0.003	0.0029 $\pm$ 0.0001
0.2	0.205 $\pm$ 0.003	0.0032 $\pm$ 0.0001
0.4	0.45 $\pm$ 0.03	0.0038 $\pm$ 0.0003

**Table 2-4** Variation of peak height and noise with concentration of  $\alpha$ -lactalbumin.

Data from Figure 2-9.

height varies more at the highest concentration tested (0.4 mg/ml). This can be accounted for by protein adsorption.

$\alpha$ -lactalbumin contains 4 tryptophan residues. However, compared to the LOD of W (3.5  $\mu$ M) in Figure 2-8, there was not a linear relationship between the number of W residues in the protein and the detection sensitivity. Yeung observed similar phenomenon for tryptophan and conalbumin<sup>15</sup>. The authors proposed several possible reasons: (1) The quantum yield of fluorescence of W changes with the nature of the microenvironment. A hydrophilic microenvironment can enhance fluorescence signal<sup>16</sup>. (2) Quenching of W fluorescence in proteins can be caused by some functional groups<sup>17, 18</sup>. (3) W and proteins might have different fluorescence and fluorescence-excitation spectra<sup>18</sup>. After the mobile phase is changed to 50 mM NaH<sub>2</sub>PO<sub>4</sub> (pH = 6.7) with 20% ACN and flow rate changed to 75 nL/min, the LOD (S/N = 3) was 41  $\mu$ g/ml (or 2.8  $\mu$ M). Although ACN can be used to minimize adsorption, it causes increased background noise.

Shihabi<sup>19</sup> reported LOD = 0.9 mg/L vs. 18  $\mu$ g/ml  $\alpha$ -lactalbumin in our study for Tamm-Horsfall protein with a molecular mass of ca. 80k-930k in conventional SEC column (250 mm $\times$ 4.6 mm i.d.) with native fluorescence detection method. However, the injection volume was 20  $\mu$ L, so the LOD in mass (18 ng) is worse than the LOD (72 pg) in this work. With 0.2  $\mu$ L injection, Legido-Quigley<sup>20</sup> achieved LOD of 41.3 fmol for ribonuclease A with 3  $\mu$ m C<sub>8</sub> Vydac nano column (100  $\mu$ m i.d.) and 7.3 fmol with reverse phase monolith column (100  $\mu$ m i.d.), which is higher than the 5.1 fmol (LOD based on injection volume) given in this work.

### 2.3.3.2 Mobile Phase

The Biosep-S2000 beads are coated with a hydrophilic layer. However, the coverage may not be complete. Under the experimental conditions used, underivatized silanol groups on the bead surface were negatively charged and could react with ionic solutes. Also, there are possible hydrophobic interactions between proteins and the bead surface.

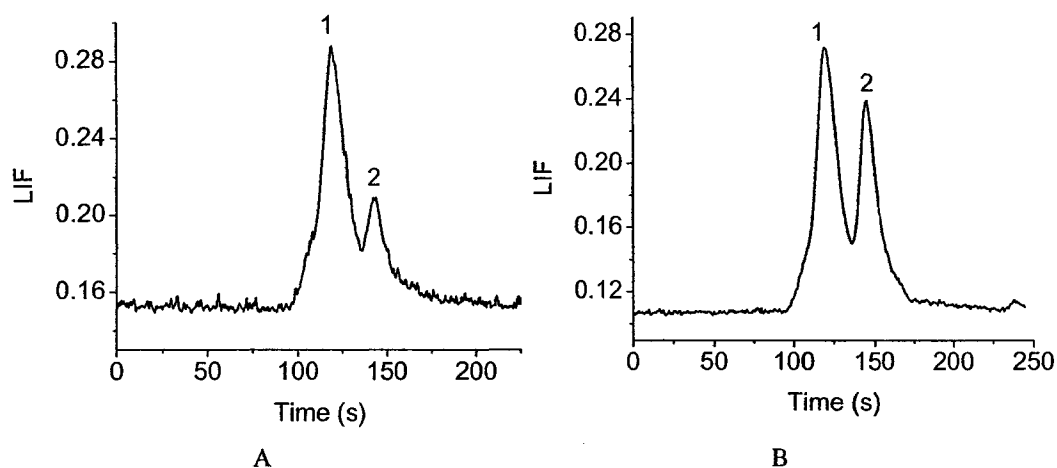


**Figure 2-10 Chromatogram for the separation of 0.25 mg/ml BSA and 0.125 mg/ml  $\alpha$ -lactalbumin in (A) 50 mM  $\text{NaH}_2\text{PO}_4$  (pH = 6.7), (B) 50 mM  $\text{NaH}_2\text{PO}_4$  (pH = 6.7) with 0.1% TFA, packing length: 12.9 cm, flow rate = 75 nL/min. Peak: 1. BSA; 2.  $\alpha$ -lactalbumin.**

To minimize ionic interactions, the use of running buffers with a high ionic strength is often suggested. However, high ionic strength will promote hydrophobic interactions. So the mobile phase condition needs to be optimized. A 50 mM phosphate buffer (pH = 6.8) is recommended by the manufacturer.

Figure 2-10 shows the separation of 0.25 mg/ml BSA and 0.125 mg/ml  $\alpha$ -lactalbumin in two different buffers. With the nano-LC system, proteins can be separated very fast, within a couple of minutes. Use of 0.1% trifluoroacetic acid (TFA) improved not only the peak shape, but also the resolution.

In this study, different buffers were tested to separate the protein mixture. The resolution ( $R_s$ ) of two adjacent peaks is calculated from Eq. (1-8), and the values in various phosphate buffers with different additives are shown in Table 2-5. Among these buffers, the additives 0.5 M NaCl, 0.01% Tween 20 and 0.2% PEG did not improve the separation efficiency. These results were not expected, since Tween 20 and PEG are usually added into running buffer to reduce protein adsorption in CE, while 0.5 M NaCl is added to reduce ionic interactions. In SEC, it may be that the pressure applied changes

or inhibits the dynamic coating process, compared to CE, so that protein adsorption is not minimized. This result agrees with what another colleague in this group observed with a commercially available non-covalently attached PEG coated capillary. Acetonitrile was helpful in reducing protein adsorption and giving higher peaks, but the resolution did not change much. Commercially available 2× SDS buffer (pH = 6.6) contains 1% SDS, 0.12 M Tris-HCl according to the information from the technical support service. However, the manufacturer does not provide the detailed composition of this SDS buffer. It was noticed that with this SDS buffer, the fluorescence signal of proteins increased a lot.

Packing length(cm)	sample	buffer	R <sub>s</sub>
12.9	0.25 mg/ml BSA 0.125 mg/ml α-lac	50 mM NaH <sub>2</sub> PO <sub>4</sub>	0.85
		50 mM NaH <sub>2</sub> PO <sub>4</sub> 20% ACN	0.81
		50 mM NaH <sub>2</sub> PO <sub>4</sub> 0.5 M NaCl	0.79
		50 mM NaH <sub>2</sub> PO <sub>4</sub> 0.1% TFA (pH~4)	0.95
12.0	1 mg/ml BSA 0.5 mg/ml α-lac	50 mM NaH <sub>2</sub> PO <sub>4</sub>	0.88
		50 mM NaH <sub>2</sub> PO <sub>4</sub> 0.01% Tween 20	0.82
		50 mM NaH <sub>2</sub> PO <sub>4</sub> 20% ACN	0.91
		50 mM NaH <sub>2</sub> PO <sub>4</sub> 0.2% PEG	0.79

**Table 2-5 Resolution between BSA and α-lactalbumin in various mobile phases. Flow rate = 75 nL/min. The phosphate buffer was pH 6.7 before mixing with other additives.**

There are two possible reasons: (1) SDS helps to minimize protein adsorption because of protein denaturation, (2) the microenvironment of tryptophan residue after protein conformational change enhances fluorescence quantum yield. However, the resolution was poor, less than 0.6. Additionally, the packed column was easily clogged after using this denaturing buffer. Takagi<sup>21</sup> reported that protein resolution obtained in SDS is markedly dependent on the phosphate buffer concentration and displays its optimum in the range of 0.05 to 0.15 M. If the phosphate buffer concentration is above 0.15M, protein resolution in the SDS buffer is dramatically reduced. The reason for this phenomenon is not understood, but this observation indicates the complexity of this buffer system.

### 2.3.3.3 Sample Solvent

The presence of ACN in the sample buffer alone, with none in the running buffer, gave sharper and higher protein peaks, as shown in Figure 2-11. However, 30% ACN may be too high for some proteins to remain dissolved. The sample syringe was often blocked after using protein with this percentage of ACN for several runs. Peak shape

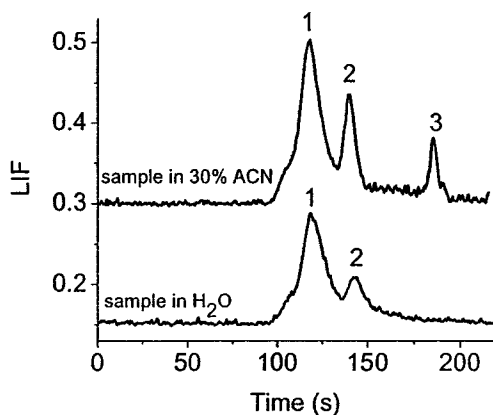


**Figure 2-11 Effect of sample solvent. 0.25 mg/ml BSA and 0.125 mg/ml ( $\alpha$ -lactalbumin were dissolved in (a) H<sub>2</sub>O, (b) 30% ACN. Mobile phase: 50 mM NaH<sub>2</sub>PO<sub>4</sub> (pH = 6.7), packing length: 12.9 cm, flow rate = 75 nL/min. Peak: 1. BSA; 2.  $\alpha$ -lactalbumin; 3. solvent peak.**

improvement was also observed with 50 mM NaH<sub>2</sub>PO<sub>4</sub> (pH = 6.7) running buffer containing 20% ACN. The additional small peak seen with added ACN may be from adsorbed protein washed off the wall by the ACN in the sample band.

The results shown above indicate that there is protein adsorption inside the column. Further, using ACN as a sample, after injecting a mixture of two proteins for several runs, resulted in elution of material from the column, as shown in Figure 2-12. There are two possible factors resulting in such adsorption: (1) to make the frits, the hydrophilic coating of the beads was burned off at high temperature, which gives an adsorptive surface.

Analyte adsorption was also found at the position of an activated reverse-phase frit and could be significantly reduced by treating the frit with diphenyltetraamethyldisilazane.<sup>22</sup> (2) the silanol group on the capillary wall shows interaction with proteins, giving some bandbroadening. (3) the imperfect coating of the silica bead causes interaction between protein and bead surfaces.

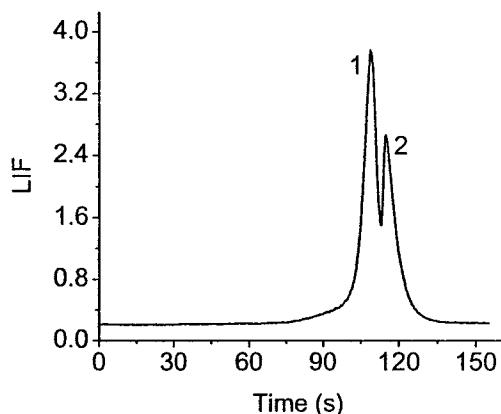


**Figure 2-12 Injecting ACN after several runs of aqueous injection. Mobile phase: 50 mM NaH<sub>2</sub>PO<sub>4</sub> (pH = 6.7) with 20% ACN, packing length: 12.2 cm, flow rate: 100 nL/min. Peak: 1. BSA; 2.  $\alpha$ -lactalbumin.**

#### 2.3.3.4 Injection Volume

The use of a sample volume that is 1-5% of the packing volume is recommended to get maximum resolution. Under these conditions, the sample volume would contribute at

most 20% to the total peak width in volume units. For the 12.9 cm packed bed used here, the volume of capillary occupied by the bed is calculated to be 250 nL, so a sample volume within 2.5-12.5 nL is acceptable. Though the 4 nL injection volume from the nanovolume injector is in this range, it is larger than the theoretical value (1.5 nL) estimated in the literature<sup>13</sup> for a 50  $\mu\text{m}$  i.d. reverse-phase column and an unretained sample. To achieve a smaller injection plug than available in the sample loop volume, a gated injection was used. The injection time was adjusted by switching the injection valve back to “load” mode after a 2 s sample injection at 1.25 nL/s to decrease the injection volume. The effect of sample volume on the resolution is shown in Figure 2-13. Proteins can be better resolved after decreasing injection volume. The injection volume is calculated by multiplication of flow rate and injection time. Resolution did not change after decreasing sample concentration. For a twice diluted protein mixture,  $R_s$  was still 0.99, implying that there was no band broadening contributed from sample overloading. Sandoval<sup>23</sup> also reported that sample volume instead of sample concentration is the limiting factor in SEC, until samples become very viscous.

Another packed capillary with a 12.2-cm packing bed was also tested for the study

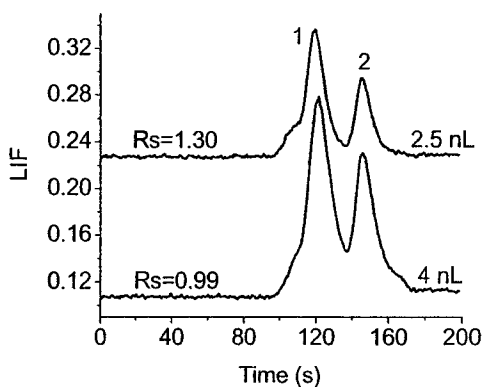


**Figure 2-13 Chromatograms of 0.25 mg/ml BSA and 0.125 mg/ml  $\alpha$ -lactalbumin. (a) 4 nL injection valve, (b) timed injection to reduce to 2.5 nL. Mobile phase: 50 mM  $\text{NaH}_2\text{PO}_4$  (pH = 6.7) with 0.1% TFA, packing length: 12.9 cm, flow rate = 75 nL/min. Peak: 1. BSA; 2.  $\alpha$ -lactalbumin.**

of the injection volume effect at a flow rate of 75 nL/min. The change of resolution for 0.1 mg/ml BSA and 0.05 mg/ml  $\alpha$ -lactalbumin with injection volume is shown in Table 2-6. Resolution increased when the injection volume changed from 4 nL to 2.5 nL while it stayed about the same when the volume decreased further to 1.25 nL. The peak area and height decreases with shorter injection times, indicating smaller volumes are injected. However, the peaks do not decrease as much as expected on going from a 2 s to a 1 s injection time. This may be because the change of injection volume is a manual operation, and injection volumes other than 4 nL are not exact.

Injection Volume (nL)	4	2.5	1.25
$R_s$	0.86	1.02	0.98

**Table 2-6 Resolution vs. injection volume. Mobile phase: 50 mM NaH<sub>2</sub>PO<sub>4</sub> (pH = 6.7), packed length: 12.2 cm, flow rate: 75 nL/min.**

### 2.3.3.5 Effect on HETP

The diffusion of molecules with high mass into and out of pores in the packing affects the efficiency of SEC. As the flow rate increases, peaks resulting from such slow

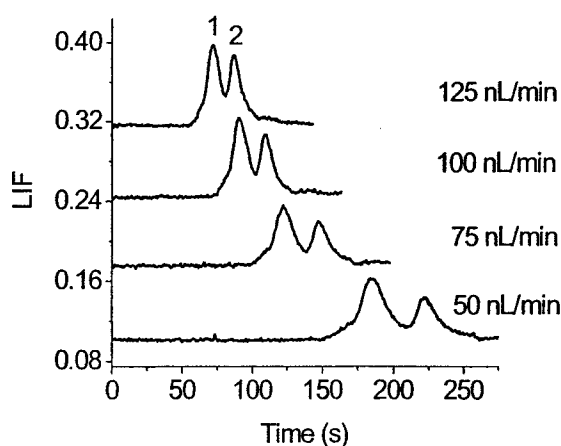


**Figure 2-14 Separation of 0.25 mg/ml BSA and 0.125 mg/ml  $\alpha$ -lactalbumin at different flow rates. Mobile phase: 50 mM NaH<sub>2</sub>PO<sub>4</sub> (pH = 6.7) with 0.1% TFA, packing length: 12.9 cm, flow rate = 75 nL/min. Peak: 1. BSA; 2.  $\alpha$ -lactalbumin.**

diffusion become broader, as observed in Figure 2-14. The van Deemter equation also states clearly that the velocity of the mobile phase influences the column efficiency more strongly than other operational variables. The fact that a slower flow rate of the mobile phase gives better resolution is shown in Table 2-7. Comparing the  $R_s$  values of BSA and  $\alpha$ -lactalbumin at 50-125 nL/min,  $R_s$  increases 19% from 0.86 to 1.02.

Flow rate (nL/min)	50	75	100	125
$R_s$	1.02	0.96	0.92	0.86

**Table 2-7 Resolution vs. flow rate. Data from Figure 2-14.**

Figure 2-15 shows the relationship between height equivalent to a theoretical plate and flow rate. The value of plate height increases with increasing flow rate. Compared to tryptophan in Figure 2-7, macromolecules show a more significant change of HETP. The flow rate dependence is caused mainly by slow mass transfer of proteins within the pores, in which restricted diffusion is dependent on the ratio of solute molecular size to pore size

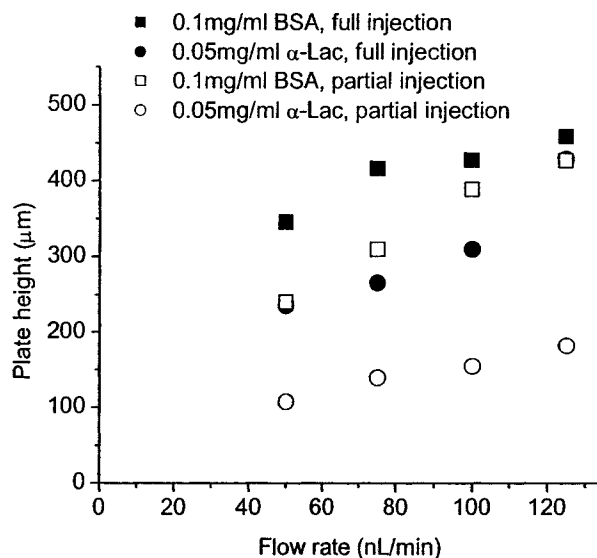


**Figure 2-15 Plate height vs. flow rate. Mobile phase: 50 mM  $\text{NaH}_2\text{PO}_4$  (pH = 6.7) with 0.1% TFA, packing length: 12.9 cm, flow rate = 75 nL/min.**

in a column. Also, the slow diffusion increases, the C term in the van Deemter equation. Besides flow rate, the injection volume also has an influence on plate height. Plate height increases with injection volume. With partial injection of sample, plate height decreased more for  $\alpha$ -lactalbumin than for BSA. This is contrary to the observation by Chervet<sup>24</sup> that the volume effect becomes less important with increasing retention factor in isocratic LC (C<sub>18</sub>, 15  $\mu$ m, 25 cm $\times$ 150  $\mu$ m). The different result for two proteins here may simply mean that adsorption phenomena play a greater role in band broadening for BSA. The little bump in front of BSA in Figure 2-14 causes increase of plate height, too. Here, the plate height is higher than the typical value in SEC, which might be accounted for by band broadening resulting from protein adsorption. Ricker<sup>23</sup> reported a plate height of 35  $\mu$ m for sodium azide in a Zorbax GF-250 SEC column (4.6 $\times$ 250 mm). Jorgenson<sup>10</sup> tested a 50  $\mu$ m i.d. capillary packed by 4-5  $\mu$ m Zorbax GF250 SEC particles with native fluorescence detection and the plate height was 10-30  $\mu$ m for BSA at mobile phase velocity of 0.01-0.075 mm/s. The very slow velocity is helpful to give the good performance. However, like most nano-LC systems, a splitting injection system was used in Jorgenson's work and most of the sample was wasted, which is not good for minute sample analysis. Also it took more than 20 minutes, even hours for protein to elute out, which is much slower than in this work.

Sample amount is another factor affecting HETP. The effect of injected sample amount on plate height is shown in Figure 2-16. Plate height increases as the amount of tryptophan increases, while it remains about the same for  $\alpha$ -lactalbumin. Based on experiments with chymotrypsinogen, Gooding<sup>25</sup> claimed that the loading capacity ( $C$ ) in mg of protein for a SEC column may be expressed by the formula

$$C = r^2 / 4.4 \quad (2-9)$$

where  $r$  is the column radius in mm. For a 50  $\mu$ m i.d. capillary, the predicted maximum protein loading capacity is 142 ng per injection. For  $\alpha$ -lactalbumin, the maximum amount injected in this study was 10 pmol (1.6 ng). As observed in Figure 2-16, the plate height

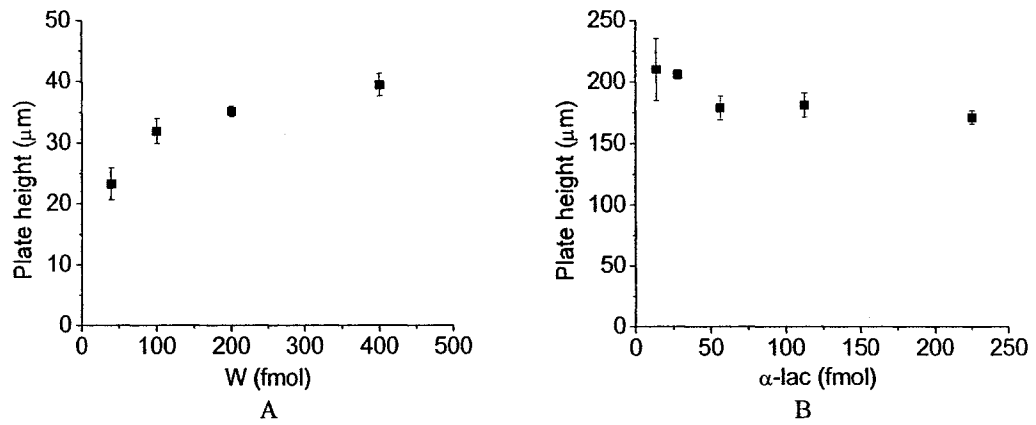


**Figure 2-16 Plate height vs. sample amount for (A) W; (B)  $\alpha$ -lactalbumin. Mobile phase: 50 mM  $\text{NaH}_2\text{PO}_4$  (pH = 6.7), packing length: 12.9 cm, flow rate = 100 nL/min. Error bars show standard deviation of three replicate measurements.**

did not change much within the tested sample load.

### 2.3.3.6 Protein Separation

Figure 2-17 shows a chromatogram for protein separation. The mixture contains 1 mg/ml BSA, 0.5 mg/ml  $\alpha$ -lactalbumin and 0.1 mg/ml peptide ( $\alpha_1$ - mating factor). 0.1%

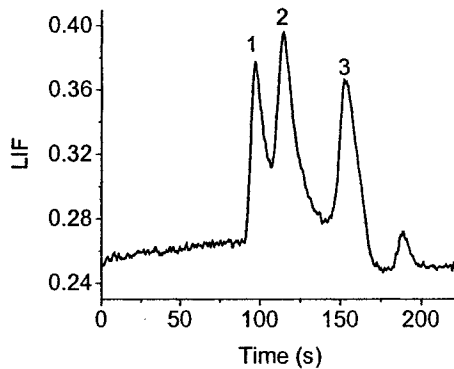


**Figure 2-17 Separation of mixture of proteins and peptide. Peak 1, 1 mg/ml BSA; 2, 0.5 mg/ml  $\alpha$ -lactalbumin; 3, 0.1 mg/ml  $\alpha_1$ -mating factor. Mobile phase: 50 mM  $\text{NaH}_2\text{PO}_4$  (pH = 6.7) with 0.1% SDS, packing length: 18 cm, flow rate: 100 nL/min.**

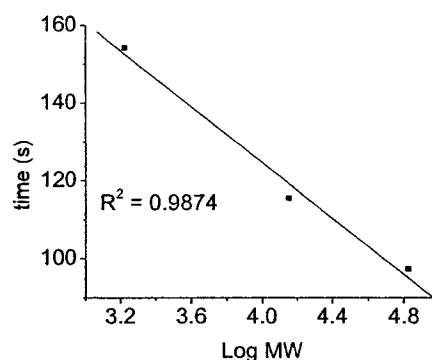


**Figure 2-18 Plot of retention time vs. log molecular weight for the mixture in Figure 2-17. Mobile phase: 50 mM NaH<sub>2</sub>PO<sub>4</sub> (pH = 6.7) with 0.1% SDS, packing length: 18.5 cm, flow rate: 100 nL/min.**

SDS was added to 50 mM NaH<sub>2</sub>PO<sub>4</sub> (pH = 6.7) to reduce protein adsorption. The small peak after the peptide may be from the desorption of sample. Although the packing length was increased to 18 cm, there was no improvement in resolution compared to the 12-cm column. For the 18-cm packing bed here,  $R_s$  for BSA and  $\alpha$ -lactalbumin was 0.77, which is similar to that reported in Table 2-5 for a 12-cm bed. The  $R_s$  for  $\alpha$ -lactalbumin and peptide D was 1.32. The calibration curve derived for SEC of protein and peptide mixtures is depicted in Figure 2-18. Based on this graph, the elution window is very small for proteins.

The separation of proteins and amino acid is shown in Figure 2-19. Here W shows the maximum time for a fully permeating component, while ovalbumin represents a weakly permeating component. Large proteins such as IgG (MW 150 kD) and  $\beta$ -galactosidase (MW 465 kD) gave peaks at about the same location as ovalbumin, but they tended to be quite broad. Thus the time window is about 70-160 s. The separation efficiency for the three samples is given in Table 2-8.

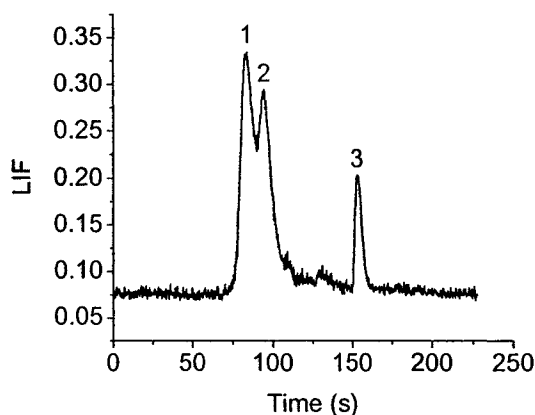


**Figure 2-19 Separation of mixture of proteins and amino acid. Peak 1, 0.2 mg/ml ovalbumin (44 k); 2, 0.1 mg/ml  $\alpha$ -lactalbumin (14 k); 3, 25  $\mu$ M W (204). Mobile phase: 50 mM  $\text{NaH}_2\text{PO}_4$  (pH = 6.7), packing length: 12 cm, flow rate: 100 nL/min.**

Protein	ovalbumin	$\alpha$ -lactalbumin	tryptophan
N (plates/m)	$5.8 \times 10^3$	$2.3 \times 10^3$	$4.5 \times 10^4$

**Table 2-8 Separation efficiency of individual components in Figure 2-19.**

#### 2.3.4 Attempt at Capillary Coating

The elution window of nano-SEC is very small, so that the number of proteins which can be separated is limited. Protein adsorption might contribute a lot to broad peaks. Here, a coating method was tried to reduce protein-wall interactions. A commercially available PEG coated capillary is used for CE separation of proteins in our lab. We found that the physically adsorbed PEG layer can only survive under low pressure of  $\sim 5$  psi. If 20 psi is applied to the coated capillary, the migration time becomes longer and longer, until finally the coated capillary failed to give protein peaks. To reduce protein-wall interaction in the nano-LC system, a permanent hydrophilic coating is



### 2.3.5 Detection with Reversed Phase Nano-LC

#### 2.3.5.1 Peptide Mixture

To demonstrate the capability of the nano-LC system, a commercially available reverse phase C<sub>18</sub> capillary from Unimicro (75 μm i.d., 20 cm packing bed) was used to analyze a peptide mixture. Figure 2-21 shows the separation of α<sub>1</sub>- mating factor fragment, luteinizing hormone releasing hormone and α<sub>1</sub>- mating factor at different flow rates. Since the peptides had been stored for a long time, the mixture gave more than

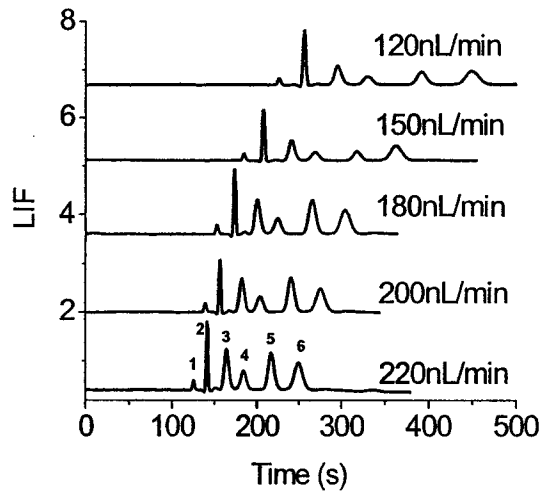


Figure 2-21 Separation of mixture of three peptides at different flow rate. Mobile phase: 0.1% TFA, 20% ACN.

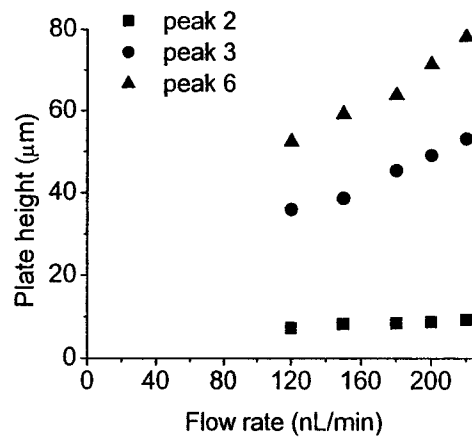
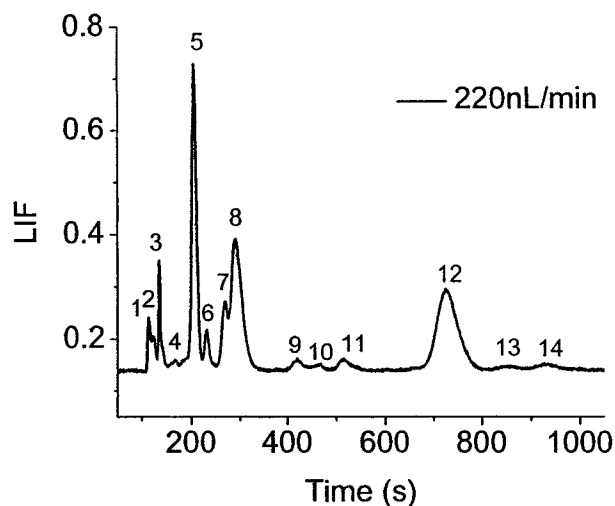


Figure 2-22 A van Deemter plot for peak 2, peak3 and peak 6 in Figure 2-21.

three peaks. However, the peptide mixture is well separated. Good separation can be achieved within 5 minutes at 220 nL/min. The van Deemter plot for three peaks in Figure 2-21 is given in Figure 2-22. As the flow rate increases, the plate height becomes larger. The weakly retained solute (peak 2) gives much smaller plate height than more strongly retained solutes (peak 3 and peak 6). The separation efficiency ranges from  $1.1 \times 10^5$  to  $1.4 \times 10^5$  plates/m for peak 2 while it is  $3.8 \times 10^3$  to  $5.6 \times 10^3$  plates/m for peak 6. The separation efficiency decreases as the retention becomes stronger. Danielson<sup>26</sup> reported efficiencies of  $1.3 \times 10^5$  plates/m for a small molecule (phenylhexane) and  $6.0 \times 10^4$  –  $1.1 \times 10^5$  plates/m for insulin with a  $33 \times 6.2$  mm reverse phase column ( $2 \mu\text{m}$  particle). However, the separation efficiency estimated from the chromatograms shown in the paper for insulin is worse than this value, around  $1.8 \times 10^4$ . Enkephalin peptides showed similar separation efficiency as insulin in chromatographs. In this study, the separation efficiency for a weakly retained peptide is comparable to Danielson's result while N for strongly retained molecules is worse. This comparison shows our system is not as efficient as the best reported, but it does give performance in a similar range. As a result, we conclude the nano-LC pump, injector and detector are not the major contributor to band broadening in the SEC study reported above.

#### 2.3.5.2 Digested Protein

The analysis of a tryptic digest of  $\alpha$ -lactalbumin with the  $C_{18}$  column used in the previous section is given in Figure 2-23. Based on database searching using Swiss-Prot for  $\alpha$ -lactalbumin, the sequence was pasted to protein prospector (prospector.ucsf.edu) to get MS-digest results. Database searching used the following parameters: trypsin digest, 2 MC, peptide N-terminus = hydrogen, peptide C-terminus = free acid, modifications considered = oxidation of M and protein N-terminus acetylated, cycteine modified by carbamidomethylation. The search results show  $\alpha$ -lactalbumin (MW = 14,223 Da, pI = 5.0) is a protein with 121 amino acids. Among these amino acids, there are 4 tryptophan



**Figure 2-23** Detection of trypsin digested  $\alpha$ -lactalbumin. Mobile phase: 20% ACN, 0.1% TFA, flow rate: 220 nL/min.

residues. However, there are 21 possibilities to obtain peptide chains with tryptophan. In Figure 2-23, 14 peaks were detected by the system, which means that the nano-LC system with native fluorescence detection has good sensitivity for tryptophan containing biomolecules. The calculated separation efficiency for peak 5, 6 and 12 is  $1.2 \times 10^4$ ,  $1.4 \times 10^4$  and  $5.9 \times 10^3$  plates/m respectively.

## 2.4 Conclusion

The application of nano-SEC for biomolecules was investigated in this chapter. The system exploited a mobile phase delivery pump which provided small and stable flow rate to get good reproducibility without the need for flow splitting, and a LINF detection method which avoids problematic labeling processes. This miniaturization of conventional SEC improves the sensitivity and analysis time. The LOD (690 nM or 2.8 fmol) of protein achieved from this system is comparable to that of CE on-chip, and even better in other nano-LC systems in terms of mass detection limits, but inferior in terms of concentration detection limits. Binary protein mixtures were separated within several

minutes. The band broadening was minimized by decreasing flow rate, using smaller injection volume, resulting in better resolution. With a commercially available C<sub>18</sub> packed capillary, good separation efficiency was achieved for weakly retained peptide while the lower separation efficiency for strongly retained peptide was in a similar range as literatures. This demonstrates the capability of the nano-LC system.

Compared to the small molecule tryptophan, protein gives much larger band broadening in nano-SEC. The difference may be caused by protein adsorption as well as the slow diffusion of large molecules. Although the beads are coated with a hydrophilic layer, the interaction of protein with the uncovered surface and capillary wall is inevitable. Within such a small column, the contribution of such protein interaction is significant compared to conventional SEC. Coating of the capillary wall may be an effective method to reduce protein adsorption. Once a good coating method is established, nano-SEC may become a promising, powerful separation technique.

## 2.5 References

- (1) Misir, K., University of Alberta, Edmonton, Canada, *M.Sc. thesis* 2004.
- (2) Ocvirk, G.; Tang, T.; Harrison, D. J. *Analyst* 1998, 123, 1429-1434.
- (3) Satchwill, T.; Harrison, D. J. *J. Electroanal. Chem.* 1986, 202, 75-81.
- (4) Harrison, D. J.; Cunningham, L. L.; Li, X.; Teclerian, A.; Permann, D. J. *Electrochem. Soc.* 1988, 135, 2473-2478.
- (5) Hjertén, S. *J. Chromatogr.* 1985, 347, 191-198.
- (6) Ahmed, F.; Modrek, B. *J. Chromatogr.* 1992, 599, 25-33.
- (7) Robson, M. M. C., M.G.; Myers, P.; Euerby, M.R.; Bartle, K.D. *J. Microcol. Sep.* 1997, 9, 357-372.
- (8) Yau, W. W.; Kirkland, J. J.; Bly, D. D. *Modern Size-Exclusion Liquid Chromatography*, 1979.
- (9) Bayle, C.; Siri, N.; Poinot, V.; Treilhou, M.; Caussé, E.; Couderc, F. *J. Chromatogr. A* 2003, 1013, 123-130.
- (10) Kennedy, R. T.; Jorgenson, J. W. *J. Microcol. Sep.* 1990, 2, 120-126.
- (11) Schmid, M.; Bäuml, F.; Köhne, A. P.; Welsch, T. *J. High Resol. Chromatogr.* 1999, 22, 438-442.
- (12) Chen, Y.; Gerhardt, G.; Cassidy, R. *Anal. Chem.* 2000, 72, 610-615.
- (13) Chervet, J. P.; Ursem, M. *Anal. Chem.* 1996, 68, 1507-1512.

- (14) Arai, T.; Norde, W. *Colloids Surf.* 1990, 51, 1-15.
- (15) Lee, T. T.; Yeung, E. S. *J. Chromatogr.* 1992, 595, 319-325.
- (16) Konev, S. V. *Fluorescence and Phosphorescence of Proteins and Nucleic Acids*; Plenum Press, 1967.
- (17) Cowgill, R. W. *Biochim. Biophys. Acta* 1963, 75, 272-273.
- (18) Teale, F. W. *Biochem. J.* 1960, 76, 381-388.
- (19) Shihabi, Z. K.; Hinsdale, M. E.; Bleyer, A. J. *J. Chromatogr. A* 2004, 1027, 161-166.
- (20) Legido-Quigley, C.; Marlin, N.; Smith, N. W. *J. Chromatogr. A* 2004, 1030, 195-200.
- (21) Takagi, T.; Takeda, K.; Okuno, T. *J. Chromatogr.* 1981, 208, 201-208.
- (22) Behnke, B.; Johansson, J.; Zhang, S.; Bayer, E.; Nilsson, S. *J. Chromatogr. A* 1998, 818, 257-259.
- (23) Ricker, R. D.; Sandoval, L. A. *J. Chromatogr. A* 1996, 743, 43-50.
- (24) Héron, S.; Tchaplal, A.; Chervet, J. P. *Chromatographia* 2000, 51, 495-499.
- (25) Gooding, K. M.; Lu, K. C.; Vanaced, G.; Regnier, F. E. *4th International Symposium on Column Liquid Chromatography* 1979.
- (26) Danielson, N. D.; Kirkland, J. J. *Anal. Chem.* 1987, 59, 2501-2506.

## Chapter 3: Size-Exclusion Electrochromatography

### 3.1 Introduction

The combination of capillary zone electrophoresis (CZE) and liquid chromatography (LC), capillary electrochromatography (CEC) has been applied mainly to neutral molecules. The separation of charged species with CEC is also reported. Fast analysis time, high separation efficiency, high sensitivity and low consumption of mobile phase makes CEC superior to LC in some ways. However, size-exclusion electrochromatography (SEEC), electrokinetically pumped SEC has not drawn much attention since its introduction in 1998. So far, most publications on SEEC are about water insoluble synthetic polymers, so the separation buffer used is an organic solvent with very low salt concentration.

The initial studies of CEC of proteins were performed on packed reverse-phase columns. These authors found that pressure had to be added to the applied voltage in order to elute proteins. They suggested that adsorption was responsible for the lack of electrokinetic migration. The work of Singh and others<sup>1,2</sup> showed that packed bed could be used for electrokinetic trapping, but that switching to pressure alone caused elution of sharp Gaussian peaks. Their result is inconsistent with an adsorption argument. Recently, other authors<sup>3</sup> have explored the behavior of microfabricated nanopores for the trapping of proteins, demonstrating that conditions that give double layer overlap can lead to protein and ion trapping near pore entrance. One of our goals in this work was to use size exclusion media in a CEC mode to develop some understanding of the failure of CEC for proteins. Size exclusion was chosen as the stationary phase because it is a well designed nanoporous media, and unlike reverse phase media it should not add an additional chromatographic process besides the role of the pores.

In this work, aqueous SEEC was explored with biomolecules. Two kinds of SEC stationary phases, silica beads and polymer beads, were tested for protein elution. The packing methods for these two stationary phases are different. The fabrication of packed

capillary with silica beads is described in Chapter 2, while the method for polymer bead packed capillary fabrication is addressed in this chapter. The mechanism of protein concentration at the inlet of the packed capillary was investigated. To change protein retention, pore size, ionic strength, pH of buffer and nature of protein were also investigated. In addition, EOF in SEEC was estimated. With the assistance of pressure in SEEC, three proteins were baseline resolved.

## **3.2 Experimental**

### **3.2.1 Reagent and chemicals**

All solutions were prepared with doubly distilled water (Millipore Canada) which was degassed by helium.  $\beta$ -lactoglobulin B from bovine milk, albumin from bovine (BSA), immunoglobulin G from rabbit serum (IgG), avidin from egg white, transferrin from human, ribonuclease A from bovine pancreas, FITC-avidin, FITC-IgG, HPLC grade acetonitrile (ACN), 3-(trimethoxysilyl)propyl acrylate, sodium dodecylbenzene sulphate (SDBS), sodium octyl sulphate (SOS), trimethylolpropane trimethacrylate (TRIM), toluene, benzoin methyl ether (BME), 2,2,4-trimethylpentane (isooctane), 2,3-epoxypropyl methacrylate (glycidyl methacrylate, GMA), tris-borate-EDTA (0.89 M tris borate, pH~8.3, 0.02 M EDTA, TBE) and 2 $\times$ SDS buffer were purchased from Sigma (USA). Sodium dihydrogen orthophosphate, NaOH and acetic acid were obtained from BDH Inc., sodium chloride from Merck (Germany), dimethyl sulphoxide (DMSO) from Caledon (Canada), sodium dodecyl sulfate (SDS) from Bio-rad, Alexa Fluo 488 protein labelling kit from Molecular Probes (USA). BioSep-SEC-S2000, PolySep-GFC-P2000 and PolySep-GFC-P3000 beads were bought from Phenomenex (USA).

A Nylon syringe filter (0.2  $\mu$ m pore size, Chromatographic Specialities Inc.) was used to filter all buffer solutions and ultrapure water used to prepare protein stock solutions. Then the protein stock solution was diluted with buffer to the desired concentration in siliconized vials (Fisher Scientific, USA). The pH of the buffer was

adjusted by titration with 1 M NaOH to the required value. Buffer solutions were degassed prior to use. Bead stock solution was made by suspending 50 mg of beads in 20 mM NaH<sub>2</sub>PO<sub>4</sub> containing 10% methanol. This stock solution was then diluted with water.

### **3.2.2 Instrumentation and Apparatus**

A Waters model 590 HPLC pump (USA) was used to pack capillaries (365 µm o.d., 50 µm i.d.) from Polymicro Technologies (USA). Unions, fittings, tubing and capillary sleeves were obtained from Upchurch (USA). Stainless steel screen (2 µm mesh, 1/16" OD) was from Western Analytical Products Inc. (USA). The packing equipment shown in Figure 2-1 was employed for all bead packing. A syringe pump from Harvard (PHD 2000 infuse/withdraw, Quebec, Canada) was used to deliver polymer solution from a 250 µL Hamilton syringe (USA) into a packed capillary to make an inlet frit through photoinitiated polymerization. An Ultraviolet (UV) Transilluminator (wavelength: 254 nm, filter size: 6×6 inch, six 15W UV tubes) from Spectroline (USA) was used. All size-exclusion electrochromatography (SEEC) was done on a Beckman P/ACE system 5010 (USA) with a 488 nm laser module. A diagram of the instrumental set-up of CE is illustrated in Figure 3-1. The CE instrument was thermostatted to 25°C.

### **3.2.3 Fabrication of Packed Capillary**

For silica beads, the same procedure outlined in chapter 2 was used. However, that procedure was modified for polymer beads because they cannot withstand the high temperature used for frit formation. Frits were fabricated with a photoinitiated polymerization method.

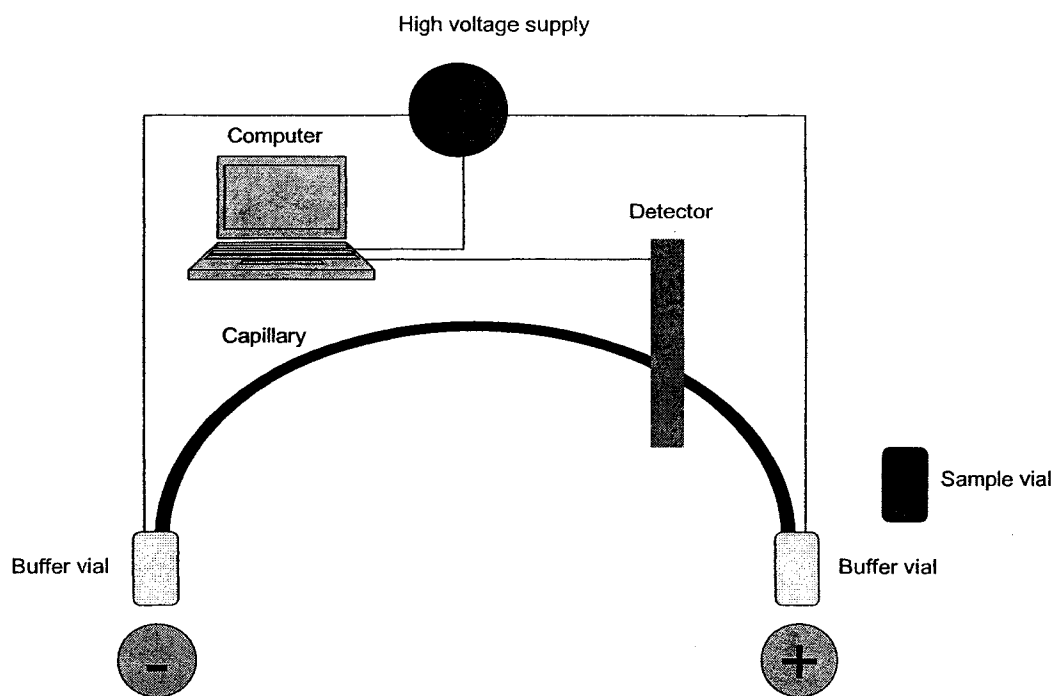


**Figure 3-1 Cartoon of a conventional capillary electrophoresis system.**

### 3.2.3.1 Silanization of Capillary Wall

A 33.5 cm long capillary was cut, then the polyimide coating was removed at 2 small regions (1 mm long each) 6.3 cm apart. A detection window (2-3 mm) was made 0.5 cm away from the outlet frit. Silane solution was prepared by mixing 1 mL of 3-(trimethoxysilyl)propylacrylate and 20 ml of a 5 mM acetic acid solution. To activate the capillary wall, it was rinsed with a Harvard syringe pump and 0.1 M NaOH, then H<sub>2</sub>O, at a flow rate of 1  $\mu$ L/min for 30 minutes each. Then silane solution was delivered at the same flow rate for 60 minutes, and left overnight. The capillary was flushed with acetone and H<sub>2</sub>O to wash away remaining solution, then dried with N<sub>2</sub>, and stored until use.

### 3.2.3.2 Frit Fabrication and Polymer Bead Column Packing

For the fabrication of a packed capillary, porous polymeric frits were made by in situ photoinitiated polymerization of GMA and TRIM, which was described by Irgum<sup>4</sup>. The

porogen mixture ratio was 50/50 isooctane/toluene while the monomer mixture was 50/50 TRIM/GMA, with 1.5% benzoin methyl ether (BME) as photoinitiator. The polymerization solution consisted of porogen and monomer mixtures in a ratio of 60/40. The preparation of polymeric columns was prepared as depicted in Figure 3-2, and outlined below.

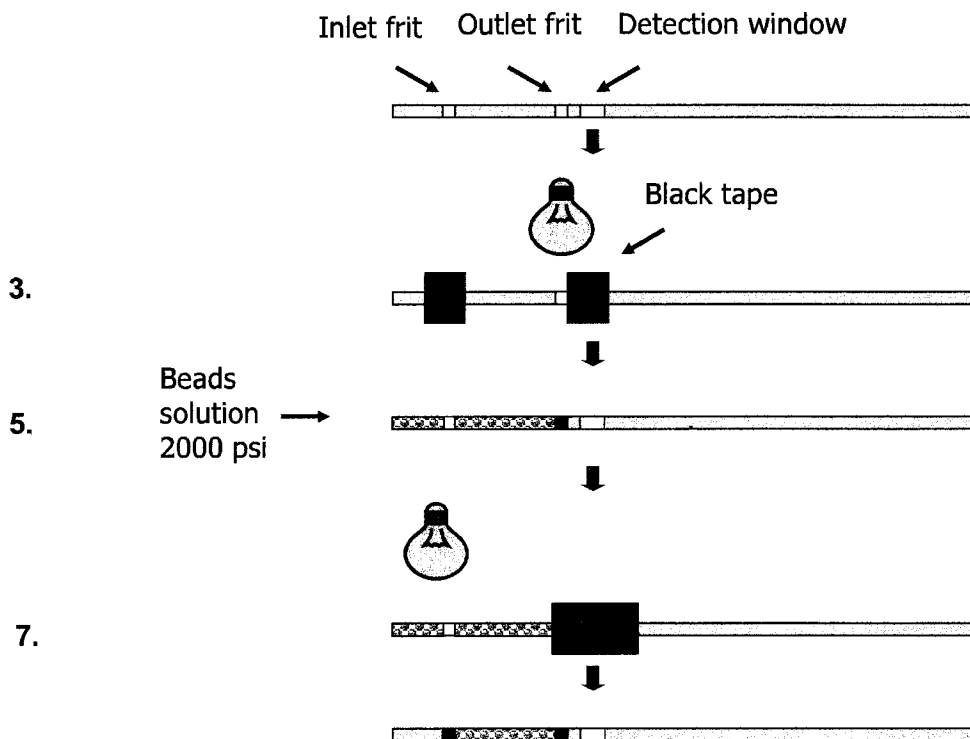


**Figure 3-2 Scheme of capillary packing with polymer beads.**

1. The polymerization solution was sonicated (Branson 1200, USA) for 3 minutes and purged with helium for 5 minutes.
2. The polymerization mixture was introduced into the capillary and sealed at both ends with parafilm.

3. The inlet frit and detection window was covered with black tape and the capillary was placed on the top surface of the UV transilluminator with the window for the outlet frit exposed to UV light (254 nm) for 8 min.
4. The reaction mixture was then removed with ethanol using a 1-mL BD syringe (USA).
5. Polymer beads were slurry packed into the capillary with Waters HPLC pump.
6. Polymer solution was transferred from a 250- $\mu$ L Hamilton syringe into packed capillary with a syringe pump.
7. The outlet frit and detection window were covered with black tape, and step 3 was repeated to make an inlet frit.
8. The capillary was washed in both directions with ethanol followed by water.

### 3.2.4 Protein Labeling

BSA from Sigma was labeled with Alexa Fluor 488 protein labeling kit. 50  $\mu$ L of 1M NaHCO<sub>3</sub> was added to 0.5 mL of 3 mg/mL BSA, then the mixture was transferred into a vial with some powder of reactive dye and mixed well. After the reaction mixture was stirred at room temperature for 1 hour, Alexa Fluor labeled BSA and Alexa Fluor were separated with BioGel P-30 fine size exclusion purification resin from Bio-Rad. The concentration of labeled BSA was calculated from the absorbance of the conjugated solution at 280 nm and 494 nm.

### 3.2.5 Measurement of Protein Electrophoretic Mobility

The measurement of electrophoretic mobility  $\mu_{ep}$  for protein was carried out in an open capillary with the same buffer used for SEEC. With a neutral marker DMSO,  $\mu_{eof}$  in open capillary can be determined.  $\mu_{ep}$  is then calculated from the difference between the apparent mobility of protein and  $\mu_{eof}$ .

### **3.2.6 Size-Exclusion Electrochromatography**

SEEC was carried out on a Beckman CE system using P/ACE system 5000 series software for system control and data acquisition. Origin 7.0 was used for data analysis. The buffer was often composed of 10 mM NaH<sub>2</sub>PO<sub>4</sub> (pH=6.7), 0.01% Tween 20, 10% ACN. For LIF detection, a 488 nm laser was used as the excitation source. For UV absorbance, 214 nm was used as detection wavelength. The packed capillary was installed into a Beckman CE cartridge and the length from inlet to detection window was about 7 cm. Proteins were diluted to 2 mg/ml with running buffer for UV detection. Before analysis, the packed capillary was first conditioned with separation buffer using an HPLC pump for at least 30 minutes, to remove any bubbles. Also, the capillary was equilibrated with mobile phase with voltage from 2 to 10 kV until stable current was obtained. All experiments were performed at 25°C.

## **3.3 Results and Discussion**

### **3.3.1 Capillary Packing with Polymer Beads**

#### **3.3.1.1 Information of Polymer Beads**

The technical information of PolySep-P2000 and PolySep-P3000 are given in Table 3-1. This polymer stationary phase is good for water-soluble polymers, proteins and peptides. The synthetic polystyrene divinylbenzene (PSDVB) particle is coated with a highly hydrophilic layer, which minimizes protein adsorption onto the particle surface. Proteins have a folding structure, which means they have a larger hydrodynamic radius than PEG and pullulan with a similar molecular weight. Therefore the exclusion limit for proteins may be smaller than the values listed in the following table. Compared to the BioSep-S2000 silica beads that are also used for size-exclusion, polymer beads have a wider pH range of 3.0-12.0.

	PolySep-GFC-P2000	PolySep-GFC-P3000
Exclusion Limits in		
Daltons:		
PEG	$9 \times 10^3$	$5 \times 10^4$
Pullulans	$1 \times 10^4$	$1 \times 10^5$
Separation Range (Da)	100-10k	250-75k
pH Range	3.0 to 12.0	

**Table 3-1 Technical data for PolySep-GFC-P beads.**

### 3.3.1.2 Activation of Capillary Wall

As recommended in the literature by Hjertén<sup>5, 6</sup>, a bifunctional compound, 3-(trimethoxysilyl)propyl acrylate, was used to derivatize the capillary wall through the reaction between methoxy groups and silanol groups at the surface of the capillary wall. Meanwhile, the acryl groups in this compound took part in later polymerization processes to anchor the polymer monolith to the capillary wall. Based on experience, without activation of the capillary wall the polymer monolith frit could not withstand the high pressure used in the packing process.

### 3.3.1.3 Frit Fabrication

The frit is a critical parameter in column performance. Bubble formation is often associated with the frit. For silica bead packing, beads are sintered together to fabricate a frit. The characteristics of beads are changed by sintering, possibly leading to nonuniform EOF at the frit. The resulting discontinuity of flow velocity at the interface of the packed and open segment of a CEC column can cause bubble formation<sup>7, 8</sup>. Bubble formation can be minimized by using short and highly permeable frits, well degassed solvents, lower temperature as well as by applying pressure at both ends of the capillary. There is little or

no control of porosity of sintered frits. Under high temperature, polymeric beads can melt, thus conventional heating methods are inappropriate for polymer beads. However, the pore size can be varied when using organic monomers to make a polymer frit. So far, several groups have tried to use photopolymer frits for capillary electrochromatography (CEC) and achieved good results<sup>9-11</sup>. Not all monoliths can be used to fabricate polymer frits. Most polymer networks collapse under high pressure (> 1000 psi) so that they cannot be used for such purposes.

Irgum<sup>4</sup> developed a photoinitiated polymerization method to make a macroporous polymer. The porogenic solvent is a mixture of toluene and isooctane, trimethylolpropane trimethacrylate (TRIM) is used as cross-linker, glycidyl methacrylate (GMA) is the reactive monomer and BME is the photoinitiator. The monolith produced has well-defined pore sizes and a narrow pore distribution. Irgum studied the effect of the porogenic solvent, percentage of cross-linking monomer and the ratio between the monomer and porogen phases on the porous properties of the monoliths. Based on these results, the recipe used in this study was selected to make the polymer frits. Based on Irgum's results, the mean diameter of the pores obtained should be 4.5  $\mu\text{m}$  while the pore diameter at the highest peak in the pore size distribution curve should be 5  $\mu\text{m}$ .

The free-radical photoinitiator benzoin methyl ether (BME) is widely used. The structure and UV absorption spectrum of BME are shown in Figure 3-3. BME adsorbs in the wavelength range of 220-380 nm with a maximum at 254 nm. Our early studies used a UV lamp to irradiate the silanized capillary. Compared to the UV transilluminator, the UV lamp produces much more heat. The exposure time of the capillary to UV light was comparable for both sources. However, the heat from the UV lamp resulted in diffusion of the monolith into the area close to the frit window. With the UV transilluminator, the edge of the polymer frit is clear and sharp, and the length of the frits is just 1 mm. From SEM images of both polymer particles the particle size was measured, using a ruler provided in the software. For PolySep-P2000 beads, the particle diameter ranges

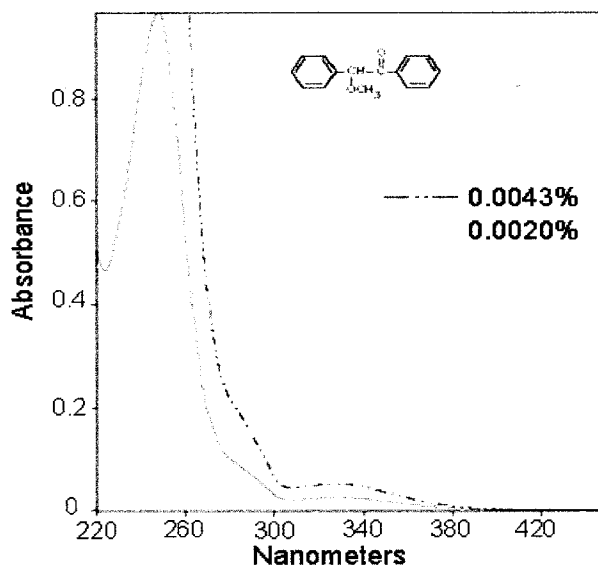
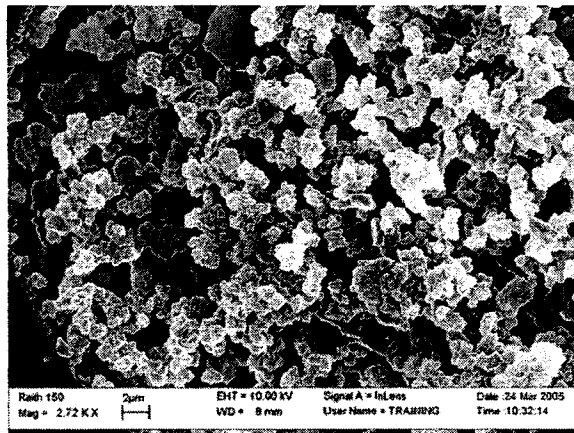


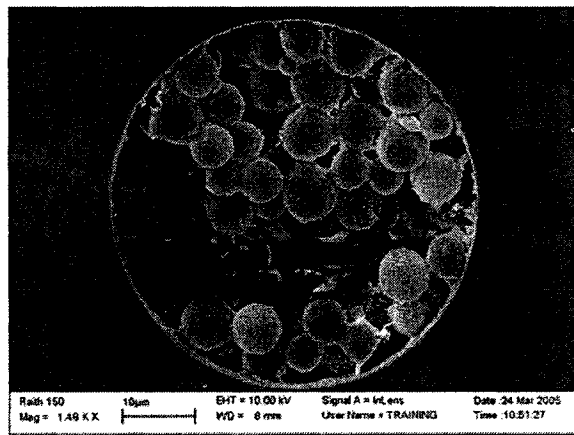
**Figure 3-3 UV absorption spectrum of benzoin methyl ether (BME). Figure taken from <http://www.sigmaaldrich.com/img/assets/3900/Photoinitiators.pdf>**

from 4.7 to 8.2  $\mu\text{m}$  while it varies from 5.7 to 8.0  $\mu\text{m}$  for PolySep-P3000 beads. Although some beads are smaller than 5  $\mu\text{m}$ , no particles were found to pass through the macroporous frit during the packing process or SEEC separations. This can be explained by the tortuous pore structure of the monolith and the “keystone effect”<sup>12</sup>; some particles act as “keystones” to block others and realize particle packing. The frits were tested to withstand at least 2000 psi.

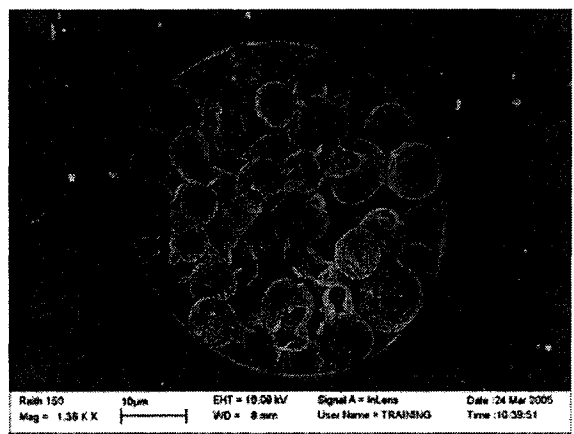
Figure 3-4 shows SEM images of frits and packed beads. Figure 3-4 (A) depicts the macroporous polymer made in a capillary. The pores are big enough to give good porosity for packing. Inlet frits and outlet frits have different appearances. This can be explained by the different composition of the polymerization mixture. During the packing process, the polymer beads filled up to the inlet of the capillary, so that the polymerization of the inlet frit was performed in a mixture of polymer solution and polymer beads.



(A)



(B)



(C)

**Figure 3-4 Scanning electron micrographs of (A) photopolymerized outlet frit, (B) embedded polymer beads, (C) photopolymerized inlet frit with embedded polymer beads.**

### 3.3.1.4 Capillary Packing

After frit fabrication, the capillary has three parts that are not polyimide coated, which makes it fragile and easily broken, so special care must be taken in capillary handling. The packing procedure described in Chapter 2 had to be modified. With the photopolymer outlet frit, no mechanical frit is needed for the packing process. Also, the ultrasonicator cannot be used because the shaking will damage the capillary. The polymer support is not as rigid as silica beads, so very high pressure is not good for the polymer beads, because it will destroy the polymer structure.

If the capillary is packed with silica beads, sometimes a very short gap was formed near a frit after voltage was applied across the column. Qi<sup>13</sup> observed similar phenomenon and reported that a gap shorter than 2 mm had little effect on migration reproducibility. Such a gap was never observed in the polymer beds. The polymer beads may swell in solutions, so that any void due to flow induced compression is filled.

### 3.3.2 SEEC with BioSep-S2000 Column

#### 3.3.2.1 Concentration Effect

When SEEC was applied to BSA, BSA was held up in a 6.3 cm packed bed and did not pass the detection window. What happened to the labeled BSA in SEEC? To study this, 20 psi was applied, instead of voltage, to drive BSA through the SEC column. The high pressure (20 psi) provided by the Beckman CE is very low for conventional LC. However, it is still high enough to make protein elute out of a packed capillary. The two traces in Figure 3-5 show the elution of BSA by different driving forces. Although, BSA did elute within 10 minutes in LC mode, it did not elute out after 50 minutes when using 10 kV. This observation agrees with that of Shepodd,<sup>1</sup> who observed that, with a monolithic silica/acrylate hybrid reverse-phase stationary phase, protein analytes were immobilized in CEC mode and released under HPLC mode. The authors explained this by electrokinetic trapping resulted from overlap of electrical double layers in nanopores.

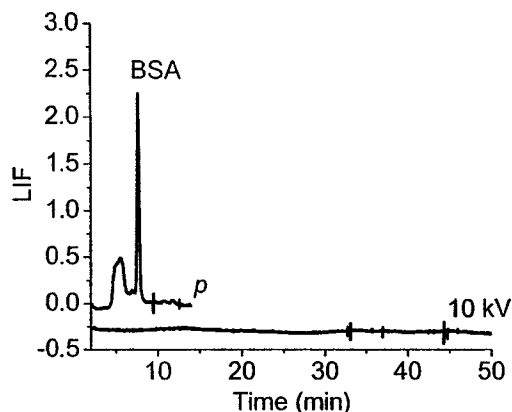


**Figure 3-5 BSA elution with pressure and voltage (10 kV). Buffer: 10 mM  $\text{NaH}_2\text{PO}_4$  (pH=6.7), 0.01% Tween 20, 10% ACN, injection: pressure 0.2 min, packed length: 6.3 cm, Bio-2000.**

Even though BSA did not elute from a packed bed with voltage, it escaped once voltage was replaced by pressure. No matter how long the voltage was applied to the SEEC system before a driving force change, BSA showed similar elution time and pattern. This is demonstrated in Figure 3-6. The BSA injected by voltage for longer times gave somewhat higher peaks. The reason why the elution time is shorter for pressure elution after applying voltage across the column for a period of time and why there are several peaks shown in Figure 3-6 is not clear. Figure 3-6 implies that the protein was trapped within a narrow zone at the entrance of the capillary. This is also confirmed by fluorescence images (Figure 3-7) of both frits. There is much stronger fluorescence signal at inlet than outlet, while no signal was observed at the detection window.

Figure 3-8 illustrates chromatograms of labeled BSA with pressure injection and electrokinetic injection. The first peak in the chromatogram is from impurity or aggregation of BSA, and the second peak represents labeled BSA. Here, the injection time has a different effect on the peak intensity for the two injection methods. With pressure injection (Figure 3-8(A)), both peaks became higher and broader as injection time increased from 0.2 min to 0.6 min. A longer injection time increases signal of these

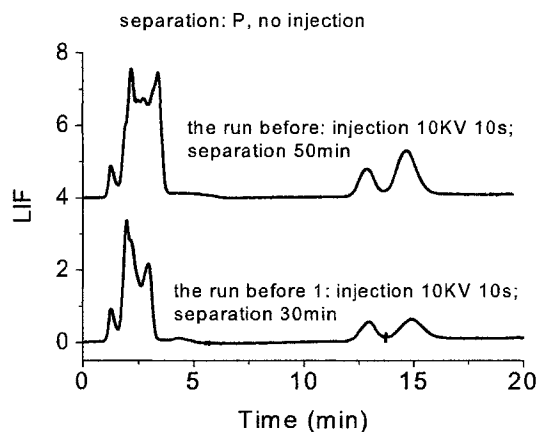


**Figure 3-6** Elution profiles of 5  $\mu\text{M}$  BSA under pressure after applying 10 kV for different length of time: 30 minutes and 50 minutes. Buffer: 10 mM  $\text{NaH}_2\text{PO}_4$  (pH = 6.7), 0.01% Tween 20, 10% ACN, injection: pressure 0.2 min, packed length: 6.3 cm, Bio-2000.

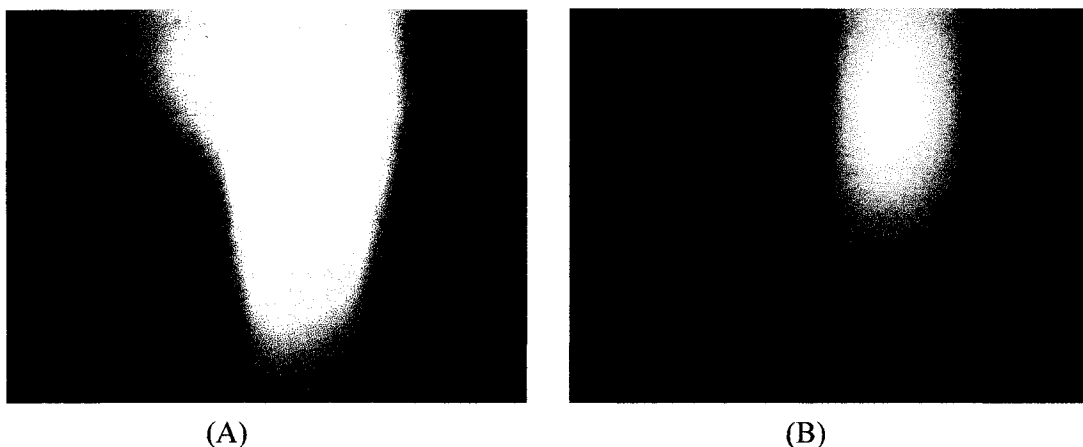


**Figure 3-7** Fluorescence images of (A) inlet frit, (B) outlet frit. The images were taken after several runs of BSA in SEEC.

2 peaks to the same degree. However, injection time has a different effect on these two species if electrokinetic injection is used. In Figure 3-8(B), the intensity and peak width of the first peak increases with injection time in a manner similar to that with pressure injection. In contrast, the peak width of the second peak (BSA) remained the same, while

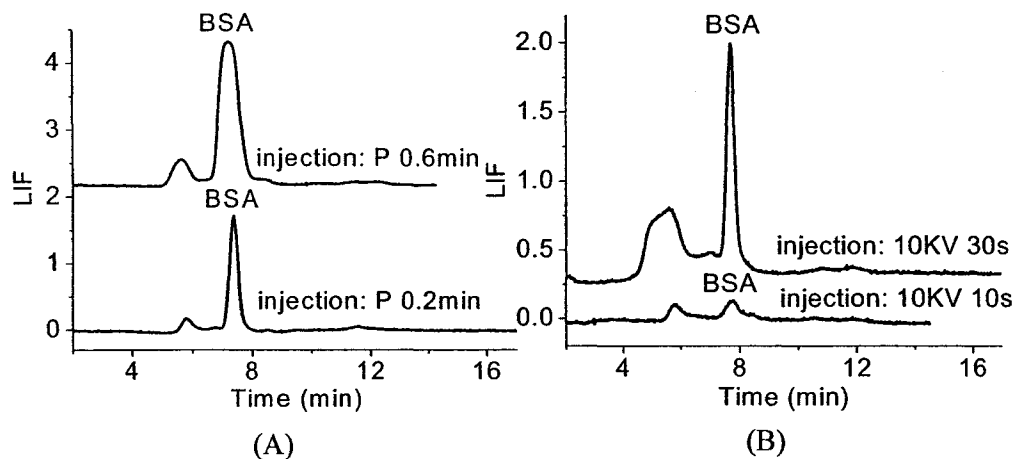


**Figure 3-8 Effect of Changing injection time for 5  $\mu$ M labeled BSA. (A) pressure injection, (B) electrokinetic injection. Pressure (20 psi) was applied to elute BSA out. Running buffer was 10 mM  $\text{NaH}_2\text{PO}_4$  with 0.01% Tween 20, 10% ACN. Separation: pressure, packed length = 6.3 cm. total length = 27 cm.**

the intensity increased dramatically. A similar concentration effect was also observed by Singh's group<sup>1, 2</sup> for several proteins in CEC. The source of this effect is explored in section 3.3.3.2.2.

### 3.3.2.2 Pressure Assisted SEEC

Pressure assisted SEEC (pSEEC) is a separation method in which both pressure and voltage are applied to a packed SEC column. pSEEC is an intermediate of SEEC and SEC wherein the separation is also an interplay of SEEC and SEC. EOF caused by the voltage is superimposed on hydrodynamic flow caused by pressure. Compared to SEEC, the pressure in pSEEC helps to suppress bubble formation under voltage and speed up the separation process, without much change in resolution. Karger<sup>14</sup> and Lubman<sup>15</sup> used pressure assisted CEC-MS to detect peptide mixtures with high efficiency.

A pressure of 20 psi was applied with various voltages to a capillary with 6.3 cm packed bed. Figure 3-9 shows the elution of native and denatured  $\beta$ -lactoglobulin B with a combination of pressure and voltage. Here,  $\beta$ -lactoglobulin B was denatured in SDS

buffer for capillary electrophoresis at 95 °C for 5 min. The migration time decreases as the electric field increases. Denatured  $\beta$ -lactoglobulin B gave sharper peaks than native protein. The protein-surface interaction was presumably minimized because denatured protein was unfolded and surrounded by SDS molecules.

IgG was also tested with pSEEC. However, poor results were obtained. Peak intensity changed a lot, and sometimes more than one peak appeared. These poor results may be induced by adsorption and/or trapping of the protein.

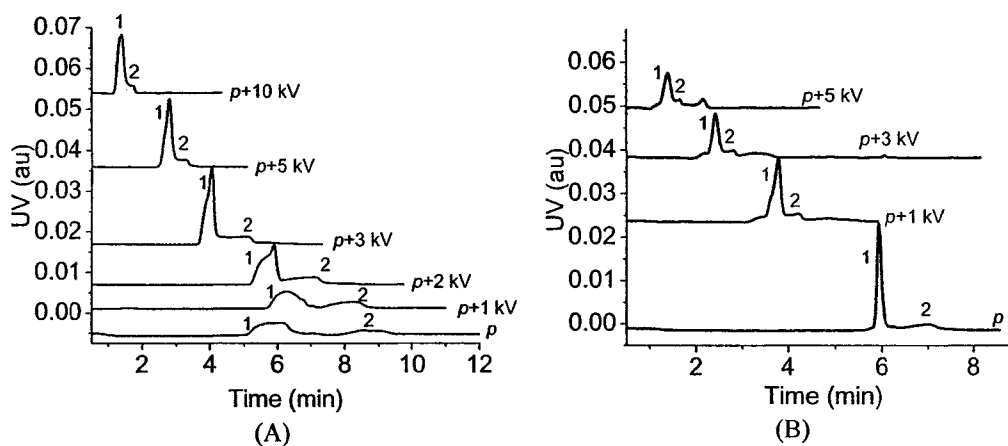


**Figure 3-9** Elution profiles of pSEEC of (A) 2 mg/mL native  $\beta$ -lactoglobulin, (B) 2 mg/mL denatured  $\beta$ -lactoglobulin. buffer: 10 mM  $\text{NaH}_2\text{PO}_4$  (pH = 6.7), 0.01% Tween 20, 10% ACN, injection: pressure 0.2 min, packed length: 6.3 cm. Peak: 1.  $\beta$ -lactoglobulin; 2. solvent peak.

### 3.3.3 SEEC with PolySep-P Column

#### 3.3.3.1 Relationship between Current and Voltage

Figure 3-10 shows a plot of the current as function of the applied field in a PolySep-P3000 packed capillary. From the good linear relationship between current and voltage, it can be concluded that no excessive heat is produced in the packed capillary within a range of 2-20 kV. Mobile phase with high ionic strength can easily cause Joule-heating in CEC, and induced bubbles leading to breakdown in an ohmic current response. In our system, 10 mM  $\text{NaH}_2\text{PO}_4$  (pH=6.7) was chosen as the buffer to

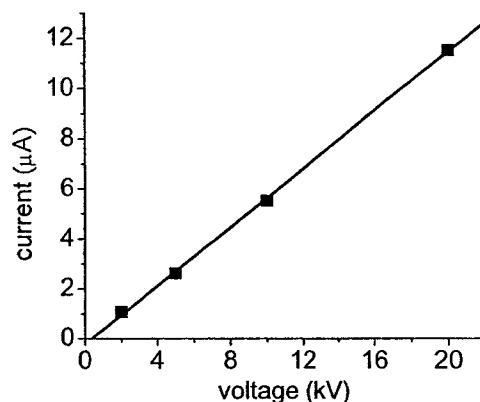


**Figure 3-10 Current as a function of voltage for PolySep-P3000 polymer beads packed capillary. Buffer: 10 mM NaH<sub>2</sub>PO<sub>4</sub> (pH = 6.7), 0.01% Tween 20, 10% ACN. Packed length = 6.3 cm. Total length = 27 cm. ( $R^2 = 0.9997$ ).**

minimize such a problem. However, when bubbles are generated they can often be removed by attaching the packed capillary to HPLC pump and flushing mobile phase through to sweep out bubbles. This process normally takes several minutes.

### 3.3.3.2 Effect of Injection Time

Results in Figure 3-11 show that electrokinetic injection time has different effects for different proteins in a PolySep-P2000 packed capillary. The first peak in these two graphs is from protein, while the second one is the solvent peak (determined by a blank) due to the mismatch of refractive index between the sample buffer and separation buffer. For  $\beta$ -lactoglobulin B, a capillary packed with polymer beads showed a similar protein concentration effect to that seen with silica beads. However, the avidin peak became both higher and broader, and did not show the kind of stacking effect seen for  $\beta$ -lactoglobulin B. For PolySep-P2000 beads, both  $\beta$ -lactoglobulin B and avidin are totally excluded from pores, based upon their molecular weight and the polymer SEC range (Table 3-1). We conclude that the protein concentration does not occur inside the pores. Avidin (66k) is much bigger than  $\beta$ -lactoglobulin B (18k), and avidin (pI = 10-10.5) is positively charged,

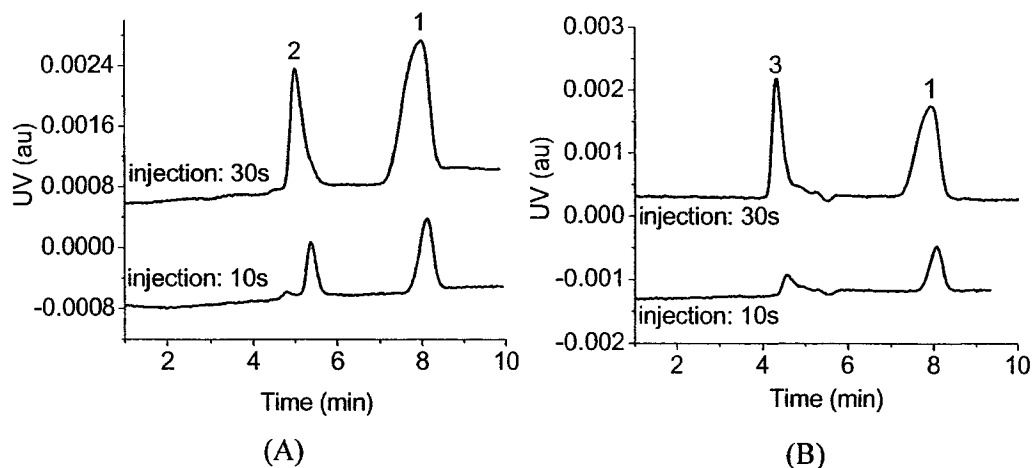


**Figure 3-11 Effect of injection time on different proteins: (A) 2 mg/ml avidin, (B) 2 mg/ml  $\beta$ -lactoglobulin B. Buffer: 10 mM  $\text{NaH}_2\text{PO}_4$  (pH = 6.7), 0.01% Tween 20, 10% ACN, injection: 10 kV, separation: 20 psi pressure, packed length: 6.3 cm, stationary phase: PolySep-P2000. Peak: 1. solvent peak; 2. avidin; 3. BSA.**

while  $\beta$ -lactoglobulin B ( $pI = 5.2$ ) is negatively charged under the experimental condition. The results show that the concentration effect does not have to occur within the pores, but that it is related to the protein charge.

### 3.3.3.2.1 Models for Concentration Effect

Compared to conventional capillaries, the fluids in nanochannels may show different properties such as reduced EOF, increased viscosity, decreased dielectric constant and rapid decrease of current. Researchers have observed concentration effects resulting from the presence of nanochannels and developed several models to explain the effects.

Timperman<sup>16</sup> found charge related molecular transport through nanoporous membranes, with results similar to those described above. Their proposed explanation is that the analytes are moved toward the poly(vinylpyrrolidone) (PVP) coated membrane (10 or 50 nm pores) by electrokinetic transport because of the small EOF in a PDMS chip, then anions are repelled by the negatively charged diffuse layer of the nanocapillaries while cations pass through. Bohn<sup>17</sup> studied the effect of surface charge density and Debye

layer thickness ( $K^{-1}$ ) on molecular transport through nanoporous membranes. The author used  $Ka$  (how much the double layer thickness occupies the pore cross section) to distinguish different transport mechanisms. “When  $Ka \sim 1$ , the electrical double layer extends over a significant fraction of the entire cross section, and electroosmosis dominates transport. When  $Ka \gg 1$ , the double layer becomes effectively confined near the walls, ion migration and diffusion dominate”. It was also found that electrostatic interaction enhances molecular transport through membrane pores while electrostatic repulsion inhibits it<sup>17-20</sup>. Swerdlow<sup>21</sup> captured negatively charged bovine carbonic anhydrase,  $\alpha$ -lactalbumin,  $\beta$ -lactoglobulin A and  $\beta$ -lactoglobulin B with Nafion tubing containing  $\sim 10$  Å pores. Negatively charged Nafion restricts passage through the membrane to small cations. The protein concentration was realized by the interaction between the hydrodynamic and electrical forces.

Shepodd<sup>1</sup> achieved efficient concentration for  $\alpha$ -lactalbumin and ovalbumin at pH = 8.4 with a monolithic silica/acrylate hybrid reverse-phase stationary phase. They found that protein analytes were immobilized in the CEC mode, yet released under HPLC mode. Thompson<sup>2</sup> from the same lab imaged this effect with a model protein (FITC-ovalbumin) in a capillary packed with porous silica beads. This effect was simply explained as electrokinetic trapping, resulting from overlap of electrical double layers in nanopores. Liu<sup>22</sup> tested positively charged rhodamine 6G and negatively charged fluorescein in a nanochannel structure and concluded that ion depletion occurs on the anode end region and ion enrichment on the cathode end region of the nanochannels with negatively charged surface, no matter what charge the ion carries. When the double layer overlaps at reduced ionic strength in nanochannels with anionic surface charge, positive ions are dominant in solution over negative ions. Liu showed their results could be explained by transport effects related to this charge imbalance. Han<sup>3</sup> used a nanofluidic filter to concentrate negatively charged proteins. The concentration factor obtained was as high as  $10^6$ - $10^8$ . Han proposed that electroneutrality is locally broken within the induced

electrical double layer at the anodic nanochannel (40 nm deep) which is created by concentration polarization, and co-ions (negatively charged biomolecules) are prohibited from this region. They also suggest that the nonlinear electrokinetic flow (electroosmosis of the second kind) induced by a tangential electric field at the anodic side speeded up the concentration process.

### 3.3.3.2.2 Possible Mechanism in This Work

We have attempted to evaluate the appropriate mechanism to explain our results in SEEC. The magnitude of EOF was tested because it may be critical to the interpretation. In an SEEC bed, a conventional EOF marker like DMSO, thiourea, acetone, etc. cannot be used because they are fully retained. Therefore, a totally excluded analyte is needed. However, charged analytes cannot give exact EOF even when they are excluded from the pores, due to their electrophoretic mobility. Here, IgG was chosen to determine the EOF in an SEEC bed, based on the assumption that its size means it should be fully excluded. The contribution of electrophoresis can be subtracted from the effective mobility, which is given by

$$\mu_{effective} = \frac{l_d l_p}{t V_p} \quad (3-1)$$

where  $t$  is migration time,  $V_p$  is the voltage applied across the packing bed, and  $l_d$  and  $l_p$  are detection length and packing length, respectively. Here,  $l_d \approx l_p$  because the detection window is very close to the outlet frit of packing bed.  $V_p$  is different from the total voltage ( $V_t$ ) across the whole packed capillary and can be deduced from a comparison between an open capillary and packed capillary of the same length. A packed capillary is composed of two parts: a packed bed and an open section.  $V_p$  is given by

$$V_p = V_t - I_p R_{os} \quad (3-2)$$

where  $I_p$  is the current in a packed capillary and  $R_{os}$  is the resistance of the open section. The resistivity of the open section is the same as that of an open capillary. Therefore the

resistance for the open section ( $R_{os}$ ) can be calculated from

$$R_{os} = \frac{R_o l_o}{l_t} = \frac{V_t(l_t - l_p)}{I_o l_t} \quad (3-3)$$

where  $l_t$  is the total length of a packed capillary, while  $l_o$ ,  $I_o$ ,  $V_t$  and  $R_o$  are the length, current, voltage and resistance for an open capillary, respectively.

The EOF in an SEEC bed ( $\mu_{eof}$ ) is given by

$$\mu_{eof} = \mu_{effective} - \mu_{ep} \quad (3-4)$$

where  $\mu_{ep}$  is the electrophoretic mobility of IgG determined in an open capillary (Table 3-3). The measured  $\mu_{ep}$  for several proteins are given in the following table. IgG is positively charged for the given pI of 7.5, but the calculated  $\mu_{ep}$  is negative. This might be due to protein-wall interaction, however people report different pI ranging from 6.5 to 7.5 for IgG. Using IgG as the marker, the calculated EOF values in a 6.3-cm long P3000 column are  $0.58 \times 10^{-4}$  and  $0.88 \times 10^{-4} \text{ cm}^2 \text{ V}^{-1} \text{ s}^{-1}$ , for two different columns.

Protein	MW (k Da)	pI	Calculated $\mu_{ep}$ ( $\times 10^{-4} \text{ cm}^2 \text{ V}^{-1} \text{ s}^{-1}$ )	Electrokinetic transport?
IgG	150	6.5-7.5	-0.18	Yes
Ribonuclease A	18.2	9.6	0.42	Yes
$\beta$ -lactoglobulin B	13.7	5.2	-1.48	No
transferrin	76-81	5.2-5.9	-0.88	No

**Table 3-2 Calculated  $\mu_{ep}$  for several proteins with an open capillary.  
Buffer: 10 mM  $\text{NaH}_2\text{PO}_4$  (pH = 6.7), 0.01% Tween 20, 10% ACN.**

The small EOF in the packed bed may be the major reason for protein concentration here. There is a 1-2 mm open section in front of the inlet frit of packing bed. The EOF in this small section is larger than the EOF in the packed bed and large enough to realize injection even for a negatively charged protein. However, the mismatch of EOF in these two sections may induce recirculating flow and certainly traps negatively charged protein at the inlet. Comparison of an EOF value of  $0.88 \times 10^{-4} \text{ cm}^2 \text{ V}^{-1} \text{ s}^{-1}$  to the values in Table

3-2 for  $\mu_{ep}$  shows that IgG and Ribonuclease A would migrate in the column while  $\beta$ -lactoglobulin B and transferrin would not, which agrees with experiment. The protein concentration observed by Shepodd<sup>1</sup> and Thompson<sup>2</sup> may also be explained by such a mismatch of EOF in a packed capillary, too. This small value of EOF also appears to account for complete retention of negatively charged proteins in SEEC.

### 3.3.3.2.3 Modification of EOF Calculation in a Packed Capillary

From Eq. (3-1),  $\mu_{effective}$  depends on the column architecture such as the  $\zeta$  potential, porosity,  $l_p/l_t$ , etc. Therefore, two columns with different  $l_p/l_t$  and porosity give different EOF. Rathore and Horváth<sup>23</sup> presented a new equation to calculate the EOF in a packed column. Because of the tortuosity ( $\tau$ ) of the packing they argue that the actual flow path of inert and neutral molecules is longer than the length of the packed bed  $l_p$ . The authors used an effective length of the flow path  $l_e$  to substitute for  $l_p$  in Eq. (3-1) and give the following equation for  $\mu_{eo,packed}$

$$\mu_{eo,packed} = \frac{l_e^2}{tV_p} \quad (3-5)$$

Here, the effective length is said to be determined from the current through an open capillary and a fully packed capillary with the same length

$$l_e = \tau l_p = l_p \left( \sqrt{I_o^* / I_p} \right) \quad (3-6)$$

where  $I_o^*$  is the current in the open capillary with the same length of packed bed. Applying this equation to our data set, and normalizing the current to account for the fact that only part of the column was packed, gives values of  $\mu_{eo}$  of  $1.3 \times 10^{-4}$  and  $2.6 \times 10^{-4}$   $\text{cm}^2 \text{V}^{-1} \text{s}^{-1}$  for the two columns we tested.

The relevant Rathore-Horváth equation (Eq. 3-6) is not explicitly derived in their publications, nor in Rathore's thesis. Our attempts to derive this equation were unsuccessful. However, Jianbin Bao in our group was able to derive a somewhat similar

looking equation, which predicts a smaller value of  $l_e$  than the Rathore-Horváth equation. The derivation is presented below.

Interparticle porosity ( $\varepsilon$ ) describes the fraction of the total volume of the capillary that is between the particles and for good packing is usually around 0.4 for a column packed with particles.<sup>24</sup> From this we obtain a relationship between the cross sectional area ( $A_f$ ) of hypothesized open column and the effective length  $l_e$ .

$$\varepsilon = \frac{V_f}{V_c} = \frac{A_f l_e}{A_c l_p} \quad (3-7)$$

where  $A_c$  is the cross sectional area of an open capillary of length  $l_p$ ,  $V_f$  and  $V_c$  are the interstitial volume for packed bed and volume for open column with the same length as packed bed.

The current in an open capillary with a length of  $l_t$  is calculated from

$$I_o = \frac{V_t A_c}{\rho l_t} \quad (3-8)$$

where  $\rho$  is the resistivity of the running buffer. Similarly, the current for a packed capillary with the same length can be calculated by

$$I_p = \frac{V_t}{\rho \frac{l_e}{A_f} + \rho \frac{l_o}{A_c}} \quad (3-9)$$

The use of  $\rho \frac{l_e}{A_f}$  for resistance in the packed bed is justified by Overbeek's model<sup>25</sup> for transport in porous media. Applying the same voltage to an open capillary of length  $l_t$  and a packed capillary segment with length  $l_p$  and open length  $l_o$ , adding to give a current ratio of

$$\frac{I_o}{I_p} = \frac{l_e^2}{l_t l_p \varepsilon} + \frac{l_o}{l_t} \quad (3-10)$$

Therefore, the effective length for the packed bed can be calculated by

$$l_e = \sqrt{\varepsilon l_p l_p \left( \frac{I_o}{I_p} - \frac{l_o}{l_t} \right)} \quad (3-11)$$

In Eq. (3-5) Rathore and Horváth have expressed the electric field as  $V_p/l_e$ . This seems to be incorrect, in that the electric field vector will be directed longitudinally along the column, which has a length  $l_p$ . Unlike the molecules it will not be directed through the tortuous pathways.

Consequently, we evaluated the mobility using the following equation

$$\mu_{eo,packed} = \frac{l_p l_e}{t V_p} \quad (3-12)$$

The values obtained from the above analysis are  $0.62 \times 10^{-4}$  and  $1.0 \times 10^{-4} \text{ cm}^2 \text{ V}^{-1} \text{ s}^{-1}$  for the two columns evaluated. The parameters used to calculate  $\mu_{eo,packed}$  are listed in Table 3-3.

	Packed Capillary 1	Packed Capillary 2	Open Capillary
Packed Length (cm)	7	7	
Total Length (cm)	27	27	27
Voltage (kV)	10	10	10
Current ( $\mu\text{A}$ )	5.3	5.6	8.6
Migration Time of IgG (min)	2.14	3.99	
$\mu_{eo,packed}$ ( $\times 10^{-4} \text{ cm}^2 \text{ V}^{-1} \text{ s}^{-1}$ )	1.0	0.62	

**Table 3-3 Parameters used for EOF calculation in packed capillary. Buffer: 10 mM  $\text{NaH}_2\text{PO}_4$  (pH = 6.7), 0.01% Tween 20, 10% ACN.  $\mu_{ep}$  for IgG under experimental condition is  $-0.18 \times 10^{-4} \text{ cm}^2 \text{ V}^{-1} \text{ s}^{-1}$ .**

Comparison of these EOF values to the electrophoretic mobilities in Table 3-2 shows that IgG and ribonuclease A would be expected to migrate to the detector, while  $\beta$ -lactoglobulin B would not, and the case for transferrin is marginal.

### 3.3.3.3 Elution of Various Proteins

The elution of native  $\beta$ -lactoglobulin B, denatured  $\beta$ -lactoglobulin B (denaturation procedure shown in section 3.3.2.3), ribonuclease A and IgG with SEEC is demonstrated in Figure 3-12. Native  $\beta$ -lactoglobulin B was retained in the capillary, while denatured  $\beta$ -lactoglobulin B, native IgG and native ribonuclease A could elute from the packed bed.

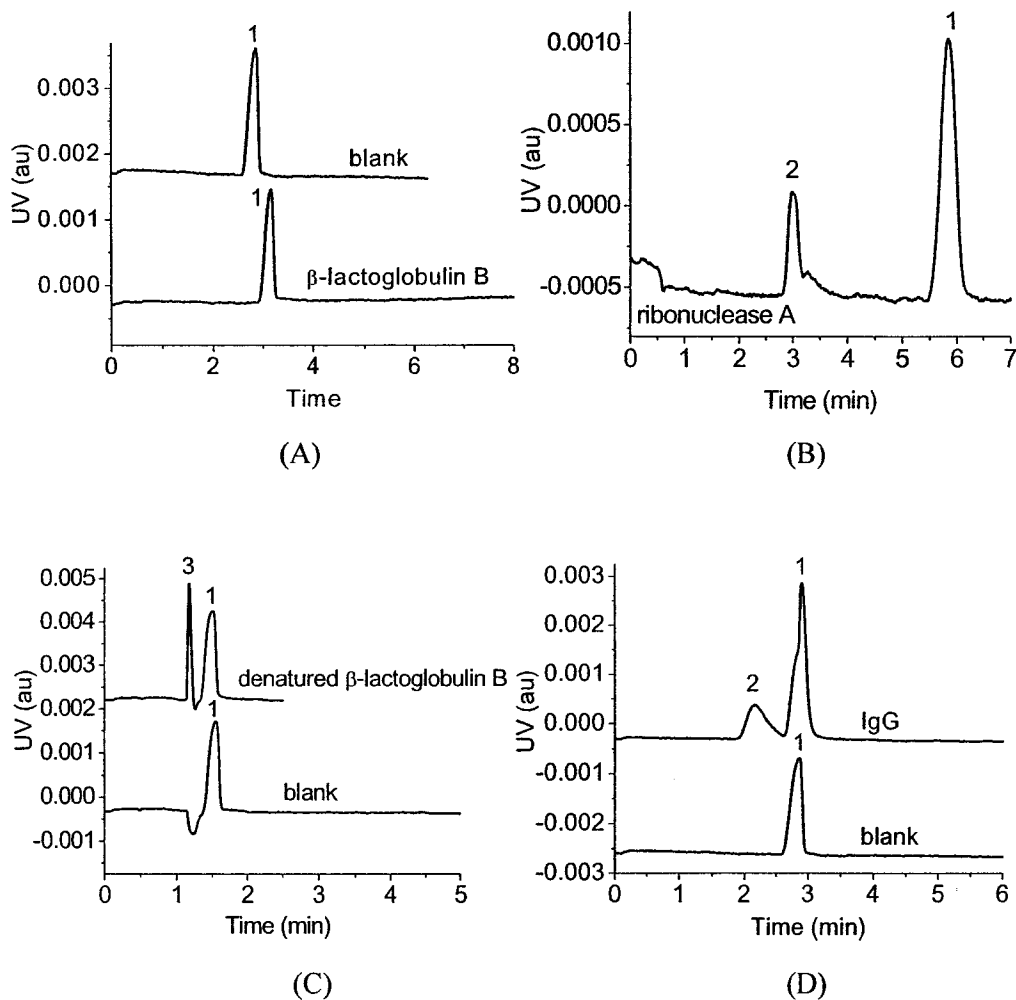


**Figure 3-12** Electrochromatograms of various proteins in SEEC. (A) 2 mg/ml  $\beta$ -lactoglobulin B, (B) 2 mg/ml ribonuclease A, (C) 2 mg/ml denatured  $\beta$ -lactoglobulin B, (D) 2 mg/ml IgG. Buffer: 10 mM  $\text{NaH}_2\text{PO}_4$  (pH = 6.7), 0.01% Tween 20, 10% ACN, injection: 10 kV 15 s, packed length: 6.3 cm, stationary phase: PolySep-P3000. Peak: 1. solvent peak; 2. ribonuclease A; 3. denatured  $\beta$ -lactoglobulin B; 4. IgG.

The larger protein BSA was similar to  $\beta$ -lactoglobulin B, with the native form being trapped, while the denatured form was not. Similar to silica bead packed columns, denatured protein eluted as a sharper peak in the polymer column, and was separated from the solvent peak. The tendency of native proteins to elute appears directly related to the net mobilities of the proteins in the packed column. The transport of negatively charged denatured protein might contradict the above trends. However, the SDS added will increase the EOF by adsorption, which will increase overall transport. Denaturing in SDS also greatly changes the shape and size of proteins, giving them a near constant, negative charge to mass ratio, which may also be a factor. It should be noted that the running buffer was the standard 10 mM modified phosphate buffer, not the high ionic strength, low mobility, SDS denaturing buffer. As a result the EOF suppressing effect of the ionic strength of the denaturing buffer would be diluted out, while the effect of SDS adsorption on EOF would cause increased EOF.

#### **3.3.3.4 Pressure Assisted SEEC**

All injections described below used pressure. In contrast to electrokinetic injection, injection by pressure can transfer the same amount of sample into a packed capillary no matter what charge the sample carries. Figure 3-13 illustrates pSEEC results for four proteins. As the voltage is increased,  $\beta$ -lactoglobulin B no longer elutes from the column, while at still larger values transferrin is also retained. The positively charged protein, ribonuclease A, always elutes. Size alone is not the issue, since  $\beta$ -lactoglobulin B and ribonuclease A have similar size, but opposite charge. Based on information in Table 3-1, both transferrin (76-81k) and IgG (150k) are excluded from the pores while  $\beta$ -lactoglobulin B (18.2k) and ribonuclease A (13.7k) are retained, based on the technical information from the manufacturer about molecular weight selectivity. Transferrin is just large enough that it will be weakly retained, given a stated exclusion limit of 75 kDalton. The observed capture trend is consistent with the net mobilities determined for these

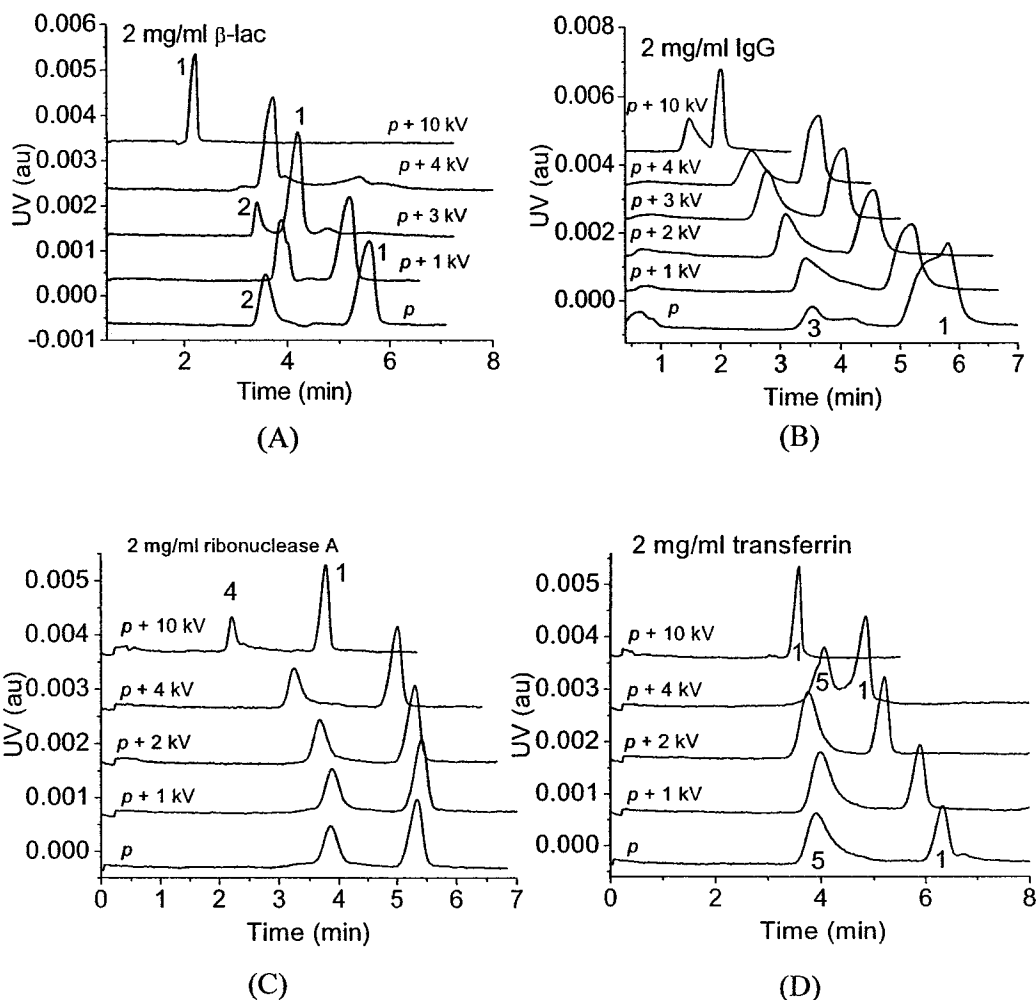


**Figure 3-13 Elution profiles of various proteins in pSEEC. (A) 2 mg/ml  $\beta$ -lactoglobulin B, (B) 2 mg/ml IgG, (C) 2 mg/ml ribonuclease A, (D) 2 mg/ml transferrin. Buffer: 10 mM  $\text{NaH}_2\text{PO}_4$  (pH = 6.7), 0.01% Tween 20, 10% ACN, sample: 2 mg/ml ribonuclease A, injection: pressure 0.2 min, packed length: 6.3 cm, stationary phase: PolySep-P3000. Peak: 1. solvent peak; 2.  $\beta$ -lactoglobulin B; 3. IgG; 4. ribonuclease A; 5. transferrin.**

proteins in the beds.

With pSEEC, the pressure can compensate for the velocity difference in opposite directions at low electric field while the latter dominates at high electric field, which is the reason why the peak of negative protein always appears in electrochromatograms under low electric field and eventually disappears as the voltage increases. The sign and

magnitude of electrophoretic mobility decides if the protein will be fully retained and which protein will be fully retained first at the same electric field.

Separation of  $\beta$ -lactoglobulin B, BSA and IgG is shown in Figure 3-14. Protein separation in pSEEC is shown in Figure 3-14(A). With 20 psi only, these 3 proteins cannot be resolved. However, when pressure and voltage were both applied to the capillary, 3 proteins could be baseline resolved. The resolution for IgG and  $\beta$ -lactoglobulin B ( $R_{s1}$ ) as well as  $\beta$ -lactoglobulin B and BSA ( $R_{s2}$ ) are given in Table 3-4. As voltage increased, the retention of BSA was stronger, so that the BSA peak became broader and almost disappeared when the voltage was increased to 10 kV. The resolution for  $\beta$ -lactoglobulin B and BSA increases with electric field. This might be due to changes in retention with changing electric field arising from the different charge and mobility. The results show that pSEEC can be used as fractionator for proteins. Protein separation with CE is shown in Figure 3-14(B). BSA got lost in open capillary, which might be due to the large  $\mu_{ep}$  or much stronger adsorption onto the wall surface than in packed capillary. Comparing these two graphs in Figure 3-14, the elution order for IgG and solvent is different, which means packed capillary still shows some SEC effect in pSEEC.

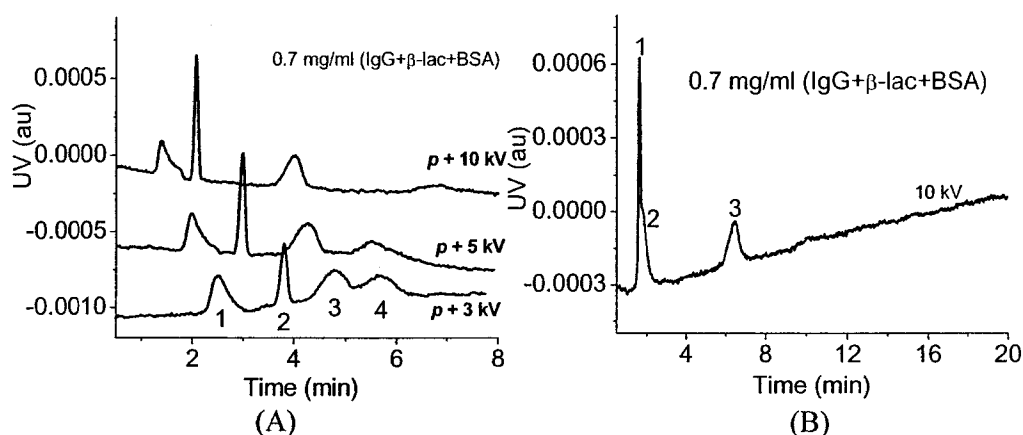


**Figure 3-14 Protein separation with (A) pSEEC, injection: pressure 0.2 min, packed length: 6.3 cm, stationary phase: PolySep-P3000; (B) CE, injection: 10 kV 6s, detection length: 7 cm. Sample: 0.7 mg/ml ( $\beta$ -lactoglobulin B+BSA+IgG), buffer: 10 mM  $\text{NaH}_2\text{PO}_4$  (pH = 6.7), 0.01% Tween 20, 10% ACN, , Peak: 1. IgG; 2. solvent peak; 3.  $\beta$ -lactoglobulin B; 4. BSA.**

Resolution	R <sub>s1</sub>	R <sub>s2</sub>
P+3 kV	2.9	0.8
P+5 kV	3.6	1.3
P+10 kV	4.6	3.3

**Table 3-4 Resolution varies with voltage for 3 proteins.**

The protein separation here is quite fast, within 7 minutes. A similar combination of pressure and voltage was also used by several groups for proteins studies. Ladisch<sup>26, 27</sup> and Cole<sup>28</sup> superimposed a small electric field (12-100 V/cm) on pressure driven flow with at least a 30 cm long column (1.5 cm i.d.) and the protein separation took more than 1 hour, up to 11 hours. Tan<sup>29</sup> applied a low-voltage electric field perpendicular to the pressure direction (pSEEC) with a column design of rectangular cross-section (12.0×0.5×1.2 cm<sup>3</sup>) and accomplished separation of BSA and myoglobin within 25 minutes. In this work, capillaries with smaller inner diameter were used so that Joule heating can be dissipated efficiently even under larger electric field (100-330 V/cm). Therefore, the separation speed is increased.

### 3.3.3.5 Effect of Pore Size

Figure 3-15 represents pSEEC results with PolySep-P2000 beads. PolySep-P2000 has a smaller exclusion limit than PolySep-P3000 column, from which we deduce that PolySep-P2000 beads have a smaller pore size. The traces in Figure 3-15 are similar to those in Figure 3-13. When the electric field is increased, the retention of negatively charged proteins became stronger until finally they were totally retained inside the packed capillary. Positively charged proteins eluted out at any voltage tested. Comparing the results for  $\beta$ -lactoglobulin B on both PolySep stationary phases, it is found that a higher electric field is needed for the protein to be totally retained in a capillary packed with PolySep-P3000 beads. This is most likely related to the larger effective pore size of PolySep-P3000 beads. The flow resistance is smaller for particles with a larger pore. Also

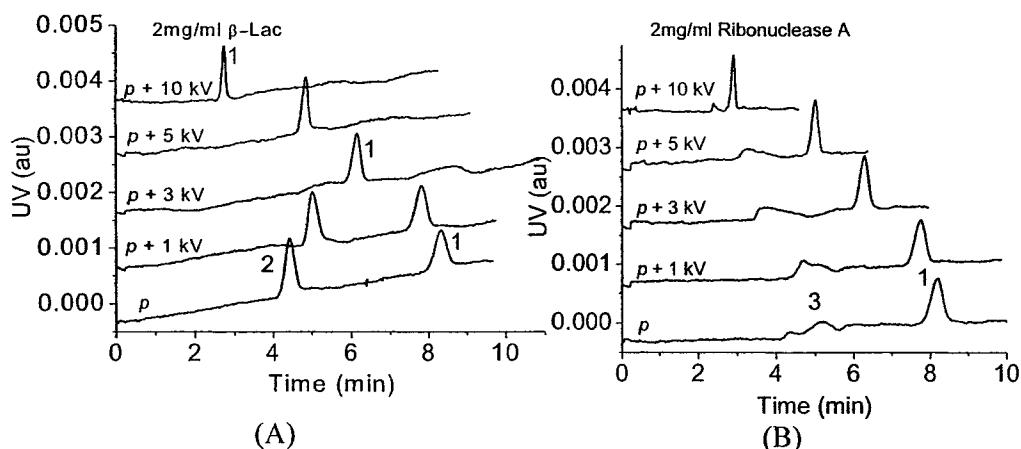


**Figure 3-15** Elution profiles of two proteins in pSEEC. (A) 2 mg/ml  $\beta$ -lactoglobulin B, (B) 2 mg/ml ribonuclease A. Buffer: 10 mM  $\text{NaH}_2\text{PO}_4$  (pH = 6.7), 0.01% Tween 20, 10% ACN, injection: pressure 0.2 min, packed length: 6.3 cm, stationary phase: PolySep-P2000. Peak: 1. solvent peak; 2.  $\beta$ -lactoglobulin B; 3. ribonuclease A.

the EOF increases with increasing pore size.<sup>16</sup> Additionally, this may be related to the role of the double layer thickness inside the pores. Martin<sup>30</sup> studied electrophoretic protein transport in gold nanotube membranes and found that the voltage required to shut down BSA transport increased with the inner diameter of a nanotube.

### 3.3.3.6 Effect of Ionic Strength

The same PolySep-P2000 bead packed capillary used in Figure 3-15 was tested at higher ionic strength. Detection of  $\beta$ -lactoglobulin B by pSEEC in 50 mM  $\text{NaH}_2\text{PO}_4$  buffer is depicted in Figure 3-16. At the higher concentration, the double layer thickness was suppressed and the EOF decreased. The lower the value of EOF the more likely it is the anionic proteins will migrate in the opposite direction to pressure driven flow. As a result, a lower field should be needed to prevent protein elution, but this was not the case.  $\beta$ -lactoglobulin B showed a peak with a combination of pressure and 3 kV in Figure 3-16, while it was retained completely in pSEEC with 10 mM  $\text{NaH}_2\text{PO}_4$  under the same experiment condition. This result supports the model developed by Han, in that a higher

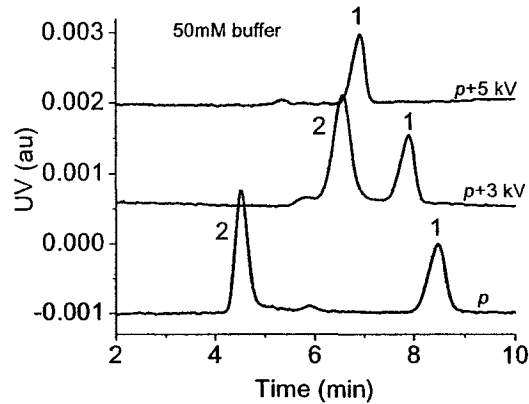


**Figure 3-16 Effect of ionic strength on protein elution in pSEEC. Buffer: 50 mM NaH<sub>2</sub>PO<sub>4</sub> (pH = 6.7), 0.01% Tween 20, 10% ACN, injection: pressure 0.2 min, sample: 2 mg/ml β-lactoglobulin B, packed length: 6.3 cm, stationary phase: PolySep-P2000. Peak: 1 solvent peak; 2. β-lactoglobulin B.**

ionic strength should result in a lower tendency to induce trapping by a charged space layer formed in the vicinity of a pore.

### 3.3.3.7 Effect of pH

The role of pH was also investigated for 2 mg/mL BSA (pI = 4.6) as shown in Figure 3-17. When pH of the mobile phase was higher than the pI, BSA was not observed

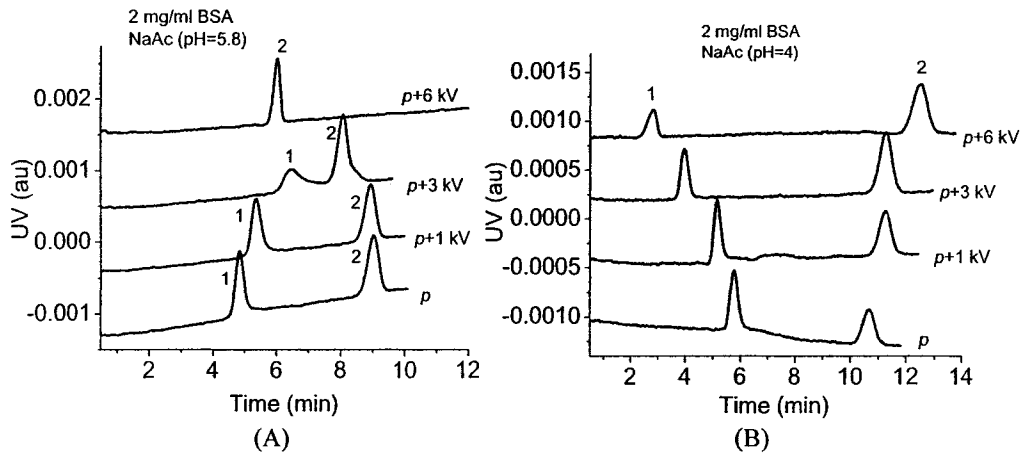


**Figure 3-17 BSA (2 mg/ml) elution in pSEEC at different pH. (A) NaAc buffer (pH = 5.8), (B) NaAc buffer (pH = 4.0). injection: pressure 0.2 min, sample: 2 mg/ml BSA, packed length: 6.3 cm, stationary phase: PolySep-P2000. Peak: 1. BSA; 2. solvent peak.**

once the voltage reached 6 kV. When the pH was less than the pI, BSA was eluted from the column at all voltages tested. Further, BSA moved faster with higher voltage, as would be expected for a cation. We also found that the positively charged BSA passed through the packing bed with only voltage applied.

### 3.3.3.8 Study of DMSO Velocity

Horváth<sup>31</sup> described two theoretical models for EOF in porous media in his review. One is Overbeek's model which is based on von Smoluchowski's work. In this model, EOF varies linearly with electric field if the field strength is low. While in the other kind of model, Dukhin's model, the calculated EOF is higher than expected by classical theories. Electroosmosis of the second kind changes with conductivity and size of particles based on Dukhin's model. This unusual EOF caused by concentration polarization was observed by several researchers.<sup>3, 32, 33</sup> The enhanced EOF can be used to speed up concentration<sup>3</sup> and separation.

7 different buffers were used to determine the mobility of a neutral marker, DMSO. The actual EOF velocity is different from the values shown in Figure 3-18 because DMSO can be retained in pores, so that the migration time is longer than for a pure EOF marker. From Figure 3-18, the measured velocity increases linearly with increasing voltage applied across the capillary. Therefore there is a linear relationship between EOF and electric field, which agrees with Overbeek's model. Here, 0.5% SDS buffer gave the highest EOF. The presence of SDS enhanced EOF in the system, resulting from SDS molecules adsorbing onto the bead surface. Zou<sup>34</sup> also reported that ionic surfactant could be used to modify uncharged monolithic capillary columns to change the direction and magnitude of EOF. However, even with 0.5% SDS buffer, negatively charged  $\beta$ -lactoglobulin B still did not elute out. The produced EOF by buffer containing 0.5% SDS is still not high enough to drive the negatively charged protein out of the bed. The commercial SDS buffer contains the same amount of SDS, but the EOF produced was

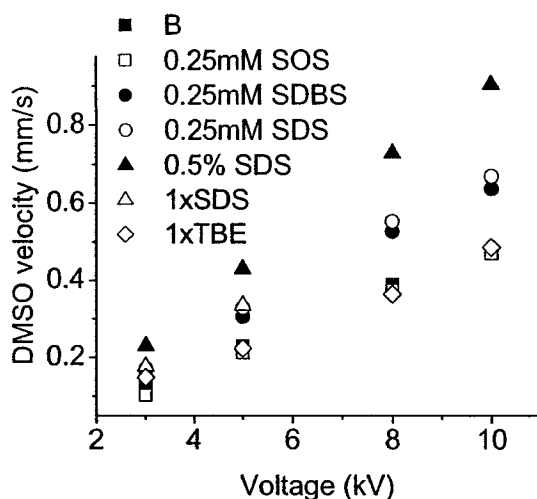


**Figure 3-18 DMSO velocity in SEEC at various voltages. Sample: 1% DMSO, injection: pressure 0.2 min, packed length: 6.3 cm, stationary phase: PolySep-P3000. Buffer (1). 10 mM NaH<sub>2</sub>PO<sub>4</sub> (pH = 6.7), 0.01% Tween 20, 10% ACN; (2). 10 mM NaH<sub>2</sub>PO<sub>4</sub> (pH = 6.7), 0.01% Tween 20, 10% ACN, 0.25 mM SOS; (3). 10 mM NaH<sub>2</sub>PO<sub>4</sub> (pH = 6.7), 0.01% Tween 20, 10% ACN, 0.25 mM SDBS; (4). 10 mM NaH<sub>2</sub>PO<sub>4</sub> (pH = 6.7), 0.01% Tween 20, 10% ACN, 0.25 mM SDS; (5). 10 mM NaH<sub>2</sub>PO<sub>4</sub> (pH = 6.7), 0.01% Tween 20, 10% ACN, 0.5% SDS; (6). 1×SDS buffer; (7). 1×TBE buffer.**

smaller. This presumably results from the high ionic strength in the commercial SDS buffer. Negatively charged biomolecules were not stacked in a microfluidic channel with 1×TBE buffer in Han's study,<sup>3</sup> suggesting nanopore transport effects are not relevant in this buffer. Still, this buffer did not work for negatively charged protein elution in our work. The pore sizes of the polymeric beads used in this work are smaller than that of the nanofilter used by Han, so that the electrical double layer overlap will be present at higher ionic strength than in Han's study, and thus proteins would be more easily concentrated in our columns at higher ionic strength. Both small EOF mobility and nanochannel induced space charge layer can cause negatively charged protein concentration in packed capillary.

### 3.4 Conclusion

The application of SEEC for protein was investigated in this chapter. Some proteins could elute out of the packed bed and give a nice peak while some others were totally retained in the column. Based on the experiment results for several proteins, it was found that protein retention is charge related. For the polymer-based stationary phase, the value of electroosmotic flow we determined for packed beds shows that the tendency of a protein to elute is directly related to its net mobility. The value of  $\mu_{eof}$  in the column is very close to that of many negatively charged proteins, so they tend to be delivered to the front of the packed bed and become trapped there. Adsorption of proteins is clearly shown to occur in both polymer and silica beds, but the clean Gaussian peaks observed show that it does not account for much of the trapping observed.

For silica-based columns we made fewer measurements of EOF, but the values are about 2-3 times higher than in the polymer beds. Thus, net mobility in the silica columns do not necessarily account for the trapping observed. Evaluation of the results for the two different pore sizes of the polymer bead beds shows that decreasing the pore size also gave greater trapping, which does not seem to be  $\mu_{eof}$  dependent. Thus, the results obtained here allow for a possible role for nanopore sized, space charge based trapping to play a role in CEC of proteins in nanoporous media.

Finally, we note that CEC of proteins in monolithic columns has been done successfully without an added pressure. In these monoliths charge was deliberately added to give high EOF, consistent with our mobility-based model of trapping. However, monoliths tend to be microporous, not nanoporous, and so will have much less tendency to exhibit double layer overlap based space charge trapping.

### 3.5 References

- (1) Artau, A.; Singh, A. K.; Shepodd, T. J. *Micro Total Analysis Systems* 2002, 1, 476-478.
- (2) Singh, A. K.; Throckmorton, D. J.; Kirby, B. J.; Thompson, A. P. *Micro Total*

- Analysis Systems* 2002, 1, 347-349.
- (3) Wang, Y.; Stevens, A. L.; Han, J. *Anal. Chem.* 2005, 77, 4293-4299.
  - (4) Viklund, C.; Pontén, E.; Glad, B.; Irgum, K. *Chem. Mater.* 1997, 9, 463-471.
  - (5) Hjertén, S. *J. Chromatogr.* 1985, 347, 191-198.
  - (6) Ericson, C.; Liao, J.; Nakazato, K.; Hjertén, S. *J. Chromatogr. A* 1997, 767, 33-41.
  - (7) Rathore, A. S.; Horváth, C. *Anal. Chem.* 1998, 70, 3069-3077.
  - (8) Wang, G.; Lowry, M.; Zhong, Z.; Geng, L. *J. Chromatogr. A* 2005, 1062, 275-283.
  - (9) Chen, J.; Dulay, M. T.; Zare, R. N. *Anal. Chem.* 2000, 72, 1224-1227.
  - (10) Mistry, K.; Cortes, H.; Meunier, D.; Schmidt, C.; Feibush, B.; Grinberg, N.; Krull, I. *Anal. Chem.* 2002, 74, 617-625.
  - (11) Mistry, K.; Krull, I.; Grinberg, N. *Electrophoresis* 2003, 24, 1753-1763.
  - (12) Ceriotti, L.; de Rooij, N. F.; Verpoorte, E. *Anal. Chem.* 2002, 74, 639-647.
  - (13) Qi, M., University of Alberta, 2002.
  - (14) Ivanov, A. R.; Horváth, C.; Karger, B. L. *Electrophoresis* 2003, 24, 3663-3673.
  - (15) Huang, P.; Jin, X.; Chen, Y.; Srinivasan, J. R.; Lubman, D. M. *Anal. Chem.* 1999, 71, 1786-1791.
  - (16) Zhang, Y.; Timperman, A. T. *Analyst* 2003, 128, 537-542.
  - (17) Kuo, T.; Sloan, L. A.; Sweedler, J. V.; Bohn, P. W. *Langmuir* 2001, 17, 6298-6303.
  - (18) Bluhm, E. A.; Bauer, E.; Chamberlin, R. M.; Abney, K. D.; Young, J. S.; Jarvinen, G. D. *Langmuir* 1999, 15, 8668-8672.
  - (19) Bluhm, E. A.; Schroeder, N. C.; Bauer, E.; Fife, J. N.; Chamberlin, R. M.; Abney, K. D.; Young, J. S.; Jarvinen, G. D. *Langmuir* 2000, 16, 7056-7060.
  - (20) Lee, S. B.; Martin, C. R. *Anal. Chem.* 2001, 73, 768-775.
  - (21) Astorga-Wells, J.; Swerdlow, H. *Anal. Chem.* 2003, 75, 5207-5212.
  - (22) Pu, Q.; Yun, J.; Temkin, H.; Liu, S. *Nano Lett.* 2004, 4, 1099-1103.
  - (23) Rathore, A. S.; Wen, E.; Horváth, C. *Anal. Chem.* 1999, 71, 2633-2641.
  - (24) Knox, J. H. *J. Chromatogr. Sci.* 1977, 15, 352-364.
  - (25) Kruyt, H. R., Ed. *Colloid Science*; Elsevier: New York, 1952.
  - (26) Rudge, S. R.; Basak, S. K.; Ladisch, M. R. *AIChE Journal* 1993, 39, 797-808.
  - (27) Basak, S. K.; Velayudhan, A.; Kohlmann, K.; Ladisch, M. R. *J. Chromatogr. A* 1995, 707, 69-76.
  - (28) Tellez, C. M.; Cole, K. D. *Electrophoresis* 2000, 21, 1001-1009.
  - (29) Tan, G.; Shi, Q.; Sun, Y. *Electrophoresis* 2005, 26, 3084-3093.
  - (30) Yu, S.; Lee, S. B.; Martin, C. R. *Anal. Chem.* 2003, 75, 1239-1244.
  - (31) Rathore, A. S.; Horváth, C. *J. Chromatogr. A* 1997, 781, 185-195.
  - (32) Mishchuk, N. A.; Takhistov, P. V. *Colloids Surf.* 1995, A, 119-131.
  - (33) Leinweber, F. C.; Tallarek, U. *Langmuir* 2004, 20, 11637-11648.
  - (34) Wu, R.; Zou, H.; Ye, M.; Lei, Z.; Ni, J. *Electrophoresis* 2001, 22, 544-551.

## Chapter 4: Summary

### 4.1 Conclusion and Future Work

This chapter summarizes the results and discussion reported in previous chapters. Further, some suggestions are given for future work.

In Chapter 2, a nano-SEC for biomolecules with a packed 50  $\mu\text{m}$  i.d. capillary was reported. The nano-SEC system developed exploited a splitless-flow mobile phase delivery pump and laser induced native fluorescence detection method. This miniaturization of conventional SEC improves the sensitivity and analysis time. The LOD (690 nM or 2.8 fmol) of protein achieved with this system is comparable to that of CE on-chip, and even better than in other nano-LC systems in terms of mass detection limits, but inferior in terms of concentration detection limits. It took only several minutes to separate binary protein mixtures. The band broadening was minimized by decreasing flow rate, using smaller injection volume, resulting in better resolution. Compared to other reported values, the separation efficiency in a commercially available  $\text{C}_{18}$  column shows our system is not as efficient as the best reported, but it does give performance in a similar range. As a result, we conclude the nano-LC pump, injector and detector are not the major contributor to band broadening in the SEC study.

Compared to a small molecule, tryptophan, protein gives much larger band broadening in the nano-LC. The difference may be caused by protein adsorption and the slow diffusion of large molecules. Although the beads are coated with a hydrophilic layer, the interaction of protein with remaining uncovered surface, activated frit and capillary wall is inevitable. Within such a small column, the contribution of protein interaction is significant compared to conventional SEC. Coating of the capillary wall and deactivation of the frits is an effective method to reduce protein adsorption. In-column detection can be used to replace on-column detection to decrease the C term in van Deemter equation as well as adsorption to the possibly activated frit. Additionally, the connection of the packed capillary to injector needs to be adjusted to minimize extra column band

broadening.<sup>1</sup>

In Chapter 3, the mechanism of protein concentration in SEEC was investigated. It was found that the protein elution was charge related, which is similar to charge trapping occurred with nanoporous membrane. Here, adsorption of proteins is clearly not the reason for trapping because of the observed clean Gaussian peaks. Although the pore size of stationary phase and ionic strength have little effect on protein retention, the pH of the buffer can change protein behavior significantly in a packed capillary, effectively since pH of the buffer can change the charge of protein, resulting in a different direction of electrophoretic mobility. The value of electroosmotic flow for beds packed with polymer-based stationary phase was determined for packed beds shows that the tendency of a protein to elute is directly related to its net mobility. The different direction of  $\mu_{eof}$  in the column and  $\mu_{ep}$  of many negatively charged proteins leads to protein trapping in the front of the packed bed. Evaluation of the results for two buffers with different ionic strength shows that protein trapping occurs at lower electric field for low ionic strength buffer, which does not support the EOF model for protein concentration. Thus, the results obtained here may indicate that nanopore induced space charge layer phenomena also play a role. In further studies, microfabricated single nanopore could be used to simplify the system to study the effect of a nanopore on protein trapping.

## 4.2 Reference

- (1) Eeltink, S.; Rozing, G. P.; Schoenmakers, P. J.; Kok, W. T. *J. Chromatogr. A* 2004, *1044*, 311-316.